Characterization of brain-derived neurotrophic factor (BDNF) and its receptor, tropomyosin receptor kinase B (TrkB), expression and function in the spinal nociceptive circuitry in a model of chronic neuropathic pain

A DISSERTATION

SUBMITTED TO THE FACULTY OF THE

UNIVERSITY OF MINNESOTA

BY

Reshma S Gore

IN PARTIAL FULFILLMENT OF THE REQUIREMENTS

FOR THE DEGREE OF

DOCTOR OF PHILOSOPHY

Dissertation Advisor

Lucy Vulchanova, Ph.D.

August 2021

ACKNOWLEDGMENTS

Lucy, for being the best thesis advisor I (or anyone) could ask for. I first met her during my interview weekend for GPN and I loved her passion for science, genuine curiosity, ability, and willingness to listen to all points of view regardless of the source. I was particularly drawn to her passion, enthusiasm, and the adorable awkwardness that is characteristic of majority of scientists. I knew very early on that she was the best PI for me, and that the Vulchanova Lab was my science home. I genuinely cannot imagine going through my graduate school journey without Lucy as my PI.

I've had the pleasure to work with and train many talented undergraduates and high school students. But it is the core lab family members I want to acknowledge. Maureen Reidl has been an amazing maternal figure and friend. Not only did she provide emotional support by listening to my countless rants, but she also helped with data collection whenever I needed it and provided a lot of delicious homemade food along the way. Alex Skorput was an amazing post-doctoral fellow and friend that provided encouragement, advice, and challenged my ideas that improved by research. His dog, Brady, certainly provided a lot of comfort and fun.

I want to thank a few more lab members from my and other labs. Tina Esmail for being a wonderful mentee and I'm proud of her achievements and feel lucky to call her my friend. Chris Honda for his kind, generous, joyful presence in lab. Even though I did not work with him directly, his presence in the lab and our casual conversations and interactions were priceless. Most of all, I miss his dry sense of humor and his laugh. I want to extend a special thanks to Dr. Cody Walters for being my best friend in grad school. And generally, the entering class of 2015 for being critical support system especially during the first few years of graduate school.

Finally, my partner Scott Spear for his support and patience during the tough last year of my thesis and the pandemic. My furbaby Kiki provides us with endless hours of joy, fun, and general goofiness. Adopting Kiki was the best decision I have made thus far, and I absolutely cannot imagine staying sane (especially the last year of grad school) without her absolute silliness and surprising intuition. My friends Heather and Serena have been a comforting presence and source of wisdom in my personal life, and I am lucky to have such a wonderful support system around me.

I feel extremely lucky to have met all the people at the U that I did during my graduate career, and I never felt homesick because I always had a science home here.

DEDICATION

To my biological and found family members.

I would not be the person I am today without my parents or my amazing friends.

ABSTRACT

Brain derived neurotrophic factor (BDNF) is widely studied for its role in plasticity that underlies learning and memory, and the maladaptive plasticity that gives rise to chronic pain. BDNF acts through its receptor, tropomyosin kinase B (TrkB), to initiate signaling cascades that result in time-, sex-, region-specific changes in nociceptive circuitry due to nerve injury. Despite great interest in the role of BDNF in neuroplasticity responsible for producing chronic pain states, including neuropathic pain, very few studies include more than one timepoint, region, sex, and methods to evaluate the presence and activity of BDNF. These gaps in the literature are especially problematic when considering reported sex-dependent or contradictory effects of BDNF on pain behaviors. Understanding the scope and exact mechanism of BDNF-TrkB signaling in neuropathic pain is crucial for the development of novel pain therapies that are safe, effective, and unbiased.

My thesis work focuses on providing a comprehensive assessment of BDNF and TrkB expression and function which includes both sexes, multiple regions of the nociceptive pathway, cell types, and timepoints after nerve injury. Using a highly sensitive in situ hybridization method, I show that changes in BDNF and TrkB mRNA in DRG and spinal cord are time- and sex-dependent. Although males had higher amounts of TrkB protein in dorsal horn (DH) of the spinal cord, the degree of TrkB activation due to injury was comparable between the sexes. A novel TrkB specific inhibitor, ANA-12, modestly but significantly reduced hypersensitivity in males in a time-dependent manner but not in females. Further investigation into this revealed that ANA-12, instead of inhibiting TrkB activity, increased DH TrkB phosphorylation in both sexes. Finally, the

role of microglia in BDNF-TrkB signaling was investigated and although BDNF mRNA was not detected in any microglial profiles in DH, TrkB mRNA was reliably identified in DH microglia after nerve injury. The microglial TrkB phosphorylation was elevated in DH of injured animals pointing to a functional role. To test that hypothesis, I generated a tamoxifen inducible microglia specific TrkB knockout line and conducted behavioral experiments to evaluate the effect of microglial TrkB on pain behaviors. No behavioral differences were detected at any timepoint in either sex. Surprisingly, tissue analysis revealed an elevation in BDNF and TrkB along with the surface area of microglia in DH indicating increased microglial activation in response to microglial TrkB deletion. These data collectively suggest that BDNF-TrkB activity is region, sex, and time-dependent and highlights the importance of validating not just the tools used, but also the effect of the manipulations on the underlying process that is being studied.

TABLE OF CONTENTS

FIGURES

INTRODUCTION

Chronic Pain

Chronic pain affects about 20% of the population, costs upwards of $200 billion in lost productivity and health care costs, and makes up for about 10-15% of doctor's visits (Stemkowski et al., 2013; CDC, 2018; CE et al., 2020). Chronic pain is defined as pain that persists or recurs for 3 to 6 months (CDC, 2018). The common treatments of pain are insufficiently efficacious and have significant long-term side-effects as well as unintended consequences such as opioid dependence and addiction. Neuropathic pain specifically is especially difficult to treat because opioid analgesics, which are currently the most prominent and commonly prescribed analgesics are not as effective in treating pain of neuropathic type (Abdulrahman and Alsafi, 2020). Newer classes of drugs including, GABA agonists, Selective serotonin reuptake inhibitors (SSRIs), and norepinephrine modulators have been found to be more effective in managing pain of neuropathic origin (Inoue, 2009). These clinical and pharmacological results suggest distinct pathology and neuroplasticity in the context of neuropathic pain as compared to other types of pain disorders.

Neuropathic pain and nociceptive pathway

Neuropathic pain is defined as pain originating because of injury or disease affecting somatosensory and nociceptive pathways. Somatosensory pathways convey information about touch, pressure, vibration, pain, and temperature from the end organs to the brain. Innocuous sensory stimuli are conveyed to the primary somatosensory cortex via the posterior-column medial lemniscus pathway. The nociceptive pathway, commonly referred to as the lateral spinothalamic tract (LST) or spinothalamic tract

(STT), carries information about painful stimuli. This pathway begins with primary sensory neurons of the pseudo-unipolar type which have two sets of processes or fibers, namely, peripherally projecting or centrally directed. The collection of cell bodies of these neurons is referred to as the dorsal root ganglia (DRG) which are nestled between spinal vertebrae. The peripherally projecting ends of the DRG neurons innervate epidermal layer of skin and can be activated by noxious stimuli presented to the skin. The centrally projecting fibers carry information from the peripheral organ to the dorsal horn of the spinal cord (superficial laminae). A dense network of excitatory and inhibitory neurons of the dorsal horn integrates the incoming innocuous and noxious stimuli and only about 1% of neurons in the DH are projection neurons that carry the integrated information to the thalamus. Axons of the projection neurons decussate at the spinal level and ascend to the contralateral ventral posterior lateral (VPL) and central nucleus of thalamus. A third order neuron from the VPL then sends information to the primary somatosensory cortex which gives rise to the conscious perception of the painful sensation. In addition, information from the central nucleus of thalamus is sent to many other brain regions including, amygdala, hippocampus, ventral striatum, anterior cingulate cortex which are responsible for the affective component of pain. Normally, the innocuous tactile sensory information is segregated from the pathways carrying noxious information. However, following nerve injury, the gating mechanisms and spinal circuitry that function to keep the two sensory pathways segregated breakdown and the innocuous information can be conveyed to the brain by the nociceptive pathway thus resulting in the sensation of pain generated by an innocuous stimulus (allodynia) (Bardoni and Merighi, 2009; Stemkowski et al., 2013). In addition to allodynia, the

existing nociceptive circuitry is sensitized such that noxious information is amplified to generate a greater sense of pain (hyperalgesia) (Bardoni and Merighi, 2009; Stemkowski et al., 2013). There are many changes throughout the ascending nociceptive pathway as well as the descending modulatory pathway that contribute to allodynia, hyperalgesia, and all the neuropathic pain components. However, the most well studied and understood mechanisms include changes that occur at the dorsal root ganglia (primary sensory neurons) and spinal cord (first site of signal convergence). Convergence and complexity of signal interpretation is greater at each higher level in the pathway. Therefore, most pre-clinical research focuses on mechanistic changes at the lower levels in the nociceptive pathways because it is relatively simpler in terms of number of converging signals. Additionally, therapeutics targeting these sites are likely to have fewer disruptive effects on the central nervous system (CNS).

Mechanisms of central sensitization

Central sensitization is a term used to refer to the changes that occur at the spinal level which are thought to be primarily responsible for producing allodynia and hyperalgesia. Various mechanisms contribute to the neuronal sensitization. Some of these include signaling factors, growth factors, neurotransmitters, and peptides released into the dorsal horn by central processes of peripheral sensory neurons following injury (Bardoni and Merighi, 2009; Stemkowski et al., 2013; Khan and Smith, 2015; Garraway and Huie, 2016; Richner et al., 2017). Several neuroimmune changes result in increased reactivity of local microglia and astrocytes that then release cytokines, chemokines, and signaling factors of their own that can directly or indirectly activate spinal neural circuits. Additionally, the expression of receptors for excitatory neurotransmitters and their open

probabilities are increased contributing to the increased sensitivity and response of spinal neurons. These mechanisms are thought to be responsible for hyperalgesia. Allodynia, on the other hand, is considered to arise due to spinal disinhibition that is triggered by microglial activity. Under normal conditions, the innocuous tactile information is gated by GABAergic inhibitory neurons that are part of the dorsal horn spinal circuits. Following nerve injury, these inhibitory gates are removed, and tactile information activates the nociceptive projection neurons and normally non-painful stimuli can produce a pain response (Chen et al., 2014a; Hildebrand et al., 2016). Microglia are thought to contribute to the disinhibition at the spinal level by releasing BDNF.

Role of BDNF in the central nervous system

Brain derived neurotrophic factor (BDNF) is a ubiquitous growth factor that plays a crucial role in neuronal survival, differentiation, and polarization during development. In the adult mammalian systems, it is thought to mediate long-term plasticity under various conditions (Borodinova and Salozhin, 2017). BDNF is produced in the neuronal endoplasmic reticulum and stored in large dense core vesicles at the axon terminals along with other neuropeptides. The mature form of BDNF (which is the form that will be referred to as BDNF in this thesis) is cleaved from its precursor, proBDNF, by proteases and convertases and thus are co-localized in large dense core vesicles. ProBDNF and mature BDNF are released from neurons in an activity dependent manner and broadly have opposing effects and different affinities for receptors(Borodinova and Salozhin, 2017). proBDNF is thought to bind with p75NTR, a member of the tumor necrosis factor family, and results in long-term depression and cell death. In contrast, the mature BDNF has a higher affinity for its cognate receptor Tropomyosin kinase B (TrkB) which auto-

phosphorylates upon BDNF binding and engages downstream substrates such as MAPK/ERK, PI3K and PLC. These pathways generally lead to activation of CREB thus bringing about long-term changes via gene-modification(Chen et al., 2014b; Borodinova and Salozhin, 2017).

BDNF activity following injury

BDNF is expressed in sensory neurons in DRG in baseline conditions and this expression increases following injuries(Obata and Noguchi, 2006; Marcol et al., 2007). Neurons of the spinal cord also express BDNF, and despite a lack of clear direct evidence, spinal microglia are thought to produce and release BDNF. Regardless of the source, the activity of BDNF at the spinal level has been shown to be necessary and sufficient for producing behavioral tactile hypersensitivity(Inoue, 2009; Stemkowski et al., 2013; Garraway and Huie, 2016). Intrathecal injections of BDNF have been shown to produce writhing, scratching behaviors which are suggestive of increased nociception(Marcol et al., 2007; Dhandapani et al., 2018). BDNF brings about these behavioral changes by sensitizing the nociceptive signaling pathways and causes long-term changes that produces maladaptive neuroplasticity which maintains the neuropathic pain state. BDNF induced activation of intracellular proteins and kinases is linked with a wide range of outcomes. These include phosphorylation and modification of endogenous receptors such that their open probability and duration increases and results in rapid and long-lasting neuronal activity(Obata and Noguchi, 2006; Marcol et al., 2007; Ding et al., 2015; Shaw et al., 2020). Additionally, activation of intracellular pathways can transiently or permanently increase or decrease receptor placement in the cell membrane. Furthermore, the long-term genetic changes can result in increased expression and

transcription of more receptors, kinases, and cellular material that can generate morphological changes.

TRKB receptor types

Tropomyosin receptor kinase B (TrkB) is a member of the receptor kinase family that functions as a cognate receptor for BDNF. All neurotrophins have an affinity for all neurotropin receptors, they have particularly high affinity for their cognate receptors (Lu et al., 2005; Ohira and Hayashi, 2009). TrkB has high affinity for BDNF and neurotrophin 3/4 (NT-3/4). The NTRK2 gene encodes for two main types of receptors, the full-length TrkB receptor (GP^{145}) that contains intracellular kinase domains, and two forms of truncated TrkB (GP^{95}) that lack intracellular kinase domains (Minichiello, 2009). The T1 and T2 truncated TrkB receptor forms have 11 and 9 unique intracellular domains, the function of which is unclear. The full-length TrkB (fl-TrkB) was thought to be the active form which allowed for intracellular signaling due to the kinase domains at the C-terminus, whereas the truncated forms are assumed to play an opposing role by scavenging BDNF thus preventing binding and activation via fl-TrkB (Klein et al., 1991; Middlemas et al., 1991; Squinto et al., 1991; Barbacid, 1994). However, more recent evidence suggests that the truncated form, T1, can produce intracellular calcium signaling (Cao et al., 2020). The precise mechanisms by which the intracellular signaling is carried out in the absence of an internal kinase domain is not known.

TRKB receptor expression and function

Like BDNF, TrkB is expressed widely and ubiquitously throughout the CNS (Yan et al., 1997; Mannion et al., 1999). Although TrkB expression in non-neuronal cells has not extensively been characterized, ultra-structural images show TrkB receptors localized

to axons, dendrites, and cell bodies of neurons in the brain and spinal cord (Yan et al., 1997). In sensory neurons, fl-TrkB receptor is expressed in cell bodies located in the DRG and the central axonal terminals that project to superficial laminae of the dorsal horn of spinal cord (Minichiello, 2009; Vaegter et al., 2011; Richner et al., 2017, 2019; Dhandapani et al., 2018). The truncated T1 form is expressed in astrocytes in the spinal cord and brain (Cao et al., 2020) . TrkB normally exists as a monomer, and it dimerizes upon BDNF binding (Minichiello, 2009). The downstream signaling which includes activation of PLC, MAPK/ERK, and PI3K are responsible for BDNF induced neural plasticity (Klein et al., 1991; Middlemas et al., 1991; Barbacid, 1994; Merighi et al., 2008; Minichiello, 2009; Ohira and Hayashi, 2009). BDNF-TrkB signaling plays a crucial role in LTP mechanisms in the CNS (Ohira and Hayashi, 2009; Khan and Smith, 2015). Similar LTP mechanisms contribute to maladaptive plasticity underlying many pathophysiological conditions, including neuropathic pain (Pezet et al., 2002; Merighi et al., 2008; Ohira and Hayashi, 2009; Cao et al., 2020). The exact localization of TrkB in different cell types has not been studied largely due to the absence of validated antibodies for the detection of fl-TrkB-immunoreactivity (-ir) as well as the truncated TrkB-ir. Majority of the data regarding expression of TrkB in various neuropathic pain states is measured via Western blot assay which does not provide information about the anatomical localization of the receptors. Furthermore, the activity of the TrkB receptors is often measured indirectly by quantifying the presence or activation of downstream markers that are thought to be activated by TrkB. Therefore, it is difficult to assess the presence of TrkB in various cell types and to quantify the expression of TrkB specifically in areas of CNS that process nociception.

Glial cell function in CNS

When glial cells were first discovered, they were believed to serve as the glue or binding agent in the CNS, however, it is clear from the mounting data that glial cells are crucial for neuronal signaling. There are five main classes of glial cells- satellite cells, Schwann cells, oligodendrocytes, astrocytes, and microglia. Schwann cells are glial cells expressed in the PNS. These cells envelop fiber tracts of primary sensory neurons and are responsible for nerve fiber myelination. Oligodendrocytes are found in the CNS and play a similar role to Schwann cells. Oligodendrocytes engage in signaling with cells and neurons to prevent neuronal regeneration in the CNS (Ji et al., 2013). Satellite cells are found surrounding DRG neurons. These cells can produce signaling factors and express receptors for various factors released by DRG neurons and peripheral immune cells. Satellite cells in turn can participate in DRG neuronal modulation by altering their excitability. Astrocytes are by far the most abundant glial cells in the CNS and are closely associated with neurons. Astrocytes not only provide neurons with essential factors required for their proper function, but also maintain proper extracellular environment. Astrocytes form dense non-overlapping networks with each other via gap junctions and are thought to control large and small blood vessels to increase blood flow to most active brain regions. Astrocytes even form tripartite synapses with axon terminals thus participating, modulating, and influencing neuronal signaling (Vallejo et al., 2010). Microglia are derived from the peripheral monocyte lineage and are the native immune cells of the CNS. These cells serve as sentinels and scan their environment for signs of damage (Ji et al., 2013).

Microglial activity following injury

Microglia function as the primary immune cells in the CNS. Under normal conditions, microglia exist in their quiescent state and are relatively stable as they monitor microenvironments for disruptions, injuries, or damage. When they detect presence of foreign objects or increased signals indicating damage, they become activated and upregulate expression of various proteins, including Iba1, a marker used to label microglia. Iba1 stands for ionized calcium binding adaptor molecule 1 (Ito et al., 1998), and is an actin-binding protein found in microglia and macrophages. It is responsible for membrane ruffling and via rac signaling it engages an intracellular signaling cascade that results in phagocytosis, microglial and macrophage proliferation, and infiltration of peripheral lymphocytes, monocytes, macrophages to the CNS (Ohsawa et al., 2000; Imai and Kohsaka, 2002; Kanazawa et al., 2002; Ramesh et al., 2013; Guan et al., 2015). These cells are phagocytotic and along with other immune cells recruited to the site of injury are responsible for cleaning up byproducts and damaged components resulting from the injury.

Contribution of microglia to nerve injury induced neuroplasticity

The contribution of microglia to nerve injury related spinal neuroplasticity has received a lot of attention and interest in recent years (Moalem and Tracey, 2006; Ji et al., 2013; Ramesh et al., 2013). Following peripheral nerve injury, the primary sensory neurons release Colony stimulating factor 1 (CSF1), along with many other signaling factors such as BDNF, in the spinal dorsal horn. CSF1 binds to its receptor, CSF1R, located on spinal microglia which causes their activation. Several downstream mechanisms including phosphorylation of p38 MAPK leads to changes that produce behavioral hypersensitivity (Jin et al., 2003; Tsuda et al., 2004; Ji and Suter, 2007).

Blocking microglial activation by non-specific microglial inhibitors, toxins or specific receptor blockers designed to inhibit certain microglial functions can reduce behavioral hypersensitivity (Jin et al., 2003; Raghavendra et al., 2003; Tsuda et al., 2004; Verge et al., 2004; Ledeboer et al., 2005; Clark et al., 2007; Guan et al., 2015). Microglia are assumed to contribute to spinal neuroplasticity by releasing BDNF thus contributing to the BDNF-TrkB signaling which sensitizes nociceptive circuitry (Coull et al., 2005; Chen et al., 2014b). However, these reports provide indirect evidence for the presence and release of BDNF from spinal microglia following nerve injury. The studies indicating microglial release of BDNF are conducted in vitro using microglial cell-cultures or in vivo using antibodies whose specificity for BDNF was not evaluated (Coull et al., 2005; Ulmann et al., 2008). Therefore, there is no evidence that microglia express BDNF and the contribution of this microglial BDNF to nerve injury induced hypersensitivity.

Sex differences in spinal mechanisms of neuroplasticity

There is compelling evidence for sex differences in various physiological processes involved in neuroplasticity (Berkley, 1997; Greenspan et al., 2007; Fillingim et al., 2009; Manson, 2010; Mogil, 2012, 2020; Sorge and Totsch, 2016; Doyle et al., 2017; Mapplebeck et al., 2018, 2019). For instance, many chronic pain conditions are more prevalent in women than in men, the intensity and duration of the pain conditions is higher in women (Greenspan et al., 2007; Fillingim et al., 2009; Manson, 2010; Mogil, 2012). In preclinical studies, many biological pathways involved in immune function after injury are different between male and female animals (Berkley, 1997; Greenspan et al., 2007; Fillingim et al., 2009; Manson, 2010; Mogil, 2020; Sorge and Totsch, 2016; Doyle et al., 2017; Mapplebeck et al., 2018, 2019). In the neuropathic pain literature, a

few reports gained attention due to their surprising conclusions that BDNF, microglia, or some aspect of BDNF-TrkB signaling or immune function do not contribute to nociceptive plasticity in females as it does in males (Greenspan et al., 2007; Manson, 2010; Mapplebeck et al., 2017, 2018; Mogil, 2020). However, these studies do not point to any mechanistic rationale for the observed sex-differences because basic functional information in females is largely absent. Almost all the current data available for the mechanisms underlying pain related neuroplasticity is collected from male subjects (Mogil, 2020). Therefore, the mechanistic explanations and points of divergence for observed behavioral sex differences remain elusive. The most influential report in the spinal neuroplasticity literature announced that microglia are dispensable in spinal neuroplasticity following nerve injury in females and instead peripheral T-cells infiltrate the CNS (Sorge et al., 2015; Sorge and Totsch, 2016). These results generated great interest, however, follow up studies that measured, and evaluated the signaling downstream of the supposed microglial functions did not show sex-differences, indicating that many signaling cascades converge and therefore would be promising targets in novel pain therapies (Mapplebeck et al., 2019). New mandates to include female subjects in all experimental protocols, with few exceptions, will provide a good base of knowledge regarding previously ignored factors that contribute to inadequate research regarding pain treatment in women. All experiments conducted here included female subjects not solely to demonstrate sex-differences, but to provide a broad framework for understanding BDNF-TrkB signaling in both sexes.

DISSERTATION OBJECTIVES

Information presented so far provides rationale for targeting components of the BDNF-TrkB signaling pathway for development of novel analgesic therapies. However, the ubiquity of BDNF-TrkB signaling in the central nervous system (CNS) poses a major problem for BDNF-TrkB inhibition as a target for pain therapies. Furthermore, the literature on region, sex, and time-specific expression and function of BDNF via its receptor in the context of nociceptive plasticity is greatly lacking. Prior studies have shown increased expression or function of BDNF, typically by proxy due to a lack of tools to directly visualization or quantification of BDNF or its receptor TrkB, at single timepoint, sex, or region of the CNS. Thus, the interpretation of data showing analgesic effects of BDNF or sex-differences in BDNF-TrkB signaling in neuropathic pain is challenging due to the absence of a comprehensive characterization of time, region and sex-specific changes following nerve injury. Understanding the region, sex, time, and injury specific changes, as well as evaluating the efficacy or action of tools used to study those changes that underlie maladaptive neuroplasticity is crucial for the development of effective pain strategies.

Towards this goal, my thesis research had three main objectives:

Chapter 1: Comprehensive characterization of BDNF and TrkB expression in regions of nociceptive pathway initially affected by peripheral nerve injury at several time-points after injury in animals of both sexes.

Chapter 2: Determine the degree of sex- and time-dependent TrkB activation after injury and evaluate whether TrkB activity is required for the establishment and maintenance of chronic hypersensitivity.

Chapter 3: Understand the role of spinal microglia in the BDNF-TrkB signaling and whether BDNF-TrkB signaling in microglia is sex-dependent.

CHAPTER 1: BDNF AND TRKB EXPRESSION IN DRG AND SPINAL CORD FOLLOWING NERVE INJURY

INTRODUCTION

Brain derived neurotrophic factor has a crucial role in neuronal development and is known to contribute to neuronal survival, neuronal proliferation, axonal growth, and neuronal migration (Lu et al., 2005). In the adult CNS, BDNF participates in mechanisms underlying neuroplasticity (Bramham and Messaoudi, 2005). Since chronic pain is a result of maladaptive plasticity in nociceptive pathways, BDNF is widely studied to understand mechanisms by which it causes long-term changes that result in chronic pain (Pezet et al., 2002). Although BDNF is greatly increased following inflammatory insults, modest increases in BDNF at specific timepoints after nerve injury have been reported (Pezet et al., 2002; Bramham and Messaoudi, 2005; Marcol et al., 2007; Merighi et al., 2008; Smith, 2014). BDNF is produced in DRG neurons and released into the spinal cord following nerve injury leading to an increase of BDNF in spinal dorsal horn (Pezet et al., 2002; Bramham and Messaoudi, 2005; Obata and Noguchi, 2006; Merighi et al., 2008; Chen et al., 2014b; Smith, 2014). In addition to the sensory neuron derived BDNF, it is also released by neurons in the superficial laminae of spinal cord (Pezet et al., 2002; Bramham and Messaoudi, 2005; Obata and Noguchi, 2006; Merighi et al., 2008; Chen et al., 2014b; Smith, 2014). Microglia are considered to play a critical role in spinal neuroplasticity by releasing BDNF into the surrounding areas of spinal cord (Coull et al., 2005; Inoue, 2009; Biggs et al., 2010). Regardless of the source, BDNF induces short- and long-term changes in the spinal cord that together increase activation of projection neuron that carry nociceptive information from spinal cord to higher brain regions

(Marcol et al., 2007; Merighi et al., 2008; Smith, 2014). The short-term changes include phosphorylation of presynaptic NMDA receptors, which increases release of glutamate and other factors into the spinal cord, phosphorylation of pre- and post-synaptic NMDA and AMPA receptors to increase their open channel probability and duration leading to increased excitability of spinal neurons, and increased trafficking of glutamate receptors in neuronal membranes (Marcol et al., 2007; Merighi et al., 2008; Chen et al., 2014b; Sikandar et al., 2018). BDNF-induced long-term changes alter the nociceptive circuitry such that innocuous stimuli can activate the nociceptive projection neurons (Bramham and Messaoudi, 2005; Coull et al., 2005; Obata and Noguchi, 2006; Obata et al., 2011; Zhou et al., 2011; Li et al., 2017; Sikandar et al., 2018). These short-and long-term changes results in long-term plasticity (LTP) in spinal nociceptive circuits. All these effects of BDNF are carried out by signaling through fl-TrkB, and methods that inhibit TrkB (such as TrkB antagonists, blockers, anti-TrkB antibodies, and genetic mutations to block TrkB function) reduce nerve injury induced hypersensitivity (Groth and Aanonsen, 2002; Yajima et al., 2002; Reichardt, 2006; Merighi et al., 2008; Ohira and Hayashi, 2009; Wang et al., 2009; Sorge et al., 2015; Hildebrand et al., 2016; Li et al., 2017; Dhandapani et al., 2018; Cao et al., 2020; Ikeda et al., 2020). Taken together, BDNF and TrkB have been independently shown to contribute to nerve injury induced behavioral hypersensitivity and increase excitability in spinal cord.

Most studies do not directly measure BDNF or TrkB expression levels in spinal cord or DRG because of the lack of validated, reliable, and sensitive antibodies and *in situ* techniques. The few reports of BDNF increase following injury includes in situ and IHC experiments that showed elevated BDNF mRNA and protein levels at multiple

timepoints after injury but only included male animals (Michael et al., 1999; Obata et al., 2003; Geng et al., 2010). Transgenic mouse lines are often used to visualize BDNF and/or TrkB in different CNS regions, however, the reports from these studies contradict data collected from wildtype (WT) animals and thus raise the possibility of altered protein regulation in transgenic mice. Again, in all these examples only male subjects are included, therefore no information about BDNF and TrkB expression or function is available in females. Many potential explanations exist for the observed behavioral or pharmacological sex-differences (Manson, 2010; Mogil, 2012; Sorge and Totsch, 2016; Mapplebeck et al., 2017, 2019), however, without any information regarding the expression and localization of BDNF and TrkB in females, it is difficult to study the point of divergence in these nociceptive signaling pathways. This study aims to fill that gap in the literature by quantifying the BDNF and mRNA expression in DRG neurons, satellite cells, as well as superficial laminae of dorsal horn of the spinal cord at multiple timepoints following peripheral nerve injury in male and female mice. The results presented in this thesis will provide comprehensive data on BDNF and TrkB expression in sex-, time-, and region-specific manner and serve as a necessary reference point for future studies aimed at understanding the root cause of observed sex-differences.

MATERIALS AND METHODS

Animals

All experiments were conducted in compliance with National Institutes of Health Guide for Care and Use of Laboratory Animals and approved by the University of Minnesota Institutional Animal Care and Use Committee. Adult male and female ICR-CD1 mice were bred in-house at University of Minnesota vivarium where male mice were housed 4 to a cage, and 5 female mice to a cage. They were kept at uniform temperature, humidity, 12-hour light/dark cycle with *ad libitum* access to food and water in a specific pathogen free environment. All animals were group housed for the entirety of all experiments, unless specific unrelated health issue required individual housing.

Spared Nerve Injury (SNI)

Tactile hypersensitivity was induced using the spared nerve injury (SNI) model as described by Decosterd and Woolf(Decosterd and Woolf, 2000). Mice were placed under isoflurane anesthesia in a recumbent position and the three terminal branches of the left sciatic nerve were exposed by bluntly dissecting the left thigh muscle. The common peroneal and tibial nerves were ligated using a 5.0 silk suture. The peroneal and tibial nerves were cut 2 mm distal to the ligation site, leaving the sural nerve uninjured. Sham animals had the left sciatic nerve exposed without ligation or cutting of the nerves.

Tactile Hypersensitivity

Mice were acclimated to the testing room prior to each behavioral test session starting the day of baseline measurements. Mice were brought into a quiet testing room and allowed to acclimate for about an hour before placing them on a wire mesh grid

platform under a glass enclosure and allowed to acclimate for 30 mins prior to testing. Synthetic Von Frey filaments were used to apply force onto the lateral plantar surface of the left and right hind paw. Using the up-down method as described by Chaplan et al (1994) and statistical framework by Dixon (2012), the 50% withdrawal threshold was calculated wherein a positive withdrawal reflex was defined as a flinching, retracting, or withdrawing of the hind paw from the filament. Baseline tactile thresholds were measured for all animals in these experiments and measured again following nerve injury but prior to tissue collection.

Spinal Cord and DRG tissue section preparation

Mice were deeply anesthetized with isoflurane and perfused via the heart with calcium-free Tyrode's solution (116mM NaCl, 5.4mM KCl, 1.6mM MgCl·26H2O, 0.4mM MgSO·47H2O, 1.4mM NaH_2PO_4, 5.6mM glucose, and 26mM Na_2HCO_3) followed by fixative (4% paraformaldehyde). Tissues were dissected, post-fixed overnight in (4% paraformaldehyde), then incubated in 10% sucrose. Spinal cords and DRG were embedded in OCT compound (Tissue-Tek), flash frozen using liquid CO_2 and stored at -80°C overnight. Sections were cut at 14 μm thickness using a cryostat microtome (OTF5000, Bright Instruments) and thaw mounted onto Superfrost Plus microscope slides (Fischer Scientific). Sliced spinal cord sections were anatomically mapped to determine slides within the L3 and L4 spinal levels. Spinal cord and DRG slides were stored at -20°C until further processing. Separate tissue blocks were made for tissues collected from each timepoint such that tissues from different timepoints were analyzed separately but comparisons were made between groups within the same experimental timepoint.

RNAscope Processing and Probes

Slides were prepared for RNAscope® processing using the RNAscope® Fluorescent Multiplex v2 Kit (Cat. No. 323100). Briefly, slides were recovered from -20^0 C, air-dried, and incubated in 4% paraformaldehyde for 5 mins. Tissue sections were dehydrated in ethanol solutions of increasing concentration (50%, 70%, 100% EtOH) for 5 mins in each solution. Slides were washed with 1X PBS for 2 mins then tissue sections were covered with hydrogen peroxide (ACDBio) for 10 mins. Slides were washed 4 times with distilled water, incubated in target retrieval reagent heated to ~96^0 C for 4 mins, washed again 4 times in distilled water, then submerges in fresh 100% ethanol for 5 mins. A hydrophobic barrier was drawn around the tissue and allowed to dry at room temperature for 30 mins. After drying, tissues were covered in RNAscope Protease III and placed in a warm 40°C humidified chamber for 15 mins. After removal from oven, slides were washed 4 times in distilled water.

Following slide and tissue preparation, mRNA was tagged using highly specific probes and associated fluorophores for visualization. Briefly, excess water was removed from slides and BDNF (cat# 424821) or NTRK2 (cat#423611), positive- and negative-control probes were added to separate slides and incubated for 2 hours at 40°C. Following incubation with probes, slides were washed 2 times in 1X wash buffer for 2 mins. Probe signal was amplified by incubating tissue sections with Multiplex FLv2 AMP1 and AMP2 for 30 mins, and in AMP3 for 15 mins at 40°C. Slides were washed 2 times in 1X wash buffer for 2 mins in between each amplification incubation and following the last amplification step. Horseradish peroxidase channel 1 (HRP-C1) signal was developed by covering tissue in RNAscope multiplex FL v2 HRP-C1 and incubated for 15 mins at 40°C. Slides were washed for 2 mins with 1X wash buffer and Cyanine 3

(PerkinElmer) diluted in TSA buffer (1:1,500) was added to the slides. Slides were incubated with Cy3 for 30 mins at 40°C. Slides were washed twice with 1X wash buffer for 2 mins, RNAscope multiplex v2 HRP blocker was added to the slides, incubated for 15 mins at 40°C, then washed 2 times in 1X wash buffer for 2 mins. DAPI was added to the slides for 30 seconds and cover-slipped using FluoroSave reagent (EMD Biosciences, Inc.). Slides were stored at room temperature. RNAscope® 20zz probes were ordered from ACDbio. The Ms-BDNF probe targeting 729-1974 mRNA region which recognize a common portion of the BDNF protein in all of the different translated proteins (NM_007540.4) and Ms-NTRK2 probe targeting 668-1582 mRNA regions encoding for FL-TrkB and truncated TrkB (NM_008745.3)

Image Acquisition and Analysis

Images were captured using a confocal Nikon A1R multiphoton confocal microscope or Olympus Fluoview upright confocal microscope at the University of Minnesota Imaging Center, with guidance from Dr. Guillermo Marquis. All images were collected on the same day or consecutive days with identical settings for all groups for direct comparison. A 25X objective was used when images were collected using the Nikon A1RMP, whereas a 20X objective was used to image tissues on the Olympus Fluoview Upright microscope. FIJI (FIJI is just ImageJ software from National Institutes of Health) was used for all image quantification. Macros were created to automate many of the repeated image processing steps.

Quantification in DRG

For quantification of the BDNF and TrkB mRNA L3 and L4 DRG ipsilateral to the injury were imaged. Three equally spaced sections were imaged for each DRG. For spinal sections, three equally spaced sections within the L3-L4 lumbar level were

selected and imaged. Images consisted of three channels for DRG images – namely, DAPI, an Alexa488 Dk anti-mouse secondary which provides background fluorescence to visualize tissue sections, and Cy3 tagged BDNF or TrkB mRNA. Gain, exposure, and offset settings were determined by using negative control probes and high mRNA signal containing tissues to determine optimal imaging parameters to avoid overexposure and underexposure. Satellite cells of the DRG were detected using the default auto threshold method and converting the image into a binary for a particle analyzer set to detect particles greater than 1micron. DRG neurons were manually circled by an observer blinded to the experimental details and groups using background observed in the 488-fluorescence channel and using DAPI staining to restrict neuron outlines to those whose nuclei are visible to avoid potential double-counting. Surface area of neurons was measured in microns by calibrating the image size based on image acquisition parameters. Manually determined cell outlines were used as ROIs and default auto-threshold was used to create an unbiased thresholding method. Signal above this threshold was considered positive signal. The area occupied by positive mRNA fluorescence was measured along with mRNA fluorescence as a function of area of the cells. Data from three sections were averaged to get single value for each L3 and L4 DRG per animal, and values from L3 and L4 were added to get a single distribution of neurons by size and mRNA signal.

Quantification in spinal cord sections

For quantification in spinal cord sections, a similar approach was used to quantify BDNF and TrkB mRNA in DRG sections. Images of spinal dorsal horn consisted of DAPI channel and Cy3 tagged BDNF and TrkB mRNA. Gain, exposure, and offset settings were determined by using negative control probes and high mRNA signal

containing tissues to determine optimal imaging parameters to avoid overexposure and underexposure. ROIs were manually drawn to outline dorsal horn of spinal cord using DAPI staining by observer blinded to experimental details or knowledge of animal groups. Spinal cord images were thresholded using the default auto-thresholding method and the area of mRNA signal and percent of mRNA area as a function of ROI size were measured. Data from three spinal sections were averaged to obtain a single value representing mRNA signal in spinal cord per animal. To quantify nuclear mRNA, auto-thresholding methods and particle analyzers were used to automatically outline nuclei using DAPI staining, and the mRNA signal within these profiles were measured. The nuclear signal was subtracted from the total mRNA signal in the Dorsal horn to obtain the extra-nuclear signal in the spinal cord.

Western blot assay

Mouse spinal cords were harvested by hydraulic extrusion. The lumbar enlargement was isolated and divided into ipsi- and contralateral halves before being homogenized in RIPA solubilization buffer (Phosphate buffered Saline (PBS) with 0.1% IPEGAL (ICN Biomedicals), 12mM sodium deoxycholate, and 0.1%SDS) containing protease inhibitors (Complete tablet, Roche) and phosphatase inhibitor (mini tablet, ThermoFischer) using a glass bead homogenizer. The homogenate was centrifuged at 1,000 G for 5 min at 4°C and the supernatant was collected. Homogenate was centrifuged again at 16,300 G for 30 mins at 4°C and the pellet was resuspended in RIPA buffer and vortexed. A protein assay was conducted to determine protein concentration of the samples. Samples were mixed with sample buffer (NuPage 4X sample buffer (Invitrogen, Grand Island, NY)) and heated to 95°C for 10 min. All samples were loaded onto a 4-12% gradient gel at 40ug per sample/ per lane (NuPage Novex bis-tris, Invitrogen) and

run at 120 volts for 1-1.5 hrs. After removal from the cassette, the gel was incubated in transfer buffer for 30 mins at RT while shaking. Gels were transferred to PVDF membranes (Immobilin-FL, Millipore) using 90 mA current overnight at 4°C. Membranes were incubated in blocking buffer (LiCor Odyssey Blocking buffer (Invitrogen)) for 1 hr at room temperature, then incubated in primary antisera rabbit anti-TrkB 1:1000 (Cell Signaling product #4603S) for 48 hours at 4°C. After rinsing with PBS containing 0.1% Tween-20, the membranes were incubated for 1 hr in secondary antisera (IR-Dye donkey anti-rabbit 800cw, LiCor). Membranes were then incubated in primary antisera for beta-actin 1:10,000 (Mouse anti-beta actin (Cell Signaling)) for 48 hours at 4°C, followed by 1 hr incubation in secondary antisera (donkey anti-mouse 680 rd, LiCor) at RT. After rinsing with PBS-Tween-20 the blot was placed in TBS until it was imaged using the LiCor Odyssey Imager. Quantification of the band signal was done using Image Studio Lite software. For each animal, TrkB signal band was normalized to actin band and this normalized signal was compared across groups. Sample size for all groups was n=5 except for female SNI group at day 3 where n=4.

Statistical Analysis

Graphical representations were prepared using GraphPad Prism (version 7; GraphPad Software, La Jolla, CA) while the data were analyzed using JMP Pro 15 (SAS Institute Inc., located at SAS Campus Drive, Cary, NC) obtained through the University of Minnesota. Data are expressed as the mean ± S.E.M. and all statistical analysis was considered significant at $\alpha \leq 0.05$. BDNF and TrkB mRNA signal between experimental groups were compared using one-way ANOVA with appropriate post-hoc test.

RESULTS

Confirmation of behavioral hypersensitivity

In all the following experiments, tactile thresholds were measured using von Frey assay and the up-down method. All animals that received SNI surgeries had significantly lower tactile thresholds on the ipsilateral paw as compared to sham operated animals (Data not shown).

Quantification of mRNA in DRG neurons and satellite cells

BDNF mRNA expression in DRG neurons

Representative images of ipsilateral L4 DRG from a male mouse at 3-days after nerve injury were collected using a confocal microscope at 20X magnification. A highly sensitive fluorescent in situ hybridization method allowed for visualization of *BDNF* mRNA in DRG. Higher punctate signal of *BDNF* mRNA in 20X image of DH of the spinal cord was observed (figure 1.1 b3) as compared to fluorescence observed in negative control probe treated DRG sections (figure 1.1 a3). Distribution of DRG neurons indicated uniform sampling of neurons across experimental groups in data sets collected at day 3 (figure 1.1 c), day 7 (figure 1.1 e), and day 28 (figure 1.1 g) post-SNI. Although the sampling was uniform across groups, the number of neurons vary across groups and therefore, the total area of DH occupied by *BDNF* mRNA signal was normalized to total area of neurons to obtain an average *BDNF* mRNA signal per micron area of neuron (figure 1.1 c, f, g). At day 3 post-SNI, an early timepoint after nerve injury, both male and female injured animals had increased *BDNF* mRNA signal in DRG neurons as

compared to their sham operated counterparts (male SNI (n=5) vs sham (n=5), $p<0.001$; female SNI (n=5) vs sham (n=5), $p<0.05$, Two-way ANOVA with Tukey's post-hoc test, figure 1.1d). No differences were detected in *BDNF* expression between any groups at day 7 post-SNI, a timepoint that represents the transitionary period between acute and chronic pain states (figure 1.1 f). At day 28 post-SNI, when chronic pain state has been established, SNI operated females had significantly lower average normalized *BDNF* expression in DRG compared to sham operated females ($p<0.05$, Two-way ANOVA with Tukey's HSD, figure 1.1 h).

TrkB mRNA expression in DRG neurons

Representative images collected from a nerve injured male 28-days post-SNI at 20X magnification show *TrkB* mRNA signal visualized using *in situ* hybridization in *TrkB* probe (figure 1.2 b3) treated and negative control treated (figure 1.2 a3) tissue sections. Distribution of neurons used for quantification of *TrkB* mRNA in DRG neurons showed uniform distribution across experimental groups at day 3 (figure 1.2 c), day 7 (figure 1.2 e), and day 28 (figure 1.2 g) post-SNI. The average normalized *TrkB* mRNA signal was calculated by dividing the total area occupied by *TrkB* mRNA in DH by the sum of total area of all neurons to get the average *TrkB* mRNA signal per micron area of neuron (figure 1.2 d, f, h). At the acute (day 3, figure 1.2 d) and chronic stages post-SNI, no differences were observed between any of the groups, but sex differences and injury induced differences were detected during the transitionary phase (day 7 post-SNI). TrkB mRNA signal in DRG neurons from nerve injured females had lower mRNA signal as compared to injured males (male SNI vs female SNI, $p<0.01$, Two-way ANOVA with

Tukey's HSD, figure 1.2 f) and sham operated females (female SNI vs sham, $p<0.05$, Two-way ANOVA with Tukey's HSD, figure 1.2 f).

BDNF mRNA in satellite cells of DRG

The proportion of *BDNF* mRNA expressing and mRNA negative satellite cells indicated lower proportion of *BDNF* expressing satellite cells at day 28 post-SNI (figure 1.3 g). To determine whether nerve injury altered the distribution of *BDNF* mRNA expression in neurons and satellite cells, the proportion of total *BDNF* signal found in satellite cell profiles was quantified and no differences were detected at any timepoint between any experimental groups (figure 1.3 b, e, h, Two-way ANOVA). The area of DH occupied by *BDNF* mRNA signal normalized to per micron area of satellite cells was used to obtain an average *BDNF* mRNA signal per micron area of satellite cell. At day 3 post-SNI, male and female SNI animals had elevated *BDNF* mRNA in satellite cells as compared to their sham counterparts (male SNI vs sham, $p<0.01$, female SNI vs sham, $p<0.05$, Two-way ANOVA with Tukey's HSD, figure 1.3 c). At day 28 post-SNI, female sham operated animals had higher amount of BDNF mRNA in satellite cells compared to sham operated males ($p<0.05$) or SNI operated females ($p<0.01$) Two-way ANOVA with Tukey's HSD, figure 1.3 i). Overall, the BDNF signal at 28day timepoint seems lower than other timepoints, which could be an artifact of the immunohistochemical processing and variability associated with the tissue freezing, sectioning and staining procedures.

TrkB mRNA expression in satellite cells of DRG

The percentage of *TrkB* mRNA expressing and *TrkB* negative satellite cells are not vastly different at any of the timepoints. The proportion of *TrkB* mRNA in DRGs that is localized to satellite cells did not indicate any differences between experimental groups

at any timepoint post-SNI (figure 1.4 b, e, h). The average normalized *TrkB* signal (calculated by dividing total area of *TrkB* mRNA in satellite cells by total area of satellite cells in microns) was not different across groups at day 3 or 7 post-SNI (figure 1.4 c, f), however, at day 28 post-SNI, nerve injured female mice had lower *TrkB* mRNA signal in satellite cells of DRG as compared to that in sham-operated females ($p<0.05$, Two-way ANOVA with Tukey's HSD, figure 1.4 i).

Quantification in Spinal Dorsal Horn

BDNF mRNA in DH of spinal cord

Representative confocal images of the DH ipsilateral to nerve injury shows DAPI stained nuclei (figure 1.5 a1, b1), *BDNF* mRNA (figure 1.5 b2) or negative control probe (figure 1.5 a2), merged image was used to determine the degree of overlap between *BDNF* mRNA and nuclei (figure 1.5 a3, b3). Quantification of the total area of *BDNF* mRNA in DH (white outlined area) was split into two components, namely *BDNF* mRNA located in nuclei (DAPI stained profiles) and extra-nuclear mRNA (total area of *BDNF* – area of nuclear *BDNF*). At day 3 post-SNI, SNI females had greater area of BDNF mRNA in extra-nuclear portion compared to male SNI animals ($p<0.05$, Two-way ANOVA with Tukey's HSD, figure 1.5 c). No other differences were detected at the other two timepoints (figure 1.5 d, e).

TrkB mRNA in DH of spinal cord

Representative images collected using a confocal microscope show DAPI stained nuclei (figure 1.6 a1, b1), *TrkB* mRNA (figure 1.6 b2) or negative control probe (figure 1.6 a2), and merged images show *TrkB* mRNA overlap with nuclei (figure 1.6 a3, b3). The only differences observed in *TrkB* mRNA in spinal DH was at the transitionary phase

at day 7 post-SNI. At day 7 post-SNI, total area occupied by *TrkB* mRNA was lower in male SNI animals as compared to sham operated males ($p<0.01$) and injured females ($p<0.05$, Two-way ANOVA with Tukey's HSD, figure 1.6 d). SNI males had lower *TrkB* mRNA in extra-nuclear cellular portions ($p<0.01$, Two-Way ANOVA with Tukey's HSD, figure 1.6 d). The *TrkB* mRNA area restricted to nuclear profiles indicated higher *TrkB* mRNA in SNI operated males as compared to sham operated males ($p<0.01$), and higher nuclear *TrkB* mRNA in female SNI as compared to male SNI ($p<0.05$, Two-way ANOVA with Tukey's HSD, figure 1.6 d).

TrkB protein levels in spinal dorsal horn

Relevant portions of the western blot membrane images are included along with the beta-actin control bands for each pair of comparisons. The fl-TrkB band appears approximately at 140-150 kDa as indicated by the protein ladder, while the truncated TrkB band appears around approximately at 95-100 kDa molecular weight. Samples from male and female animals are marked by colored arrows, and the quantification of the signal (normalized to actin) is included below the images of the membranes. At each timepoint 3-, 7-, and 28-day post-SNI, three comparisons were done, namely, male SNI vs female SNI (figure 1.7 a, d, g), male SNI vs male sham (figure 1.7 b, e, h), female SNI vs female sham (figure 1.7 c, f, i). Nerve injury did not increase protein levels of fl-TrkB receptor or truncated TrkB, however at day 3 (figure 1.7 a) and day 28 (figure 1.6 g) post-SNI female SNI animals had significantly lower fl-TrkB and truncated TrkB receptor forms in DH as compared to SNI males (Two-way ANOVA with Tukey's HSD, figure 1.7 a, g).

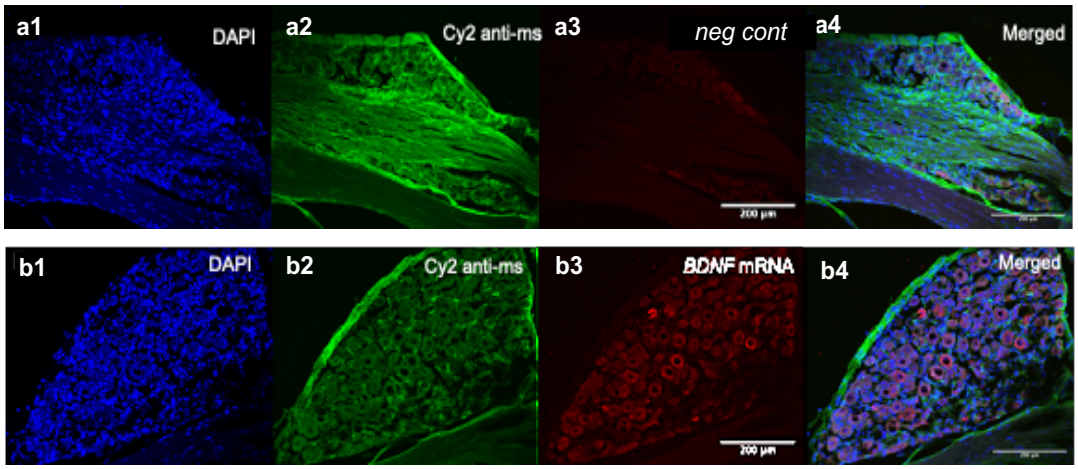

Day 3 post-SNI (c, d)

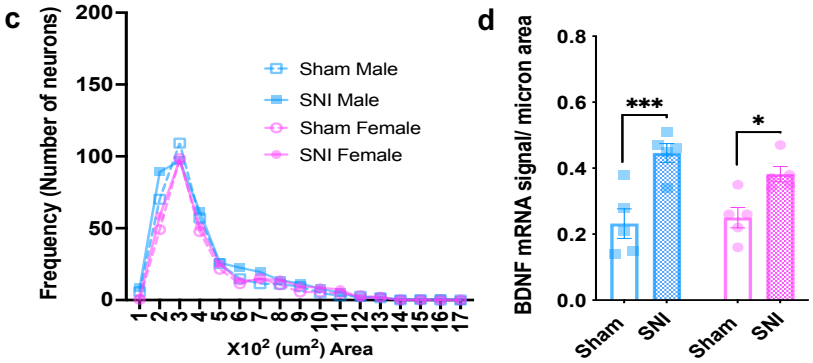

Day 7 post-SNI (e, f)

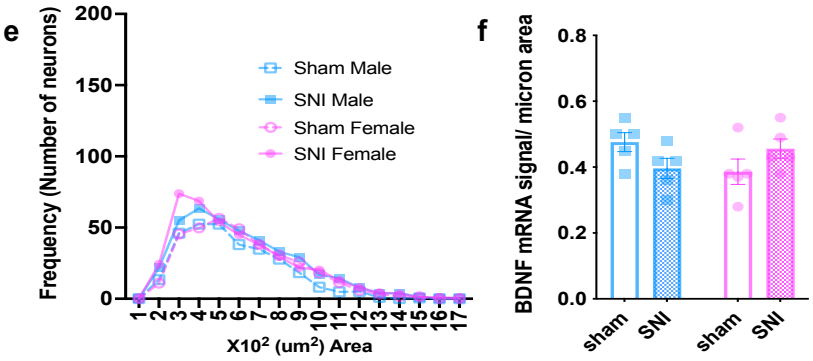

Day 28 post-SNI (g, h)

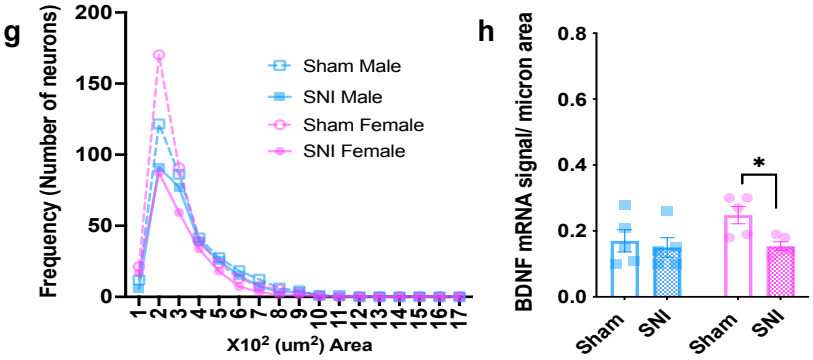

Figure 1.1: Quantification of BDNF mRNA in DRG neurons at 3 days, 7 days, and 28 days post-SNI.

Representative confocal images of L4 DRG from a male mouse 3 days post-SNI ipsilateral to the injury (Negative control: a1-4, BDNF mRNA: b1-4). DAPI staining (a1, b1), non-specific staining with Cy2 conjugated donkey anti-mouse antibody to visualize DRG cell outlines (a2, b2), BDNF mRNA (b3) or control probe fluorescence (a3) Scale bar = 200um, 20X objective. Frequency distribution of neurons by size was consistent across experimental groups at the three timepoints tested (c, e, g). BDNF mRNA signal was obtained by normalizing total BDNF mRNA area for the unequal total neuronal surface area (d, f, h). At day 3 post-SNI, male and female nerve injured animals had significantly higher amount of BDNF mRNA in DRG neurons as compared to their sham counterparts (d, Two-Way ANOVA with Tukey's HSD). Nerve injured females has significantly less BDNF mRNA in DRG neurons as compared to sham operated females at the 28-day post-SNI timepoint (h, Two-Way ANOVA with Tukey's HSD). N=5 mice per group, $p<0.05$*, $p<0.01$**.

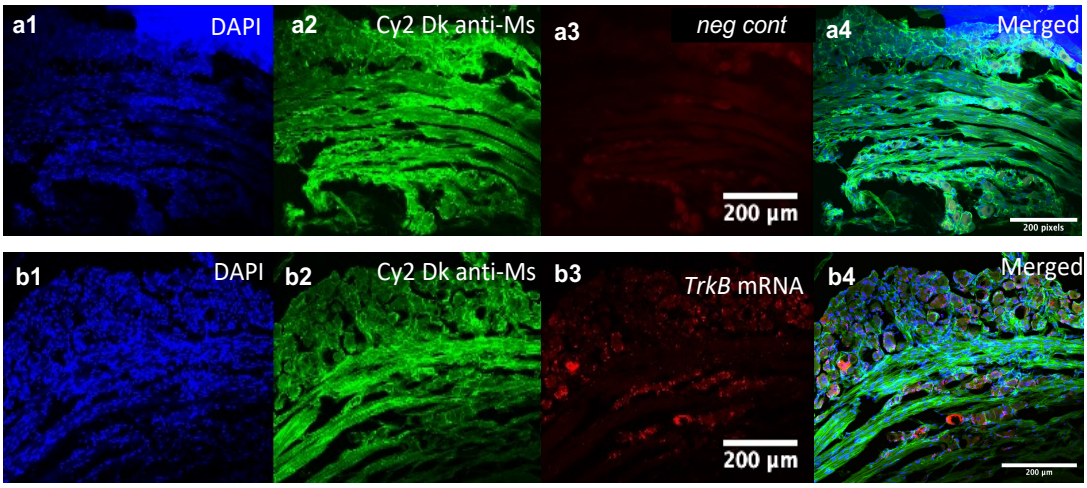

Day 3 post-SNI (c, d)

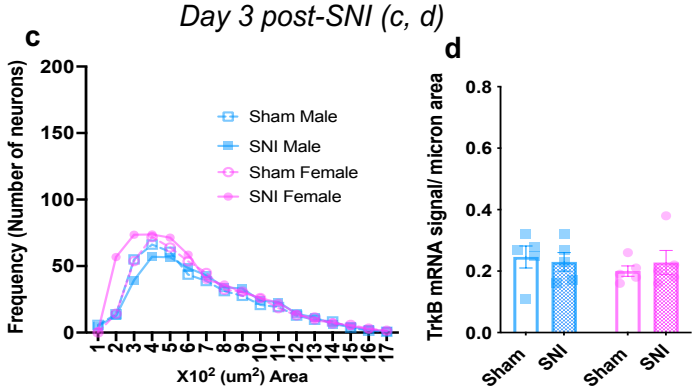

Day 7 post-SNI (e, f)

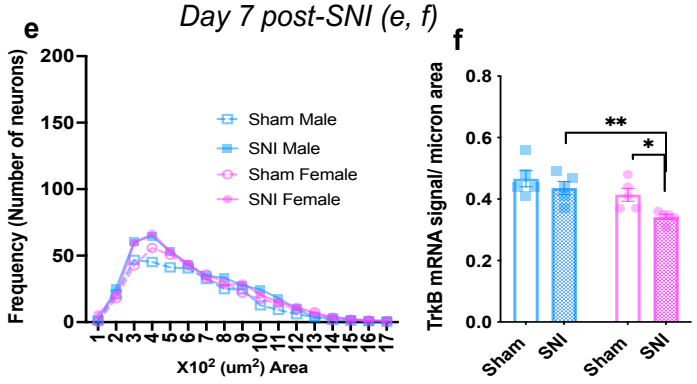

Day 28 post-SNI (g, h)

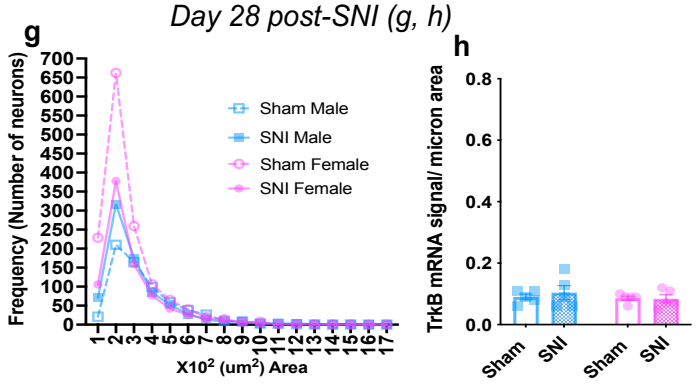

Figure 1.2: Quantification of TrkB mRNA in DRG neurons at 3 days, 7 days, and 28 days post-SNI. Representative images collected from SNI male 28 days post-SNI. DAPI (a1, b1), non-specific staining with Cy2 conjugated donkey anti-mouse antibody (a2, b2), *TrkB* mRNA (b3) or neg control probe (a3), and merged images (a4, b4). Scale bar = 200um. 25X objective. Frequency distribution of neurons by size was consistent across experimental groups at the three timepoints tested (c, e, g). *TrkB* mRNA signal was obtained by normalizing total *TrkB* mRNA area for the unequal total neuronal surface area (d, f, g). At day 7 post-SNI timepoint, injured males and sham operated females had significantly higher *TrkB* mRNA in DRG neurons compared to nerve injured females (d, Two-Way ANOVA with Tukey's HSD). N=5 mice per group, $p<0.05$*, $p<0.01$**.

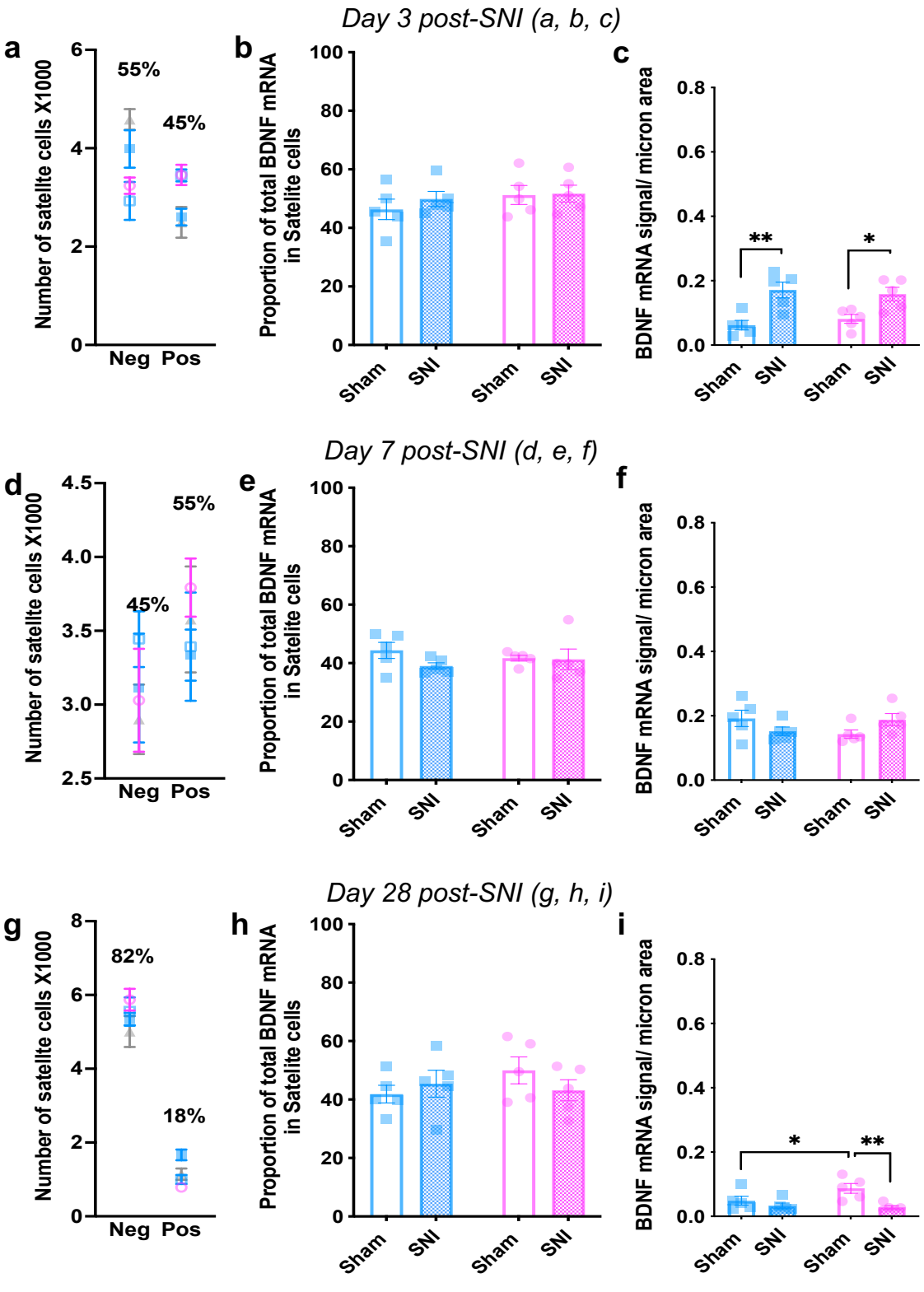
Day 3 post-SNI (a, b, c)
a
Number of satellte cells X1000
55%
45%
Neg Pos
b
Proportion of total BDNF mRNA in Satelite cells
Sham SNI Sham SNI
c
BDNF mRNA signal/ micron area
**
*
Sham SNI Sham SNI
Day 7 post-SNI (d, e, f)
d
Number of satellte cells X1000
55%
45%
Neg Pos
e
Proportion of total BDNF mRNA in Satelite cells
Sham SNI Sham SNI
f
BDNF mRNA signal/ micron area
Sham SNI Sham SNI
Day 28 post-SNI (g, h, i)
g
Number of satellte cells X1000
82%
18%
Neg Pos
h
Proportion of total BDNF mRNA in Satelite cells
Sham SNI Sham SNI
i
BDNF mRNA signal/ micron area
*
**
Sham SNI Sham SNI

Figure 1.3: Quantification of BDNF mRNA in DRG satellite cells. The number of *BDNF* mRNA positive satellite cells and those not expressing *BDNF* mRNA at days 3(a), 7(d), and 28(g) post-SNI reveals that at day 28 timepoint, fewer satellite cells express *BDNF* mRNA as compared to the other timepoints (a, d, g). The proportion of total *BDNF* mRNA that is expressed in satellite cells was not different between any of the groups at any timepoint (b, e, h). The *BDNF* mRNA signal was also measured as average signal density per micron (um^2) area of satellite cells (c, f, i). Interestingly, at day3 post-SNI, Male and female injured animals had significantly higher *BDNF* mRNA signal in satellite cells as compared to their sham counterparts (c, Two-Way ANOVA with Tukey's HSD). Additionally, at day28 post-SNI, injured females had significantly lower *BDNF* mRNA in satellite cells as compared to sham operated females, and sham females had higher *BDNF* mRNA compared to sham operated males (i, Two-way ANOVA with Tukey's HSD). At each timepoint, each group included 5 animals. $p<0.05$*, $p<0.01$*

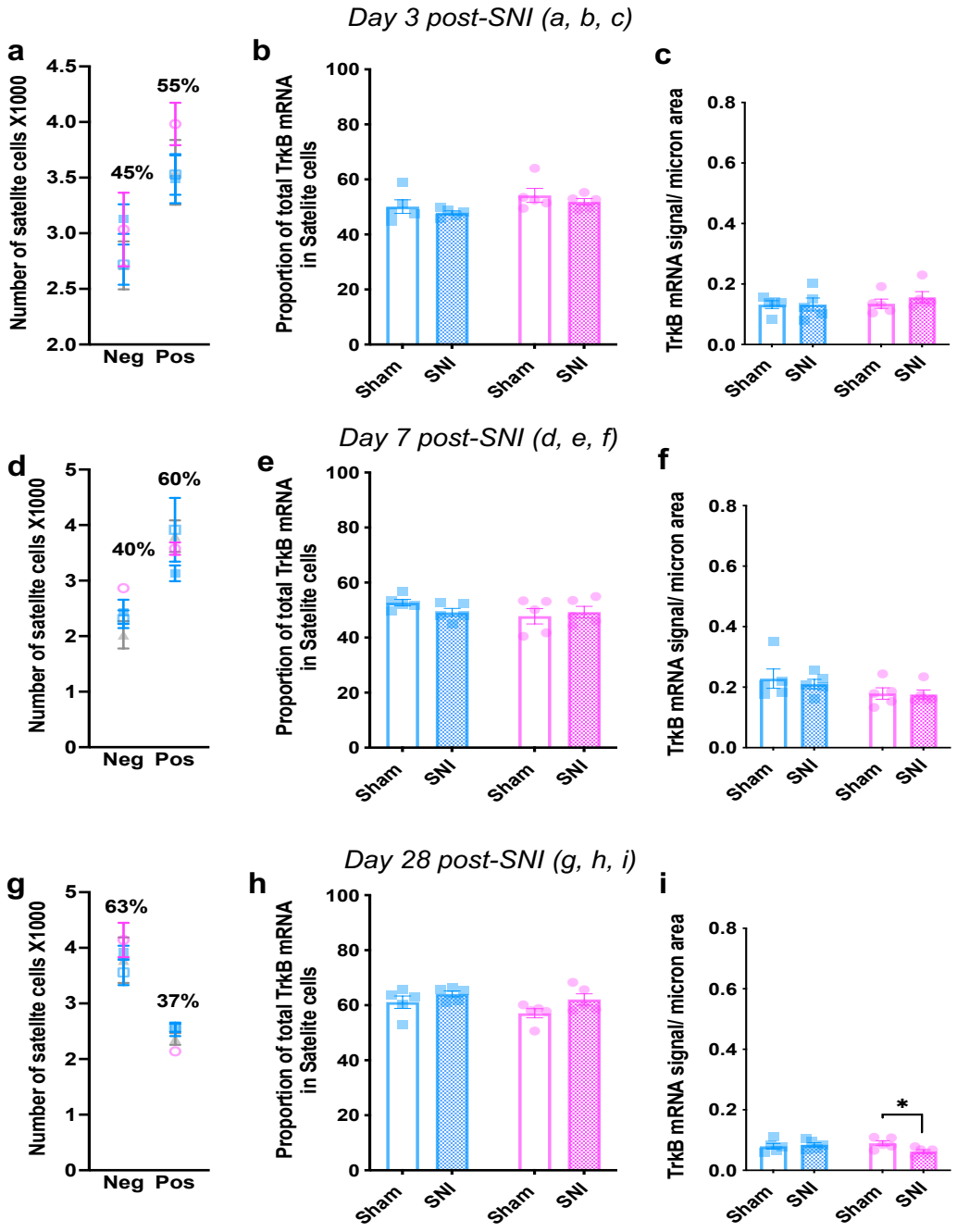

Figure 1.4: Quantification of TrkB mRNA in satellite cells of DRG at days 3 (a, b, c), 7 (d, e, f) and 28 (g, h, i) post-SNI. The proportion of *TrkB* mRNA expressing satellite cells was higher at days 3, and 7 but not at day 28 post-SNI (a, d, g). Across all experimental groups and timepoints, proportion of TrkB mRNA signal was not different between any groups (b, e, h). However, at day 28 post-SNI, nerve injured females had significantly lower TrkB expression density in satellite cells compared to sham operated females (i, Two-Way ANOVA, Tukey's HSD). N=5 per group all timepoints. $p<0.05$*. N=5 animals per group per timepoint.

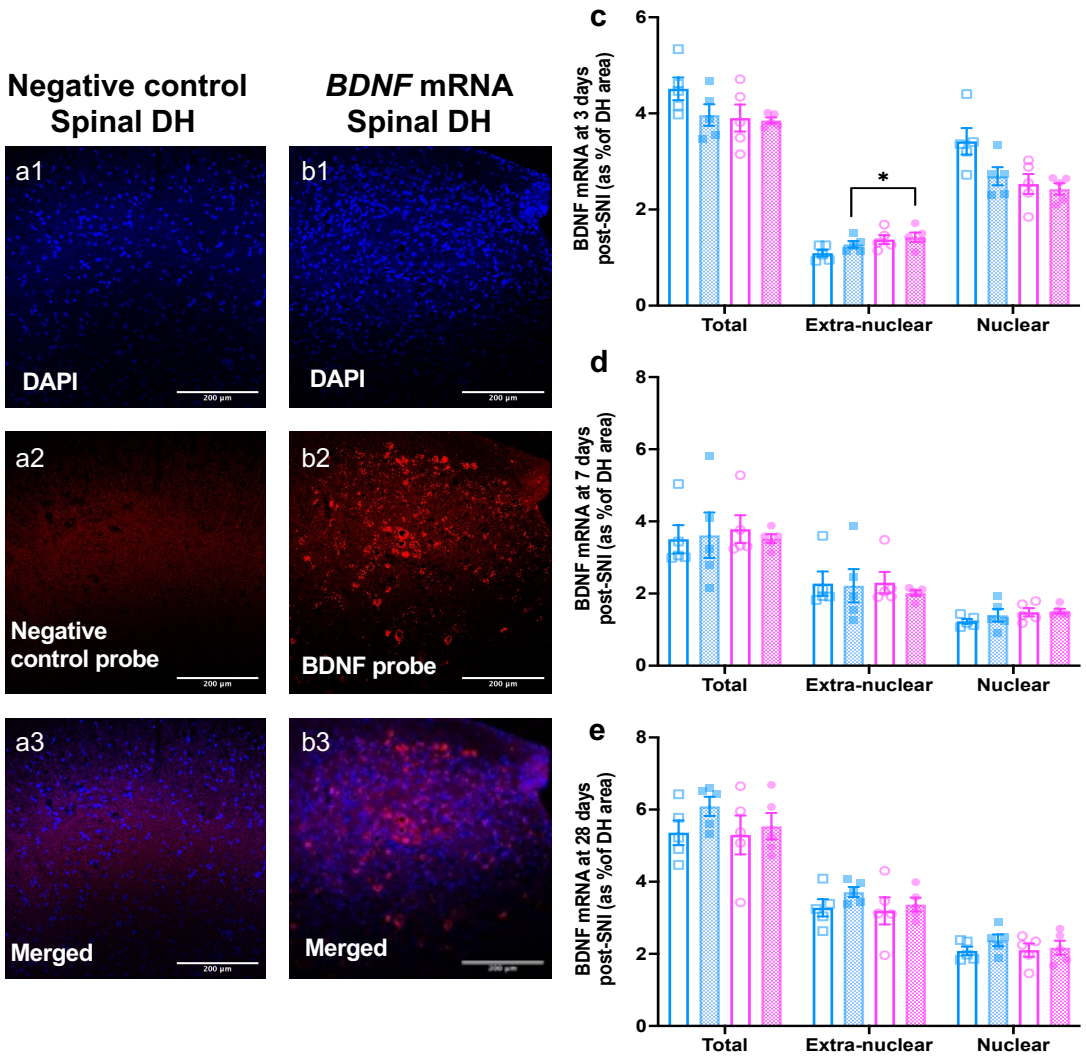

Figure 1.5: Quantification of BDNF mRNA in dorsal horn of spinal cord at days 3 (c), 7 (d) and 28 (e) post-SNI. Representative images visualizing *BDNF* mRNA (b2) and negative control probe (a2) in DAPI stained nuclei (a1, b1) and extranuclear portion in dorsal horn (DH) spinal sections collected from SNI males at day 28 post-SNI (a, b). Scale bar = 200um, 20X objective. The total, extranuclear and nuclear portion of *BDNF* mRNA in DH ipsilateral to nerve injury or sham surgery at day 3 (c), day 7 (d), day 28 (e). At day 3 post-SNI, female SNI animals have higher extra-nuclear *BDNF* mRNA (c, Two-Way ANOVA with Tukey's HSD). 5 animals/group per timepoint. $p<0.05$*.

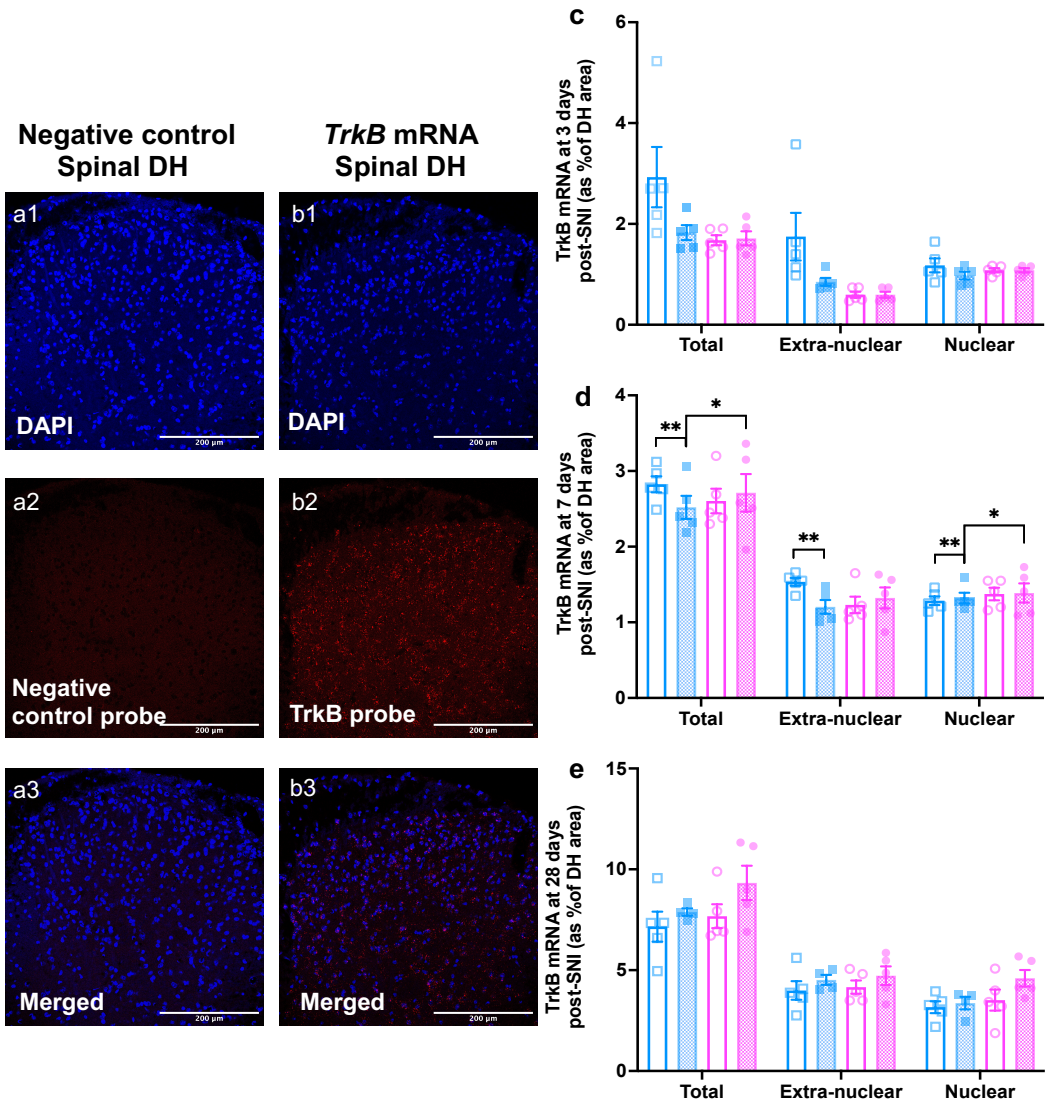

Figure 1.6: Quantification of TrkB mRNA in dorsal horn of spinal cord ipsilateral to nerve injury at days 3(c), 7(d) and 28(e) post-SNI. Representative images collected from male SNI animals at day 3 post-SNI were used to visualize *TrkB* mRNA in DH (b2) and negative control probe (a2) and quantify mRNA signal in DAPI stained nuclei (a1, b1). Scale bar = 200um, 20X objective. The total amount of *TrkB* mRNA, the mRNA in nuclear and extra-nuclear portion of DH cells was quantified 3 days (c), 7 days (d) and 28days post-SNI (e). At day 7 post-SNI timepoint, male SNI animals had lower total and extranuclear *TrkB* mRNA compared to sham operated males (Two-way ANOVA with Tukey's HSD, d). The total amount and nuclear proportion of *TrkB* mRNA was higher in SNI females compared to SNI males on day 7 post-SNI (Two-way ANOVA with Tukey's HSD). Interestingly, SNI males had higher nuclear *TrkB* mRNA compared to sham males at day 7 post-SNI (d, Two-way ANOVA with Tukey's HSD). N=5 animals per group for each timepoint $p<0.05$*, $p<0.01$**

Day 3 post-SNI (a, b, c)

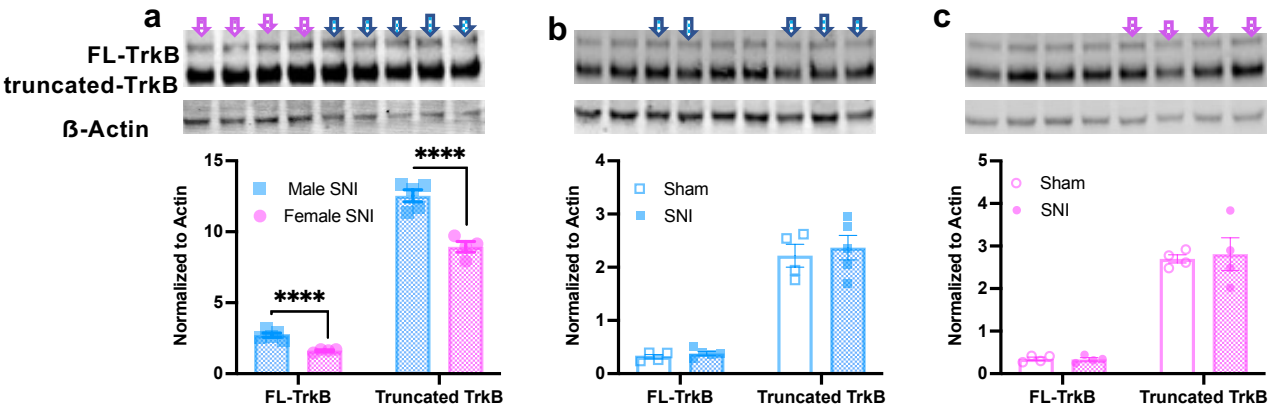

Day 7 post-SNI (d, e, f)

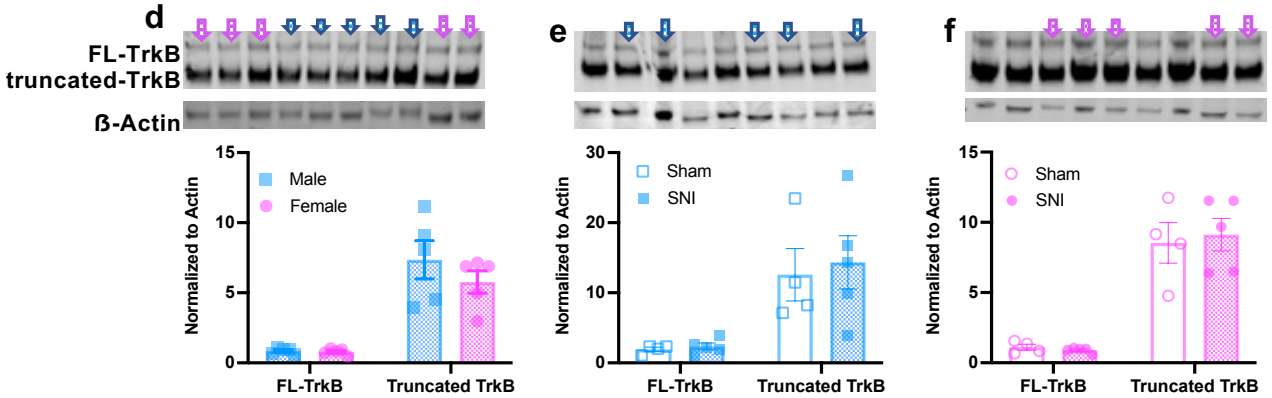

Day 28 post-SNI (g, h, i)

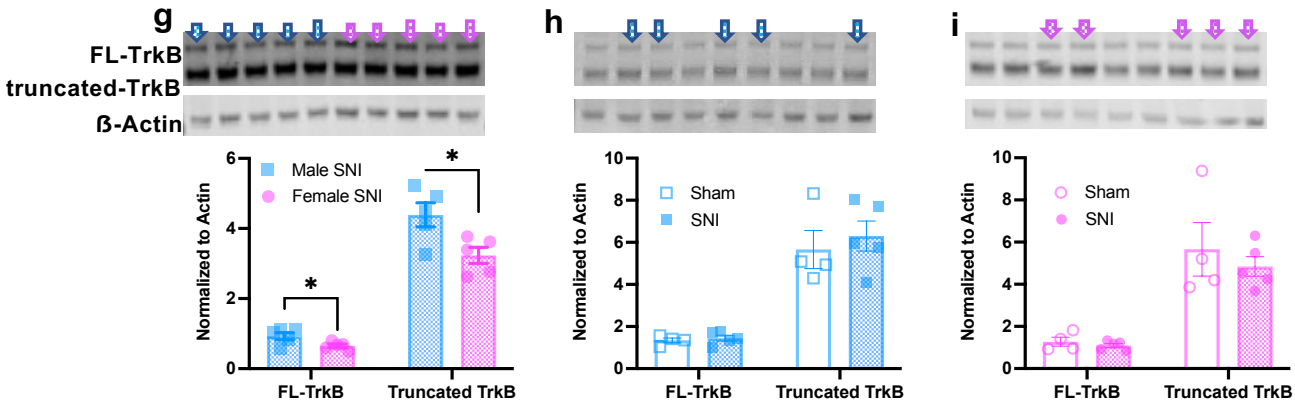

Figure 1.7: Western Blot analysis quantifying full-length TrkB receptor (fl-TrkB) and truncated form of TrkB in the dorsal horn of spinal cord at 3, 7, and 28 days post-SNI. Fl-TrkB is about 150kD, while the truncated form is more abundant and weighs about 100kD. Relevant portion of the western blots along with the beta-actin control lanes are marked with arrows indicating the male or female SNI animals (a, d, g). These data are quantified and visualized in the figures below the western blot images. At the 3-day and 28-day post-SNI timepoint there is a significantly higher amount of fl-TrkB and truncated TrkB in male injured animals as compared to injured females (a, g), whereas no sex differences were observed at the 7-day post-SNI timepoint. Interestingly, no differences were observed in the TrkB protein expression between injured and uninjured counterparts at any of the timepoints tested. Paired Student's t-test. $p<0.05$*, $p<0.0001$. N=5 for all groups, except day 3 female SNI group (n=4).

DISCUSSION

mRNA detection in DRG and spinal cord

Despite tremendous focus and interest in the role of BDNF-TrkB signaling in spinal neuroplasticity associated with nerve injury, very little is known regarding the changes in expression of *BDNF* and even smaller subset of the literature focuses on visualizing and quantifying TrkB. Early reports used *in situ* hybridization to demonstrate presence of *BDNF* mRNA in sensory neurons and antibodies that are either no longer available or unvalidated to detect BDNF immunoreactivity (-ir) to measure BDNF changes following nerve injuries (Michael et al., 1999; Fukuoka et al., 2001; Ha et al., 2001; Obata et al., 2003; Geng et al., 2010; Terada et al., 2018). In our dataset, we observed a greater number of *BDNF* and *TrkB* positive neurons compared to prior reports. This could be explained by our use of RNAscope® technology which is highly sensitive and can detect a single mRNA strand. Therefore, it is possible that many neurons express low levels of *BDNF* or *TrkB* mRNA, but it does not participate in BDNF or TrkB protein synthesis or meaningfully contribute to BDNF-TrkB signaling.

BDNF mRNA in DRG neurons and satellite cells

Previous reports of *BDNF* mRNA in DRG neurons demonstrate higher *BDNF* mRNA levels in DRG neurons for up to 4 weeks after nerve axotomy, and even report a rightward shift in the neuronal distribution such that the frequency of larger neurons increased starting 4 days after axotomy (Michael et al., 1999). Another report of *BDNF* mRNA in DRG cells following chronic constriction injury (CCI) in rats show more

modest increase in *BDNF* mRNA at 14 days after injury (the only timepoint investigated) and did not report any shifts in *BDNF* expressing neuronal distribution (Obata et al., 2003) Yet another report measuring *BDNF* mRNA in rat DRG after spinal nerve ligation model of nerve injury, reported an increase in *BDNF* mRNA as early as day 4 after injury that remained elevated up to 4 weeks when the study ended (Fukuoka et al., 2001) These studies collectively indicate injury-, time-, and region-specific changes in *BDNF* mRNA, however, none of these studies measure changes at the DRG and spinal level or investigate its presence in different cell types or sexes.

Data presented in this chapter indicates SNI induced increase in *BDNF* mRNA in DRG neurons at day 3 post-SNI timepoint in males and females (figure 1.1d). Distribution of *BDNF* expressing neurons resembles that of general neuronal distribution included in figure 1.1 (c, e, g) since over 90% of DRG neurons express *BDNF* mRNA. The distributions across experimental groups were not different and no rightward shift was observed in our data set. The mismatch between results in this chapter and previous reports can be explained by the difference in nerve injury model and a more sensitive mRNA detection method. However, when *BDNF* mRNA area is normalized to the neuronal area, we observed an injury induced increase suggesting an overall increase in *BDNF* mRNA after injury. Interestingly, our experiments did not show significant elevation in *BDNF* mRNA in DRG neurons at days 7 or day 28 post-SNI, but nerve injured females had lower *BDNF* mRNA in DRG neurons as compared to sham operated females at day 28. These results indicate a sex-, time-, and injury-dependent effects on *BDNF* mRNA expression. Therefore, during early stages of nerve injury, male and

female systems respond similarly by increasing *BDNF* expression in DRG neurons (figure 1.1 d), whereas during the chronic pain stage at day 28 post-SNI, nerve injured females downregulate *BDNF* expression compared to sham females (figure 1.1 h) suggesting a compensatory decrease in females after injury.

BDNF mRNA in satellite cells

Although the role of satellite cells in modulating DRG neuron activity has been appreciated, its participation in *BDNF*-TrkB signaling in DRG is unclear. Satellite glial cells closely associate with DRG neurons and engage in increased signaling to maintain neuronal excitability (Ji et al., 2013; Milosavljević et al., 2020). Satellite cells are known to release ATP, inflammatory factors, cytokines, and chemokines that can maintain an inflammatory state at the DRG level thus contributing to the maintenance of the neuropathic pain state (Scholz and Woolf, 2007; Ji et al., 2013; Milosavljević et al., 2020). Since not much is known about *BDNF* and *TrkB* expression in satellite cells, we evaluated the proportion of satellite cells that express *BDNF* mRNA, and at day 3 and 7 post-SNI, about half of all satellite cells expressed *BDNF*. At day 28, the overall signal was lower and therefore the proportion of *BDNF* positive satellite cells was also lower. The increased *BDNF* mRNA in injured males and females at day 3 post-SNI compared to shams match those seen in DRG neurons, indicating that similar kinds of changes due to injury occur in DRG neurons and satellite cells. Furthermore, the *BDNF* mRNA signal pattern at day 28 post-SNI is like that seen in neurons, such that female SNI animals had lower *BDNF* mRNA compared to sham females (figure 1.3 i). Interestingly, female sham

group had higher *BDNF* mRNA expression compared to sham males which points to sex- and time-dependent reversal of *BDNF* mRNA expression.

TrkB mRNA expression in DRG neurons and satellite cells

The limited information about *TrkB* expression in DRG usually extends to demonstrating *TrkB* expression in DRG neurons (Foster et al., 1994; Yan et al., 1997). Here, we characterized the *TrkB* expression pattern in DRG neurons. We found that during the transitionary period from acute to chronic pain state, *TrkB* expression in injured females was lower than males which may either indicate the lack of *TrkB* involvement in this transition, or a compensatory decrease to reach homeostasis.

The proportion of *TrkB* positive to *TrkB* negative satellite cells, or the proportion of total *TrkB* mRNA localized to satellite cells was not affected by injury or sex-dependent variables. The only difference detected was at day 28 post-SNI where injured females had lower *TrkB* expression compared to sham, which matches the pattern of *BDNF* mRNA expression. This may indicate that *TrkB* is not a major player in maintaining neuropathic pain state in females or it might suggest that once chronic pain state is established, most signaling factors are downregulated.

BDNF and TrkB expression in spinal cord

BDNF expression in spinal dorsal horn ipsilateral to the nerve injury is not significantly different between experimental groups. Interestingly, about half of the total *BDNF* mRNA signal was located outside of nuclear profiles. Typical quantification methods limit mRNA quantification to nuclear region, however, by doing so a significant portion

of mRNA signal is missed. At day 3 post-SNI, female SNI mice had higher *BDNF* mRNA in extra-nuclear portion compared to male injured animals. The significance or difference between the role of mRNA in nuclear profiles vs cytoplasm is unclear. Unlike *BDNF* expression in DH, sex- and injury- dependent effects on *TrkB* mRNA are detected at day 7 post-SNI, wherein injured males had lower *TrkB* expression compared to sham operated males and injured females. Similar effects were noticeable in the extra-nuclear and nuclear portions. These data largely match those seen in DRG cells in that *TrkB* expression seems to change at the day 7 timepoint. It may mean that TrkB receptor activity is crucial for the transitioning of acute to chronic pain. Collectively, these results suggest that injury induced changes in BDNF and TrkB expression is altered in regions initially affected by peripheral nerve injury.

TrkB protein expression in spinal cord

Immunohistochemistry for TrkB protein has proven difficult due to the absence of validated and reliable antibodies, however, most experiments that involve measuring fl-TrkB or truncated TrkB use western blot assays (Yajima et al., 2002; Geng et al., 2010). Unlike these reports, we did not find injury induced increase in fl-TrkB or truncated TrkB protein levels in DH in males or females. It is possible that the amount of detectable of fl-TrkB is low which may mask any subtle effects between groups. Interestingly, at early and late timepoint after nerve injury, injured male mice had higher fl-TrkB and truncated TrkB protein levels in DH as compared to that of injured females (figure 1.7 a,d). This suggests an underlying sex-difference such that the expression of TrkB protein levels is

lower in females at baseline or injury induced increase in females is lower than that seen in males.

Collectively these data point to sex-, region-, and times-dependent changes in BDNF and TrkB mRNA and protein levels in areas of the pathway that are initially affected by nerve injury. We noticed an increase in BDNF expression in DRG neurons and satellite cells at day 3 post-SNI, and a decreased BDNF expression by 28days post-SNI, however, TrkB expression is only reduced in injured females at day 7 when the pain state transitions from acute to chronic. In contrast to the TrkB mRNA expression in DRG, nerve injured females have increased TrkB expression in SC as compared to injured males. The exact role of these receptors expressed in different components of the pain pathway in a sex-, time- and region-specific manner will greatly advance our knowledge about the differences and commonalities in BDNF-TrkB signaling in different models of pain and the two sexes.

CHAPTER 2: FUNCTIONAL ROLE OF TRKB ACTIVATON IN SNI INDUCED HYPERSENSITIVITY

INTRODUCTION

BDNF signaling contributes to spinal neuroplasticity underlying central sensitization (Pezet et al., 2002; Marcol et al., 2007; Merighi et al., 2008; Smith, 2014). Many signaling cascades are involved in this process which collectively modifies the spinal nociceptive circuitry to amplify noxious and innocuous stimuli evoked sensory perception (Bramham and Messaoudi, 2005; Coull et al., 2005; Geng et al., 2010; Zhang et al., 2011a; Zhou et al., 2011; Chen et al., 2014b; Khan and Smith, 2015; Hildebrand et al., 2016; Kitayama et al., 2016; Li et al., 2017; Wang et al., 2019). These changes due to BDNF are thought to occur via activation of TrkB receptor which is the high affinity receptor for BDNF. The *NTRK2* gene encodes for three distinct forms of the TrkB receptor (Middlemas et al., 1991; Minichiello, 2009). The full-length receptor (fl-TrkB) often referred to as $gp145^{TrkB}$ consists of 821 amino acid sequence and has an intracellular kinase domain that autocatalyzes upon ligand binding (Middlemas et al., 1991; Minichiello, 2009). The two alternatively splices truncated forms - T1 (often referred to as $gp45^{TrkB}$) and the less well-known and uncharacterized T2 share the transmembrane and extra-cellular sequence with fl-TrkB, however the T1 and T2 forms have 11 and 9, respectively, unique intracellular amino acid sequences and lack

intracellular kinase domains and this cannot engage in canonical downstream signaling cascades.

Since intracellular signaling from BDNF is thought to be carried out because of fl-TrkB phosphorylation (pTrkB), the truncated forms were thought to lack the ability to induce intracellular signaling. Some believed the truncated TrkB receptors hinder TrkB activity by sequestering BDNF thus inhibiting or lowering fl-TrkB activation and the subsequent downstream signaling (Middlemas et al., 1991; Squinto et al., 1991; Barbacid, 1994; Lu et al., 2005; Reichardt, 2006; Mitre et al., 2016). More recent evidence indicates that T1 TrkB can induce intracellular calcium signaling in astrocytes via an unknown mechanism (Cao et al., 2020). And the consequences of those downstream signaling cascades in contrast to the signaling initiated by fl-TrkB activity is undetermined.

Major roadblock in investigating the extent and anatomical specificity of TrkB activity is the lack of methods to visualize or measure TrkB activity while preserving anatomical information. Usually, TrkB activation is indirectly measured by evaluating processes and markers downstream of TrkB phosphorylation (Yajima et al., 2002; Coull et al., 2005; Geng et al., 2010; Zhou et al., 2011; Chen et al., 2014b; Hildebrand et al., 2016; Li et al., 2017; Wang et al., 2019). These types of analyses can be used to assess the overall consequences of TrkB signaling at large, however, they do not provide information regarding the spatial extent of context dependent TrkB activity. Furthermore, activity of downstream factors is often used to construe the effect of TrkB activation of signaling factors or substrates in the same cell or region, however such information is

obtained indirectly and does not provide the necessary context for TrkB activity in injury induced neuroplasticity (Geng et al., 2010; Hildebrand et al., 2016; Li et al., 2017).

Inhibition of TrkB activation is another avenue of investigation to study the causal role of TrkB in BDNF-TrkB signaling mediated changes. However, this goal too is hindered by the lack of specific tools to block TrkB activity. For instance, the drug previously widely used as a TrkB inhibitor, K252a, later was found to block most Trk receptors along with intracellular kinases including PKC (Buchholz et al., 2018; León et al., 2020). Other methods like BDNF sequestration or deletion of cell types assumed to release BDNF (Mannion et al., 1999; Raghavendra et al., 2003; Ledeboer et al., 2005; Xiaodi et al., 2010; Zhang et al., 2011b, 2011a; Zhou et al., 2011; Li et al., 2017) following increased neuronal activity are also commonly used and pose a problem regarding the specificity of these tools to alter TrkB activity.

The issues in data interpretation stemming from indirect results is compounded by the lack of information in related domains, for instance, sex differences in BDNF-TrkB signaling have been broadly advertised and accepted. However, the experiments that gave rise to these speculations primarily targeted microglial function and manipulated microglial activity without confirming the mechanistic consequences of those manipulations (Zhou et al., 2011; Sorge et al., 2015). As a result, the behavioral sex-differences that were observed were prematurely attributed to differences in BDNF-TrkB signaling. Another study generated a pharmacogenetic mutant line in which the endogenous TrkB receptor is replaced with a modified TrkB receptor which can be

manipulated using a drug specifically designed for these receptors (Wang et al., 2009). In this study male and female mice were tested but the results did not specify sample sizes or any observed sex-differences. It is unclear if they did not detect any sex-differences or if they did not look for them. Since majority of the studies in this field only used male subjects, the dearth of information regarding the expression and function of BDNF, TrkB, and downstream factors in females sparked interest in sex-differences in the BDNF-TrkB signaling pathway. Experiments in this chapter were designed to evaluate if TrkB activation is absent in SNI operated female mice or whether TrkB is functionally required for the maintenance of behavioral hypersensitivity.

Given these challenges in studying the degree and spatial limits of TrkB activation due to peripheral nerve injury, we validated an antibody directed against the phosphorylated form of TrkB (pTrkB) and quantified changes in TrkB activity at various timepoints after injury to assess sex-differences in injury-induced TrkB activation. Next, we employed a novel small molecule TrkB inhibiting drug, ANA-12, that was initially characterized in hippocampal learning and memory paradigm (Cazorla et al., 2011). Using this TrkB antagonist, we conducted experiments to test whether ANA-12 has time- and sex-dependent effects on behavioral hypersensitivity. Finally, additional control studies were performed to evaluate and understand behavioral and biological side-effects arising from the vehicle used in behavioral experiments.

MATERIALS AND METHODS

Animals

All experiments were conducted in compliance with National Institutes of Health Guide for Care and Use of Laboratory Animals and approved by the University of Minnesota Institutional Animal Care and Use Committee. Male and female ICR-CD1 WT mice (20-40 g) were used for all the following experiments. Animals were group house 4 males per cage, and 5 females per cage in a temperate and humidity-controlled SPF facility on a 12-hour light/dark cycle. The animals had free access to food and water.

Spared Nerve Injury (SNI)

This procedure is described in more detail in Chapter 2. Briefly, while under deep anesthesia, the thigh muscle on the left side was exposed and bluntly dissected to visualize the sural nerve. Two of the branches, tibial and common peroneal, were ligated with 5.0 silk suture and about 2mm portion of the nerve was cut and removed to prevent nerve regeneration. Muscle was closed with 4-0 monofilament absorbable suture and the overlaying skin was stapled. Animals were monitored for 3 days post-operatively.

Behavioral hypersensitivity assay

A detailed description of the Von Frey assay is described in methods section of Chapter 2 as well as in (Chaplan et al., 1994) and (Dixon, 2012). A 50% threshold calculation is used to determine withdrawal thresholds by applying a series of synthetic monofilaments to the lateral portion of the mouse hand paw. For all groups, male and female animals were tested separately to avoid any confounds due to pheromonal effects.

Males and females were either tested on different days or the room was thoroughly cleaned if the two were tested on the same day in separate sessions.

Tissue preparation and sections

Following behavioral assessment, mice were deeply anesthetized with isoflurane and perfused via the heart with calcium-free Tyrode's solution (in mM: 116 NaCl, 5.4 KCl, 1.6 MgCl2·6H20, 0.4 MgSO4·7H2O, 1.4 NaH2PO4, 5.6 glucose, and 26 Na2HCO3) followed by fixative (4% paraformaldehyde and 0.2% picric acid in 0.1 M phosphate buffer, pH 6.9). The spinal cord or brains (for hippocampal sections) were removed, cryoprotected in 10% sucrose overnight, covered with OCT and frozen using liquid CO_2, and cryostat-sectioned into 14 μm sections that were slide-mounted. Sections were preabsorbed in T/T/T buffer (TBS containing 0.2% Triton-X 100 and 0.2% Tween 20) for 30 min followed by incubation with a rabbit anti-pTrkB (Y816) 1:500 (Millipore Sigma-Aldrich ABN1381) diluted in T/T/T overnight at 4°C in a humidified chamber. Tissue sections were then washed 3X 10 mins each in TBS, incubated with a secondary antibody solution containing Cy3 Donkey anti-Rabbit 1:300 (Jackson Labs) in T/T/T for 1hr at room temperature. Slides were then washed in TBS 3X10 mins each and cover slipped with FluorSave™ (Millipore 345789). Sections were allowed to dry and stored at room temperature until being imaged.

Phosphatase Treatment

Slide mounted tissue sections (mentioned above) were treated with Lambda Protein Phosphatase (LPP) (BioLabs P0753S). A NEB buffer solution was prepared by

adding 1ml of 10XNEB and 1ml of $MnCl_2$ to 10mls of dH_2O and aliquoted and stored at -80° C. Each tissue section was treated 100ul/slide with LPP containing or LPP lacking NEB

buffer. To prepare the LPP solution, 20ul of LPP stock was added to 350ul of NEB buffer, while for control slides were treated with NEB buffer alone. Tissue sections were circled with hydrophobic pen and treated with either LPP solution or NEB solution overnight at 37° C in a humidified chamber for 8 hours. Sections were washed with TBS 3X10 mins each and IHC protocol for pTrkB staining was conducted as described above.

Western Blot Analysis

SNI male and female mouse spinal cords were harvested by hydraulic extrusion 28days post-SNI. Hippocampal tissue was collected by rapidly dissecting and extracting brains from mice euthanized at day 28 post-SNI. The lumbar enlargement was isolated and divided into ipsi- and contralateral halves for tissue analysis. Tissue samples were flash frozen using liquid nitrogen and stored at -20^{O} C. Tissues were allowed to thaw on ice before being homogenized in RIPA solubilization buffer (Phosphate buffered Saline (PBS) with 0.1% IPEGAL (ICN Biomedicals), 12mM sodium deoxycholate, and 0.1%SDS) containing protease inhibitors (Complete tablet, Roche) and phosphatase inhibitor (mini tablet, ThermoFischer) using a glass bead homogenizer. The homogenate was centrifuged at 1,000 G for 5 min at 4°C and the supernatant was collected. Homogenate was centrifuged again at 16,300 G for 30 mins at 4°C and the pellet was resuspended in RIPA buffer and vortexed. A protein assay was conducted to determine

protein concentration of the samples. Samples were mixed with sample buffer (NuPage 4X sample buffer (Invitrogen, Grand Island, NY)) and heated to 95°C for 10 min. All samples were loaded onto a 4-12% gradient gel at 40ug per sample/ per lane (NuPage Novex bis-tris, Invitrogen) and run at 120 volts for 1-1.5 hrs. After removal from the cassette, the gel was incubated in transfer buffer for 30 mins at RT while shaking. Gels were transferred to PVDF membranes (Immobilin-FL, Millipore) using 90 mA current overnight at 4°C. Membranes were incubated in blocking buffer (LiCor Odyssey Blocking buffer (Invitrogen)) for 1 hr at room temperature, then incubated in primary antisera rabbit anti-pTrkB (Y816) 1:500 (Millipore Sigma-Aldrich ABN1381 for 48 hours at 4°C. After rinsing with PBS containing 0.1% Tween-20, the membranes were incubated for 1 hr in secondary antisera (IR-Dye donkey anti-rabbit 800cw, LiCor). Membranes were then incubated in primary antisera for beta-actin 1:10,000 (Mouse anti-beta actin (Cell Signaling)) for 48 hours at 4°C, followed by 1 hr incubation in secondary antisera (donkey anti-mouse 680rd, LiCor) at RT. After rinsing with PBS-Tween-20 the blot was placed in TBS until it was imaged using the LiCor Odyssey Imager. Quantification of the band signal was done using Image Studio Lite software. Results normalized to actin were averaged within group n=4 or n=5 per group.

Imaging and Quantification

A Nikon A1RMP confocal microscope (25X objective, 1.1 NA) at the University of Minnesota Imaging Center was used to obtain images of tissue sections. Imaging parameters were set using negative controls (NEB treated controls for LPP treated sections, Sham control for SNI vs sham comparisons) to set the lower parameters and the sections with highest fluorescence was used to determine the maximum exposure settings

to avoid saturation. All images in a single data set were collected on the same day at the same microscope settings. Tissue blocks for the purposes of sectioning were grouped by the duration after SNI, therefore, data from the three timepoints cannot be compared across time. Three images from evenly spaced tissue sections of L3 and L4 region of spinal cord were collected. All quantification was conducted using FIJI software by an experimenter blinded to the treatment conditions and groupings. An ROI was manually drawn to outline the dorsal horn of spinal cord, and minimum threshold was manually selected for each tissue section. The Area of pTrkB-ir (denoted as %area of pTrkB-ir) as a function of ROI size were obtained and used to compare pTrkB-ir in different groups. For all quantification in Fig 3.1-3.5, only ipsilateral dorsal horn images were collected from three evenly spaced spinal sections and averaged to get a single value per animal. The data presented in Fig 3.6 was collected from naïve animals in which we do not expect any laterality of effect. Therefore, bilateral images of dorsal horn were collected from three evenly spaced spinal sections and a single value per animal was obtained for further analysis.

TrkB inhibitor

ANA-12 is a novel small molecule drug that was previously described for its antidepressant and anxiolytic properties in a mouse model (Cazorla et al., 2011). A 10mM stock of ANA-12 with DMSO were aliquoted and frozen at -20°C. For injections, 200uM solution was prepared by diluting the 10mM ANA-12 stock into a 1:1.5 diluent of PEG300: sterile saline. Vehicle control solution was made by substituting ANA-12 stock with DMSO in 1:1.5 PEG300: sterile saline. 5ul of the 200uM solution (1nmol) of ANA-12 was injected intrathecally into each animal as described previously (Mestre et al.,

1994). ANA-12 solution for intraperitoneal injections was made by dissolving the 10mM DMSO containing stock in sterile PBS at 5mg/ml solution and animals were injected 0.5mg/kg per mouse. Vehicle for experiments in which ANA-12 was injected intraperitoneally replaces ANA-12 with DMSO.

Statistical Analysis

All datasets were assessed for normality to determine whether a parametric or non-parametric test was appropriate. Student's t test, One-Way ANOVA or Two-Way ANOVA were run using JMP Pro 15 licensed through University of Minnesota. Data are expressed as the mean ± S.E.M. and all statistical analysis was considered significant at $\alpha \leq 0.05$.

RESULTS

Validating antibody in hippocampal tissue

To determine if the pTrkB antibody detects a protein of the correct molecular weight, we performed western blot assay on hippocampal tissue collected from male and female SNI mice 28 days after surgeries and were able to visualize a band around 140kDa which likely corresponds to the phosphorylated fl-TrkB receptor (figure 2.1 a). Hippocampal tissue was used for Western blots because of the well-defined protocols for tissue processing for pTrkB visualization. Since the original report of ANA-12 inhibition of TrkB phosphorylation used Western blot assay to confirm reduction in TrkB phosphorylation in hippocampal tissue, we followed the same drug dosage (0.5mg/kg) and timeline (2 hrs post drug) to collect hippocampal tissue for histology. Representative images of pTrkB-ir in hippocampus tissue sections from vehicle (figure 2.1 b1) and ANA-12 (figure 2.1 b2) treated animals showed a significant decrease in pTrkB-ir in dentate gyrus of ANA-12 injected mice ($p<0.05$, Student's t test, figure 2.1 c).

Detecting a phosphorylated protein in spinal DH

To verify that the antibody detects a phosphorylated protein, tissue sections collected from male SNI operated animals 3 days post-SNI and were treated with lambda protein phosphatase (LPP) to dephosphorylate protein residues, or with a control NEB solution that does not have any dephosphorylating activity. Representative images show dorsal horn of spinal cord from animals 3 days after SNI (figure 2.2 a, b, c). Ipsilateral DH treated with NEB (vehicle control) has higher fluorescence associated with pTrkB-ir, as compared to contralateral DH treated with NEB (figure 2.2 a, b). Ipsilateral DH tissue sections were incubated in LPP solution or NEB overnight at 37°C in a humidified

chamber. Our quantification indicates that SNI increased pTrkB-ir in DH ipsilateral to nerve injury as compared to the contralateral DH ($p<0.00001$ One-Way ANOVA with Tukey's multiple comparison test figure 2.2 d), and LPP treatment significantly reduced pTrkB-ir as compared to the ipsilateral DH ($p<0.00001$) and even the contralateral DH of sections treated with NEB ($p<0.05$ figure 2.2 d).

TrkB activity in spinal DH after nerve injury

To determine if the pTrkB signal is increased following nerve injury, pTrkB-ir in ipsilateral dorsal horn of male and female mice after SNI or sham procedures. Representative images collected at day 3 post-SNI showed pTrkB-ir in ipsilateral DH (figure 2.3 b), but not the contralateral dorsal horn in SNI operated male (data not shown), while ipsilateral DH of sham operated male had lower pTrkB-ir (figure 2.3 a). Behavioral testing was conducted to screen for behavioral sex-differences. Baseline tactile thresholds were measured prior to surgical procedures, and 3 days after the surgery when behavioral hypersensitivity develops in this model. Both male and female SNI animals had significantly lower 50% withdrawal thresholds as compared to sham operated controls indicating that the injured animals were hypersensitive on the side of injury ($p<0.01$, $p<0.0001$, Two-way repeated measures ANOVA with Tukey's post-hoc comparison, figure 2.3 c). The quantification of pTrkB-ir in DH of spinal cord revealed increased pTrkB-ir in ipsilateral DH in nerve injured males and females as compared to their sham operated counterparts ($p<0.0001$, Two-way ANOVA with Tukey's post-hoc test, figure 2.3 d). SNI-operated male and female mice had comparable amount of pTrkB-ir in ipsilateral DH. However, sham females had significantly higher amount of pTrkB as compared to sham males, suggesting that females have higher amount of baseline TrkB

activity or the sham surgical procedure results in greater inflammatory reaction in female sham mice as compared to sham males ($p<0.001$, Two-Way ANOVA with Tukey's post-hoc test).

TrkB activity in males at multiple timepoints after injury

Since we did not detect any sex differences in the SNI induced increase in pTrkB-ir between male and female nerve injured animals, we performed additional experiments to compare SNI induced pTrkB-ir at 3 different timepoints to test whether sex-differences are time-dependent. At all three timepoints, male and female mice were hypersensitive in the paw on the ipsilateral side of injury and no sex-differences were detected in the level of hypersensitivity (figure 2.4 a, c, e). Additionally, pTrkB-ir was similarly increased in both sexes at 3 days (b), 7 days (d), 28 days (f) after nerve injury (Student's t test, figure 2.4 b, d, f). Therefore, we did not detect sex-differences in the SNI induced behavioral hypersensitivity or increase in pTrkB-ir.

Functional role of TrkB activity in male and female mice

Although female mice had a similar degree of TrkB activation in DH after SNI, the functional role of that activity was undetermined. We hypothesized that in female mice, TrkB activity does not functionally contribute to the SNI induced behavioral hypersensitivity as it does in male mice. To test this hypothesis, we injected male and female SNI operated animals at multiple timepoints after injury and the animals were injected with a single 1nM dose of ANA-12 (i.t.) or vehicle once at the beginning of test days. All animals were baselined before SNI surgeries, and all animals were hypersensitive on the injured side when tested at day 3 post-SNI and remained hypersensitive for the duration of the study (figure 2.5). Interestingly, ANA-12 had a

modest but significant anti-hyperalgesic effect on days 7, 14 and 28 post-SNI (Repeated measures Two-way ANOVA with Tukey's HSD for multiple comparisons, p values indicated by asterisks on graphs indicate significant difference from control group at the matching timepoint, figure 2.5 a). Unexpectedly, ANA-12 did not significantly reduce hypersensitivity in female mice, and in fact, vehicle treatment had a small anti-hyperalgesic effect in females (Repeated measures Two-way ANOVA with Tukey's multiple comparisons, figure 2.5 b). Collectively, these data indicate that the effect of ANA-12 on behavior is sex-dependent.

Efficacy of ANA-12 in spinal TrkB inhibition in male and female mice

The sex-differences in the behavioral effect of TrkB inhibitor, ANA-12, in female mice gave rise to two possible explanations for the sex difference – first, TrkB activity does not contribute to SNI induced hypersensitivity, or second, ANA-12 acts differently in male and female animals. To determine which of these possibilities is the likely explanation, we collected DH tissues from animals at 2 hrs post-drug at day 7 post-SNI (day and time post-injury, and post-drug with maximal drug effect) after ANA-12 or vehicle treatment. Although the behavioral experiment did not show significant reduction in hypersensitivity in males, the pattern of ANA-12 reducing hypersensitivity in males and increasing hypersensitivity in females as compared to their sham counterparts observed previously was maintained (figure 2.6 a). Immunohistochemical assessment of degree of TrkB inhibition in male and female SNI mice yielded surprising results (figure 2.8 b). ANA-12 treatment which in another dataset significantly reduced behavioral hypersensitivity, had higher pTrkB-ir as compared to vehicle treated SNI males (Student's t test, $p<0.05$, figure 2.6 b). In contrast, ANA-12 treatment previously did not

have a significant anti-hyperalgesic effect on SNI induced hypersensitivity, the pTrkB-ir in ANA-12 treated female cords was lower compared to their vehicle treated counterpart (Student's t test, $p<0.05$, figure 2.6 b). Taken together, the results presented here suggests that TrkB activity negatively regulates SNI induced hypersensitivity, and that the drug effects were sex dependent.

ANA-12 effects on naïve male and female animals

Since we detected some effects of vehicle on SNI females as compared to ANA-12 treated SNI females, we conducted additional experiments to test the effects of ANA-12 and vehicle on tactile sensitivity and TrkB activity in naïve mice. Naïve male and female animals were injected with ANA-12, vehicle, or saline intrathecally, and tested at 2 and 4 hours after injections. ANA-12 or vehicle did not influence tactile thresholds in naïve males and females as compared to saline injected control counterparts (figure 2.7 a). We then collected spinal tissue at 5 hours post-drug injections to quantify pTrkB-ir in different groups. We detected significant main effect of sex ($p<0.0001$) as well as treatment ($p<0.0060$) without significant interaction between the two ($p=0.27$) in a Two-Way ANOVA. Multiple comparisons test revealed that saline injected naïve female mice had higher pTrkB-ir as compared to saline injected naïve males, suggesting that females normally may have higher baseline TrkB activity which is consistent with the data from 3days post-SNI where sham operated females had higher pTrkB-ir in ipsilateral DH compared to that of the male sham operated mouse (Two-way ANOVA with Tukey's HSD $p<0.05$, figure 2.7 b). This sex difference is maintained in ANA-12 injected groups where female ANA-12 injected animals had higher proportion of pTrkB-ir as compared to their male counterparts ($p<0.001$). Although the decreased pTrkB-ir in vehicle treated

male and female mice was not significantly difference from saline controls, it was sufficient to mask the latent sex differences in pTrkB-ir. Finally, in naïve females, vehicle injected females had significantly less pTrkB-ir as compared to ANA-12 treated females, neither of which were significantly difference from saline injected females. On the other hand, none of the treatments significantly altered pTrkB-ir in males, which might suggest that the female CNS is more susceptible to the effects of DMSO, PEG300, and ANA-12 as well as nerve injury induced changes.

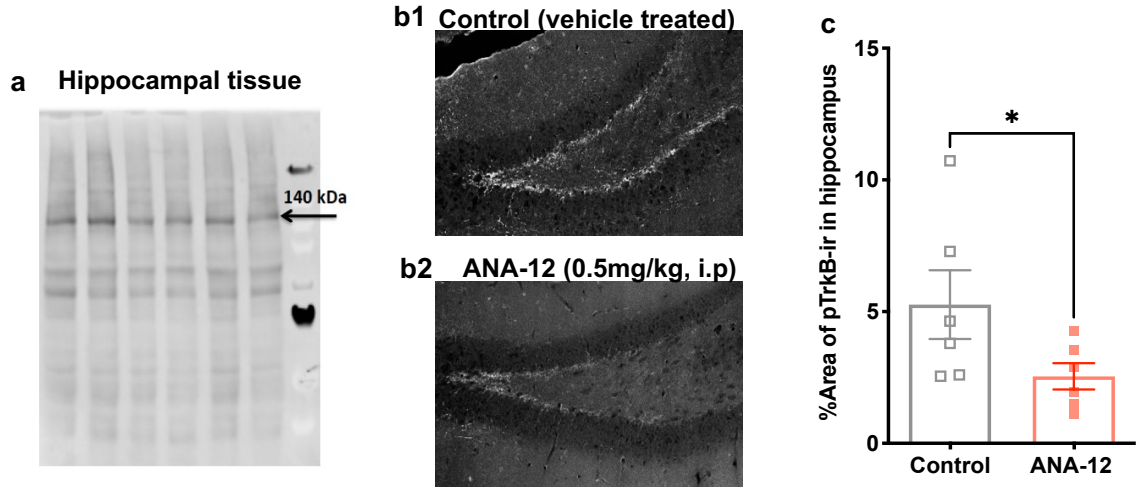

Figure 2.1: Validation of antibody in hippocampal tissue. Western blot assay of hippocampal tissue collected from male SNI and female SNI mice 28-days post-SNI showed a bright band with molecular weight of ~140kDa which corresponds to the weight of the full-length TrkB (150kDa) receptor (a). Confocal images of dentate gyrus of hippocampus collected from TrkB inhibitor, ANA-12 (i.p), injected male mice 3 days post-SNI had significantly lower pTrkB-ir (b2) as compared to hippocampal tissue from vehicle treated mice (b1). Quantification of pTrkB-ir in dentate gyrus indicates significantly lower amount of immunoreactivity in ANA-12 treated animals (b2) as compared to vehicle treated controls (c). Student's t test. $p<0.05$*. N=6 animals per group for Western blot assay, and IHC analysis with ANA-12 and vehicle treatment.

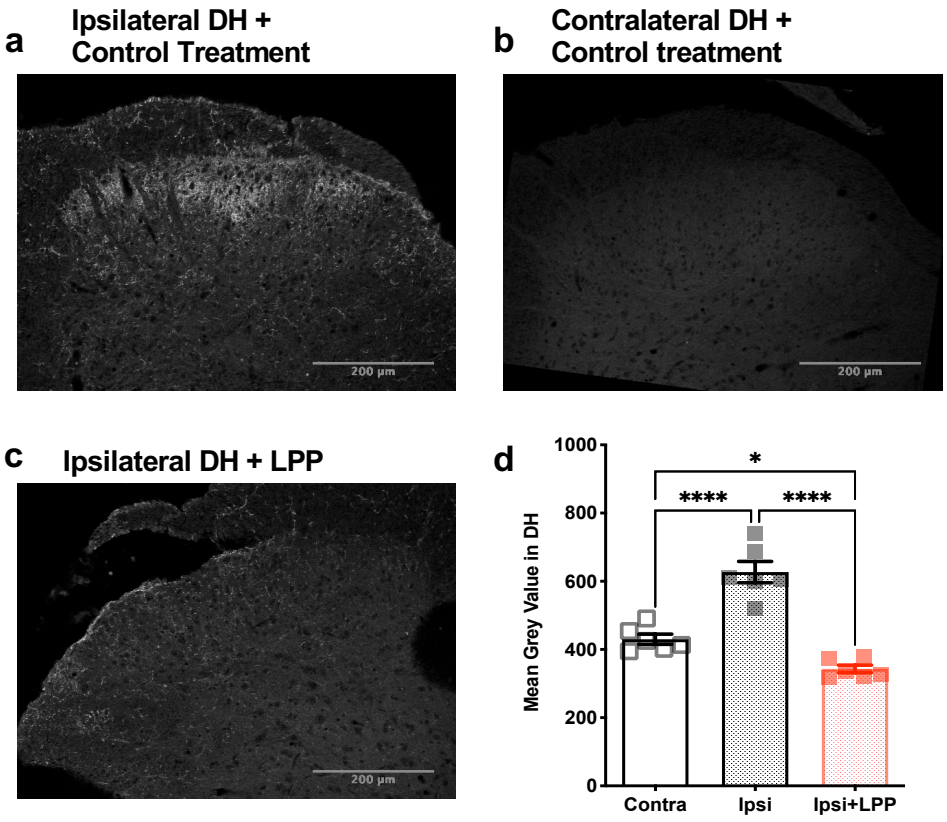

Figure 2.2: Validating antibody directed against phosphorylated TrkB in spinal cord after nerve injury. Confocal images of ipsilateral (a, c) and contralateral (b) DH of SC sections treated with a phosphatase (LPP) (c) or control buffer (NEB, MnCl2, DMSO) vehicle (a, b). Ipsilateral dorsal horn of SNI males has visible pTrkB-ir (a) compared to the contralateral dorsal horn (b). LPP treatment of spinal sections significantly reduces pTrkB-ir in dorsal horn (c), even lower than staining in contralateral dorsal horn (d). One way ANOVA, with Tukey's post-hoc test. $p<0.05$*, $p<0.0001$*** Scale bar = 200um. N=6, tissues from same animals used for the treatments and comparison.

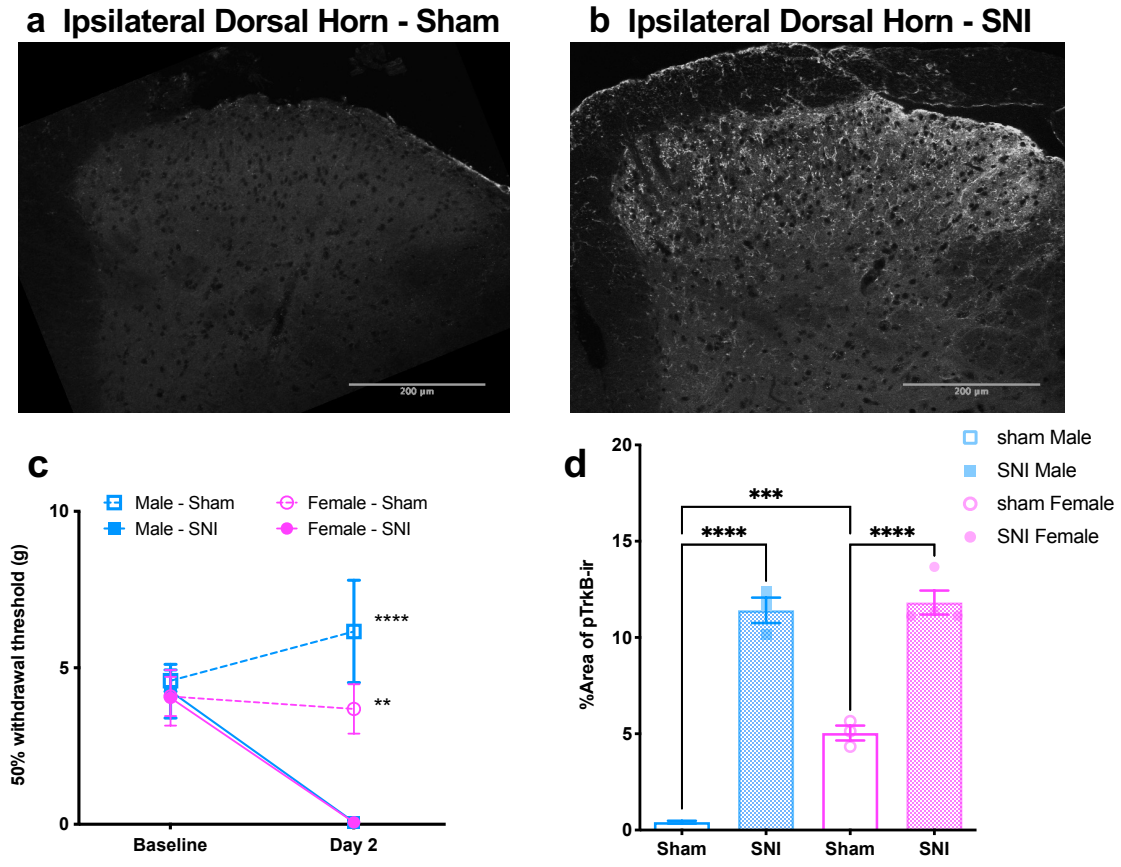

Figure 2.3: Quantification of TrkB phosphorylation at day 3-post SNI. A confocal image of the left dorsal horn from a sham operated male (a) and nerve inured male (b) immunostained for phosphorylated form of TrkB (p-TrkB) is visualized. scale bar=200um, 20X magnification. The behavioral data from Von Frey assay shows that both male and female SNI operated animals were significantly more hypersensitive as compared to their sham operated counterparts (c). Consequently, male and female SNI operated animals had significantly higher pTrkB immunoreactivity at day 3 post-SNI as compared to their sham counterparts (d). A significantly higher pTrkB-ir was observed in sham operated females as compared to males at day 3 post-SNI (d). Two-way ANOVA with Tukey's post-hoc comparisons. N=3 per group, except female SNI (n=4) $p<0.01$**, $p<0.001$***, $p<0.0001$***

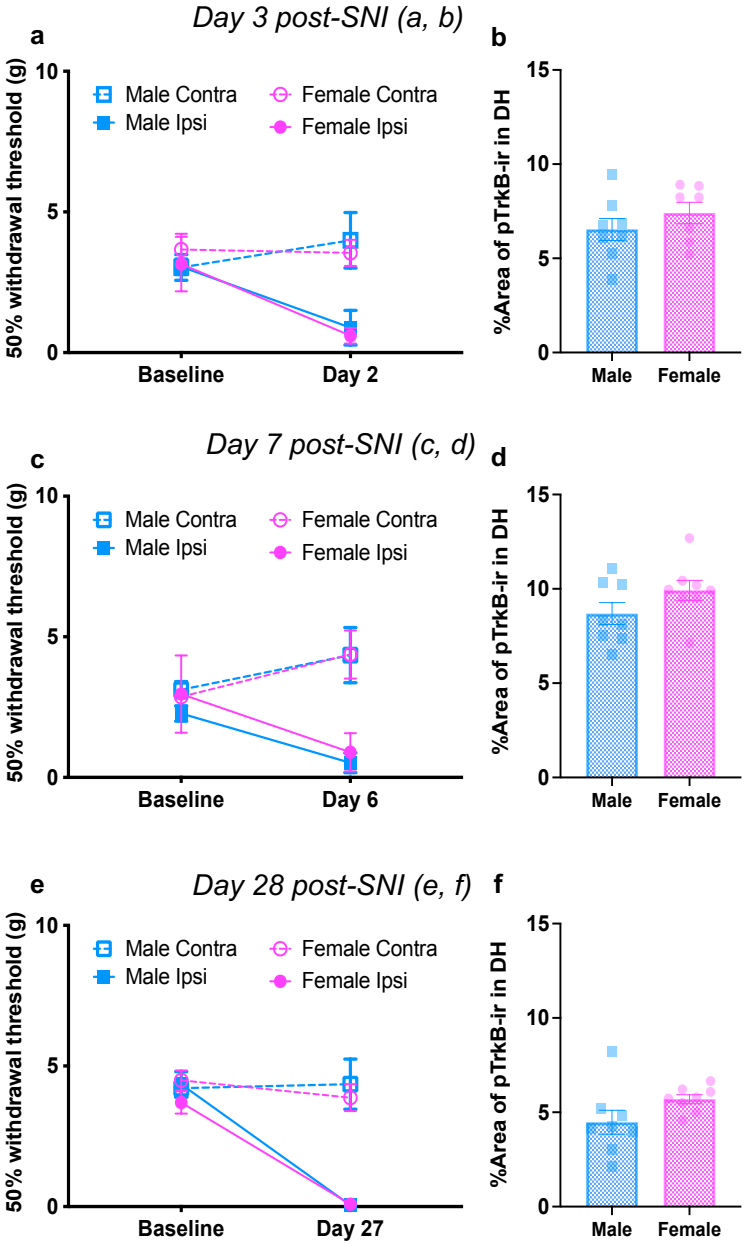

Figure 2.4: SNI induced TrkB activation in male and female mice at day 3 (a, b), day 7 (c, d), and day 28 (e, f) after injury.

We did not detect any behavioral sex differences in tactile thresholds at baseline or any timepoint after injury (a, c, e). Correspondingly, Nerve injured male and female mice had similar levels of pTrkB-ir in the ipsilateral dorsal horn at all time-points (b, d, f). Two-way repeated measures ANOVA for behavioral analysis, Student's t test or pTrkB-ir. N=8 for all groups except 3day female SNI (n=7).

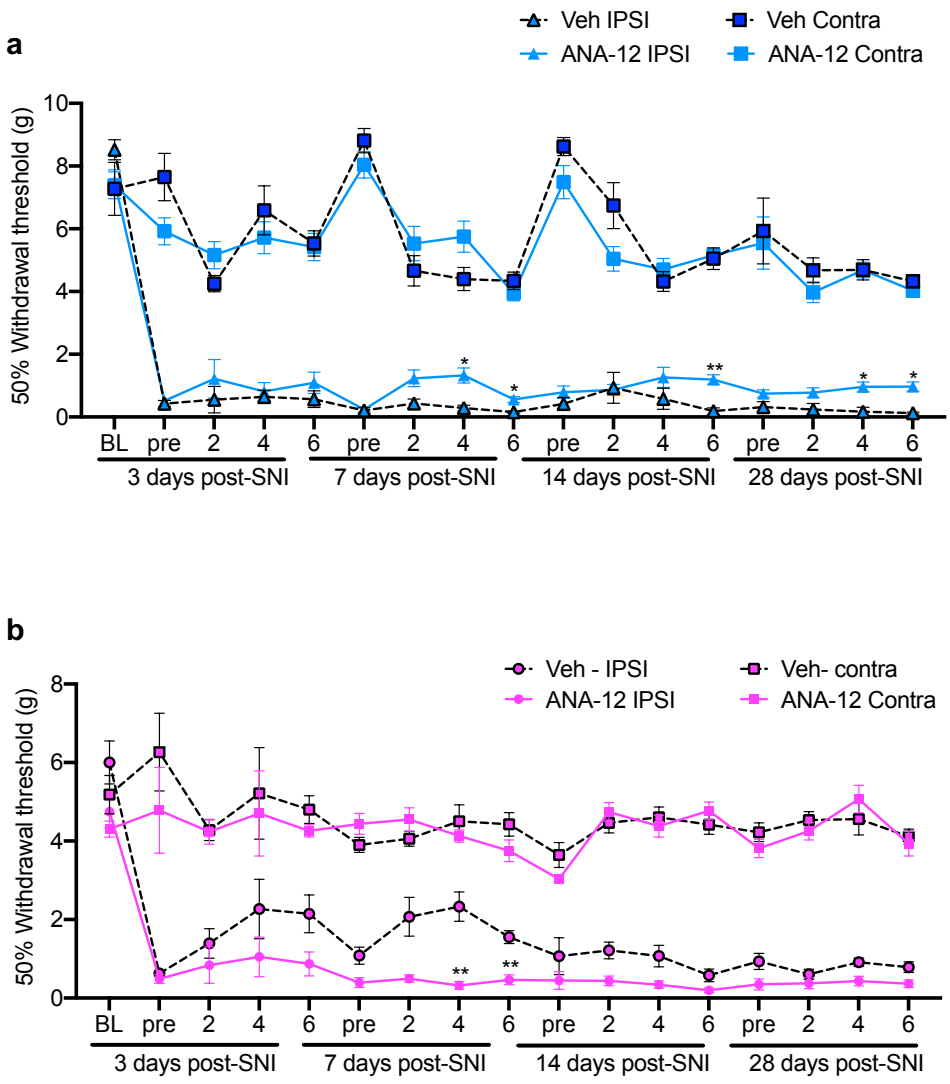

Figure 2.5: Repeated injections of ANA-12 (i.t.) in male and female nerve injured mice. Male (a) and female (b) SNI mice were baselined before SNI and at days 3, 7, 14, and 28 post-SNI. On days post-SNI, tactile thresholds were tested prior to drug injections, and at 2hrs, 4hrs, and 6hrs after ANA-12(i.t.) or vehicle (i.t.). ANA-12 treated SNI males had significantly higher tactile thresholds on day 7 (4 and 6 hrs after drug), day 14 (6 hrs after drug), day 28 (4 and 6 hrs post drug) after SNI (a). In female animals, ANA-12 did not increase behavioral tactile thresholds, but vehicle treated SNI female mice were significantly less hypersensitive compared to ANA-12 treated animals, specifically on day 7 (4 and 6hrs after drug) post-SNI (b). Female ANA-12 and vehicle group had n=10 each. Male ANA-12 group n=8, male vehicle group n=7.

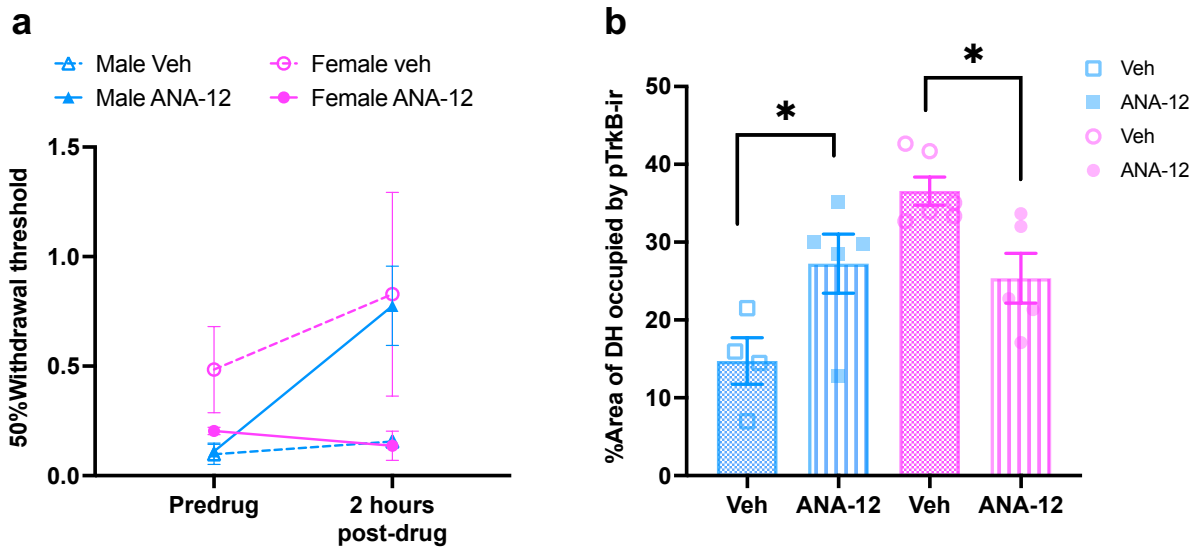

Figure 2.6: Effects of ANA-12 (i.t.) on SNI induced pTrkB-ir in male and female mice 7 days post-SNI. Nerve injured male and female mice were tested pre-drug and 2 hours post-drug (ANA-12(i.t.) or Veh) 7 days after injury (A). pTrkB-ir in spinal cords of these animals 4 hours after drug was quantified to determine the effects of the drug on TrkB activity (B). Unexpectedly, In males that show slight reduction in hypersensitivity at 2 hours after ANA-12(i.t) administration, ANA-12 increased pTrkB-ir in SNI operated males as compared to vehicle treated SNI males ($p<0.05$, Student's t test). In contrast, female SNI mice in which the vehicle treatment showed mild anti-allodynic effect, pTrkB-ir in spinal cord was significantly higher in vehicle treated SNI females as compared to ANA-12 injected SNI females ($p<0.05$, Student's t test). $p<0.05$* sample sizes: Male veh = 4 mice, male ANA-12 = 5 mice, female veh = 6, female ANA-12 = 5.

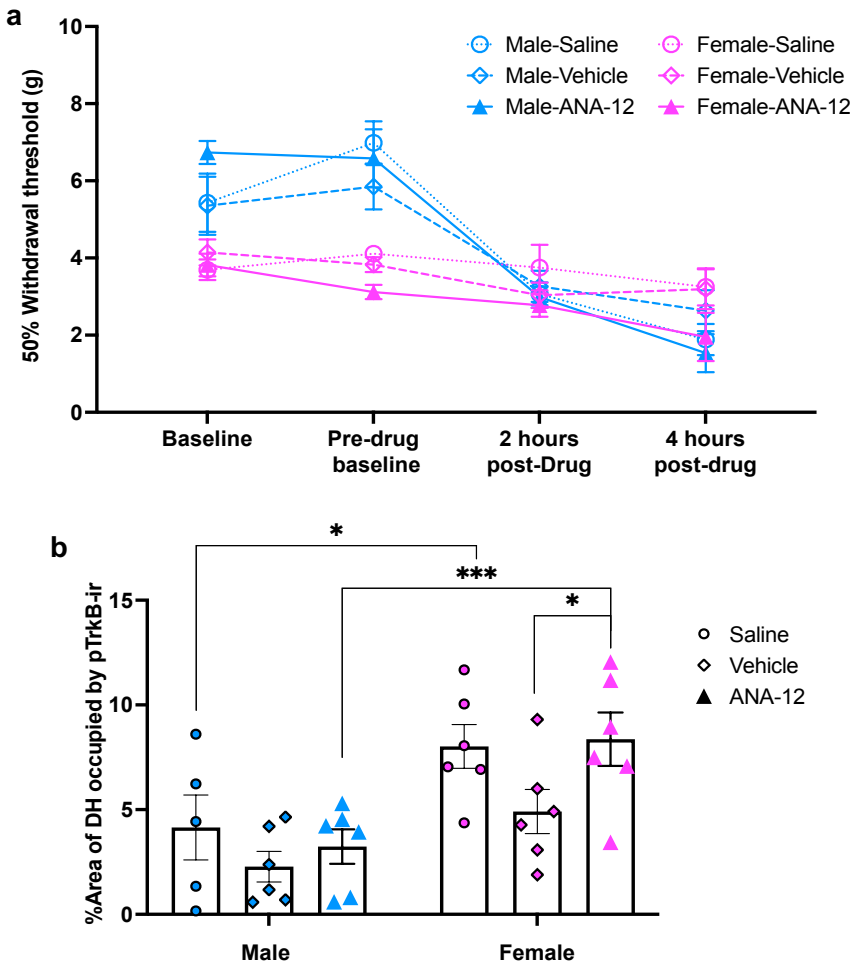

Figure 2.7: Effects of intrathecal administration of ANA-12 and vehicle on spinal pTrkB-ir in naïve mice. Naïve, uninjured, male and female mice were injected with ANA-12 (i.t.), vehicle (i.t.), and saline (i.t.) and their tactile thresholds were measured, and no differences were detected due to drug treatment (a). pTrkB-ir in spinal cord was significantly higher in naïve ANA-12 injected females as compared to vehicle treated females (b). Significant sex differences were observed in terms of baseline pTrkB-ir and effects of ANA-12, with female mice expressing higher amount of pTrkB-ir at baseline (saline treated males vs females), or after ANA-12 treatment (b). Two-Way ANOVA with Tukey's HSD, $p<0.05$*. N=6 per group, except Male saline group (n=5).

DISCUSSION

Most studies that report TrkB activation after injury indirectly measure TrkB activity because reliable and validates antibodies directed against TrkB receptors and TrkB specific antagonists or blockers are rare. In this study, we measured the level of TrkB activity after nerve injury using a commercially available antibody directed against phosphorylated fl-TrkB^{Y816}. Validation efforts revealed that the antibody detects a phosphorylated protein with the same molecular weight as fl-TrkB receptor, whose immunoreactivity is reduced by TrkB antagonist treatment. These experiments allow for site, region, and injury specific evaluation of TrkB activity in spinal cord.

TrkB function in nerve injury induced changes in male and female mice

The data presented here indicate that activation of TrkB in spinal cord following nerve injury is increased comparably in male and female mice, but the functional role of TrkB may differ between the sexes. A novel, small molecule, TrkB receptor specific antagonist, ANA-12, minimally but significantly reduced nerve injury-related hypersensitivity in male mice as compared to vehicle treated mice, however in females, the effects were reversed, and the vehicle treated group was significantly less hypersensitive at certain timepoints. This indicates that either the role of TrkB receptor or the function of the drug is different between males and females.

Evaluating sex-specific effects of drug on TrkB activity

To understand and verify drug activity on spinal TrkB function, we collected spinal tissues from male and female injured mice injected with ANA-12 or vehicle 7 days post-SNI. ANA-12 had significant yet opposite effects in male and female mice. In males, ANA-12 increased pTrkB-ir in DH as compared to males that received vehicle. In

contrast, ANA-12 injected females had significantly reduced pTrkB-ir in DH as compared to vehicle treated females. These counterintuitive results raise several possibilities as to the role of BDNF-TrkB signaling after nerve injury.

ANA-12 has opposite effect in male and female mice: ANA-12 was first characterized in male mice, and the only two reported uses of it in context of nerve injury tested it in males. Therefore, the pharmacological and pharmacodynamic properties of the drug have not been evaluated or tested in females.

TrkB activation reduces behavioral hypersensitivity: Our results show that the modest reduction in hypersensitivity corresponded with increased pTrkB-ir in males, while the vehicle which produced mild hyperalgesic effect in females also increased pTrkB-ir, suggesting a positive relationship between antinociceptive effects and increased TrkB activation. These results seem to oppose the conventional framework which suggests that BDNF-TrkB signaling is responsible for pain behaviors, however, it is possible that the TrkB signaling has dual properties and that activation of a specific set of TrkB receptors act in opposition to the neuroplasticity promoting mechanisms.

Misinterpretation of existing data: Just as validated antibodies for TrkB receptors are difficult to find, so are other tools to specifically manipulate TrkB function. Often, the role of TrkB or BDNF in specific area after nerve injury is evaluated using methods that indirectly influence BDNF or TrkB activity. For instance, the two reports of sex-differences in neuroimmune signaling, and specifically BDNF-TrkB signaling in spinal cord were evaluated by eliminating microglia, inhibiting microglial function with non-specific toxins, inhibiting activation of kinases present in multiple cell types using methods that do not spatially restrict their activity. Thus, the confluence of these effects

on the simple behavioral output does not provide information regarding the mechanism by which pain behavior is regulated in the context of injury. Furthermore, when these techniques are used, their effectiveness or specificity is not verified. Therefore, these methods are assumed to exert the intended effect on a system, but it is possible that the means used for experimental manipulations may have sex-, time-, region-, and context specific effects that go unnoticed, thus leading to a misinterpretation of the results.

Dual role of BDNF-TrkB signaling in pain processing

Although the data presented here seem to oppose established ideas of BDNF-TrkB signaling, it is difficult to speculate or hypothesize how these sex-differences impact downstream signaling. Some reports find that BDNF signaling in certain contexts can reduce pain hypersensitivity, suggesting dual effects of the neurotrophic factor (Miki et al., 2000; Eaton et al., 2002). Furthermore, a study investigating the KCC2 channel reduction that is a downstream consequence of BDNF-TrkB signaling found that the changes were conserved in male and female mice, which indicated to them that although the BDNF-TrkB signaling may diverge at the level of microglial signaling, the downstream changes attributed to BDNF-TrkB are preserved in males and females (Mapplebeck et al., 2019). Therefore, although the pattern of TrkB activity and its role in tactile hypersensitivity might be different between male and female mice, the signaling pathways converge further down the signaling pathway. This also raises the possibility that sex-dependent, BDNF-TrkB independent mechanisms produce downstream changes like those initiated by BDNF-TrkB signaling and they have a common target. Studying the similarities and differences between signaling pathways in males and females can

tremendously accelerate identification of targets for novel therapeutics that are efficacious in males and females.

Sex-dependent injury-specific effects of ANA-12 and vehicle

Finally, we tested ANA-12 and the vehicle (2%DMSO and 33%PEG300 in Saline) in naïve mice and found that in females, vehicle suppressed TrkB activity and ANA-12 elevated back to levels comparable to saline controls. Similar patterns were present in males, but the effects did not reach significance. These data show that the nerve injury alters the BDNF-TrkB system, the drugs interact with that altered system in a sex-dependent manner. Additionally, there are certain baseline differences that should be considered since naïve females overall had higher TrkB activation in DH as compared to naïve males, a trend also seen in sham operated animals where females have higher TrkB activation compared to sham operated males.

Taken together, the experiments in this chapter highlight the necessity for validation studies to understand sex-, time-, region-, assay-dependent patterns in signaling cascades. Furthermore, the results presented here can provide context, framework, and baseline data regarding the level of BDNF-TrkB activity in male and female animals, and the nuances of the signaling pathway in the two sexes.

CHAPTER 3: ROLE OF SPINAL MICROGLIA IN INJURY INDUCED SPINAL BDNF-TRKB SIGNALING

INTRODUCTION

Microglia and macrophages act as the first line of immune defense in the CNS and respond to damage or injury threat signals. Although peripheral monocytes and macrophages were thought to infiltrate the spinal cord following peripheral nerve injury, recent studies indicate that the increase in microglial markers in spinal cord is due to rapid proliferation and expansion of native microglia (Guan et al., 2015). Activated microglia serve many functions, including recruitment of other immune and glial cells, increased surveillance of CNS tissue, eliminating foreign object or damaged components (Milligan and Watkins, 2009). In the nerve injury literature, spinal microglia are considered important for their role in producing and releasing BDNF (Coull et al., 2005; Tsuda et al., 2005; Moalem and Tracey, 2006; Ji et al., 2013) which initiates a signaling cascade that ultimately results in disinhibition of spinal circuitry and increased nociceptive signaling (Ji et al., 2013).

A few reports investigated the role and contribution of sensory neuron derived BDNF and found that it contributes minimally or partially to the injury induced hypersensitivity (Dembo et al., 2018; Sikandar et al., 2018). These studies highlight the importance of microglia as a source of BDNF, which is further supported by the fact that microglial inhibitors, or interventions aimed at blocking microglial function, significantly reduce pain behaviors in models of neuropathic pain (Jin et al., 2003; Raghavendra et al., 2003; Tsuda et al., 2004; Ledeboer et al., 2005; Marchand et al., 2005; Zhuang et al.,

2005; Clark et al., 2007; Zhang et al., 2011b; Zhou et al., 2011; Sorge et al., 2015). However, the exact role of microglia in signaling cascades following nerve injury has not been well-characterized.

Despite the great interest in microglia for their role as BDNF producers and triggering long-term maladaptive neuroplasticity, there is no direct evidence to suggest microglia produce or release BDNF *in vivo*. Coull et al (2002) showed minimal BDNF release by ATP stimulated cultured microglia (Coull et al., 2005). Additional experiments included the intrathecal injection of ATP stimulated cultured microglia into rat spinal cords which produced behavioral hypersensitivity (Coull et al., 2005), however, these experiments did not test whether the pronociceptive effect of microglia were due to BDNF. Although, Ulmann (2008) performed immunohistochemistry to detect BDNF-ir, the antibody used was not validated by them or others, and additional tests were not presented to show specificity (Ulmann et al., 2008). Other studies generally assume microglial BDNF release and design experiments under that assumption (Tsuda et al., 2005; Moalem and Tracey, 2006; Ji et al., 2013). Sorge et al (2015) generated a tamoxifen inducible microglial BDNF knockout line to specifically study the role of microglial BDNF in pain behaviors but did not provide any evidence to show the degree of BDNF knockdown in these mice (Sorge et al., 2015). Finally, newer mouse lines designed to visualize BDNF expressing cells using genetically encoded fluorescent reporter proteins did not show reporter expression in microglia (Dembo et al., 2018). Therefore, expression of BDNF in spinal microglia has not been confirmed. Sex-differences complicate the interpretation of these data since blocking, sequestering, or inhibiting BDNF activity seems to reverse hypersensitivity in male mice only, and

inducible genetic deletion of BDNF from microglia showed similar pattern of reduced hypersensitivity in males (Sorge et al., 2015). These data led to much speculation regarding the fundamental role of BDNF-TrkB signaling in female mice (Sorge and Totsch, 2016; Mapplebeck et al., 2017, 2018). However, since the exact role of microglia in BDNF-TrkB signaling in spinal cord is unknown, the mechanistic reason for the sex-differences cannot be discovered.

Since some evidence indicates presence and release of BDNF from spinal microglia, it is possible that microglia do not themselves express BDNF but sequester extracellular BDNF via TrkB receptors. As discussed in an earlier chapter, TrkB receptors come in three forms. The fl-TrkB receptor contains an intracellular kinase domain which is thought to be responsible for intracellular signaling (Barbacid, 1994; Minichiello, 2009; Ohira and Hayashi, 2009). In contrast, the truncated forms were long thought to sequester BDNF thus acting as an antagonist to fl-TrkB by preventing its activation (Middlemas et al., 1991). The truncated T1 receptor is known to internalize BDNF upon binding, the BDNF is then transported and rereleased in an activity-dependent manner in DRG neuronal cultures.

We evaluated the expression of *BDNF* and *TrkB* mRNA in spinal microglia using a high sensitivity *in situ* hybridization assay. We did not detect any instances of *BDNF* mRNA signal overlapping with microglial profiles, however, *TrkB* mRNA in microglia was evident. Additional experiments to evaluate if microglial TrkB is activated after nerve injury. We found that much of the injury induced increase in pTrkB-ir was localized to spinal microglia in injured mice. This is a novel finding because microglia were thought to lack the fl-TrkB receptor. Finally, we tested the functional role of

microglial TrkB receptors in nerve injury-induced hypersensitivity using a mouse line which permits tamoxifen-inducible microglia-specific TrkB deletion. We confirmed the degree of KD since we did not see any behavioral differences due to microglial TrkB deletion. In all these experiments, we did not detect any sex-differences in terms of the TrkB activation after nerve injury or the microglial TrkB deletion.

METHODS

Animals

All experiments were conducted in compliance with National Institutes of Health Guide for Care and Use of Laboratory Animals and approved by the University of Minnesota Institutional Animal Care and Use Committee. Animals were group house 4 males per cage, and 5 females per cage in a temperate and humidity-controlled SPF facility on a 12-hour light/dark cycle. The animals had free access to food and water. Male and female 4–12-week-old mice of the following genotypes: ICR-WT (CD-1), C57/Bl6, Iba1-eGFP, Ai14, Cx3Cr1cre^{ERT2} XAi14, Cx3Cr1cre^{ERT2} X TrkB$^{fl/fl}$. ICR (CD-1) WT and C57/Bl6 mice were bred in house. Iba1-GFP, a transgenic line in which enhanced green fluorescent protein (EGFP) is controlled by the Iba1 promoter, generated on a C57/Bl6 background, were provided by Dr. Kohsaka, National Institute of Neuroscience, Tokyo, Japan (Hirasawa et al., 2005). Ai14, B6.Cg-Gt(ROSA)$^{26Sortm9(CAG-tdTomato)Hze}$/J (Stock Number #007909) mouse line was bred with B6.129P2(C)-Cx3cr1$^{tm2.1(cre/ERT2)Jung}$/J mouse (Stock Number #020940)from Jackson labs and the colony was maintained at the University of Minnesota vivarium. The TrkB$^{fl/fl}$ line was obtained from Dr. Lino Tessarollo, Center for Cancer Research, NCI, Frederick, MD 21702[109]. Heterozygous Iba1-GFP, heterozygous Ai14, Cx3Cr1cre^{ERT2}XAi14 mice heterozygous for both genes, Cx3Cr1cre^{ERT2}XTrkB$^{fl/fl}$ heterozygous for Cre and homozygous TrkBfl/fl animals were used for the following experiments. 4-hydroxytamoxifen (50mg/kg, i.p.) was injected for 3 consecutive days, starting 2 days before SNI and ending on the day of SNI surgeries. In experiments in which animals were treated with tamoxifen, all animals, including littermate controls were injected with

tamoxifen. A 10mg/ml solution of 4-OHT in corn oil was heated to 40^0C to dissolve the drug. 4-OHT solution was used within 5 days of dilution.

Spared Nerve Injury (SNI)

Tactile hypersensitivity was induced using the spared nerve injury (SNI) model as described by Decosterd and Woolf (Decosterd and Woolf, 2000). Mice were placed under isoflurane anesthesia in a recumbent position and the three terminal branches of the left sciatic nerve were exposed by bluntly dissecting the left thigh muscle. The common peroneal and tibial nerves were ligated using a 5.0 silk suture. The peroneal and tibial nerves were cut 2 mm distal to the ligation site, leaving the sural nerve uninjured. Sham animals had the left sciatic nerve exposed without ligation or cutting of the nerves.

Tactile Hypersensitivity

Mice were brought into a quiet testing room and allowed to acclimate for about an hour before placing them on a wire mesh grid platform under a glass enclosure and allowed to acclimate for 30 mins prior to testing. Synthetic Von Frey filaments were used to apply force onto the lateral plantar surface of the left and right hind paw. Using the up-down method as described by (Chaplan et al., 1994) and statistical framework by (Dixon, 2012), the 50% withdrawal threshold was calculated wherein a positive withdrawal reflex was defined as a flinching, retracting, or withdrawing of the hind paw from the filament. Baseline tactile thresholds were measured for all animals in these experiments and measured again following nerve injury but prior to tissue collection.

Spinal Cord and DRG tissue section preparation

Mice were deeply anesthetized with isoflurane and perfused via the heart with calcium-free Tyrode's solution (116mM NaCl, 5.4mM KCl, 1.6mM MgCl·26H2O,

0.4mM MgSO·47H2O, 1.4mM NaH_2PO_4, 5.6mM glucose, and 26mM Na_2HCO_3) followed by fixative (4% paraformaldehyde). Tissues were dissected, post-fixed overnight in (4% paraformaldehyde), then incubated in 10% sucrose. Spinal cords were embedded in OCT compound (Tissue-Tek), flash frozen using liquid CO_2 and stored at -80°C overnight. Sections were cut at 14 μm thickness using a cryostat microtome (OTF5000, Bright Instruments) and thaw mounted onto Superfrost Plus® microscope slides (Fischer Scientific). Sliced spinal cord were anatomically mapped to determine slides within the L3 and L4 spinal levels. Spinal cord and DRG slides were stored at -20°C until further processing.

RNAscope Processing and Probes

Slides were prepared for RNAscope® processing using the RNAscope Fluorescent Multiplex v2 Kit (Cat. No. 323100). Briefly, slides were recovered from -20^0 C, air-dried, and incubated in 4% paraformaldehyde for 5 mins. Tissue sections were dehydrated in ethanol solutions of increasing concentration (50%, 70%, 100% EthOH) for 5 mins in each solution. Slides were washed with 1X PBS for 2 mins then tissue sections were covered with hydrogen peroxide (ACDBio) for 10 mins. Slides were washed 4 times with distilled water, incubated in target retrieval reagent heated to ~960 C for 4 mins, washed again 4 times in distilled water, then submerges in fresh 100% ethanol for 5 mins. A hydrophobic barrier was drawn around the tissue and allowed to dry at room temperature for 30 mins. After drying, tissues were covered in RNAscope Protease III and placed in a warm 40°C humidified chamber for 15 mins. After removal from oven, slides were washed 4 times in distilled water.

Following slide and tissue preparation, mRNA was tagged using highly specific probes and associated fluorophores for visualization. Briefly, excess water was removed from slides and BDNF (cat# 424821) or NTRK2 (cat#423611), positive- and negative-control probes were added to separate slides and incubated for 2 hours at 40°C. Following incubation with probes, slides were washed 2 times in 1X wash buffer for 2 mins. Probe signal was amplified by incubating tissue sections with Multiplex FLv2 AMP1 and AMP2 for 30 mins, and in AMP3 for 15 mins at 40°C. Slides were washed 2 times in 1X wash buffer for 2 mins in between each amplification incubation and following the last amplification step. Horseradish peroxidase channel 1 (HRP-C1) signal was developed by covering tissue in RNAscope multiplex FL v2 HRP-C1 and incubated for 15 mins at 40°C. Slides were washed for 2 mins with 1X wash buffer and Cyanine 3 (PerkinElmer) diluted in TSA buffer (1:1,500) was added to the slides. Slides were incubated with Cy3 for 30 mins at 40°C. Slides were washed twice with 1X wash buffer for 2 mins, RNAscope multiplex v2 HRP blocker was added to the slides, incubated for 15 mins at 40°C, then washed 2 times in 1X wash buffer for 2 mins. DAPI was added to the slides for 30 seconds and cover-slipped using FluoroSave reagent (EMD Biosciences, Inc.). Slides were stored at room temperature. RNAscope® 20zz probes were ordered from ACDbio. The Ms-BDNF probe targeting 729-1974 mRNA region which recognize a common portion of the BDNF protein in all of the different translated proteins (NM_007540.4) and Ms-NTRK2 probe targeting 668-1582 mRNA regions encoding for FL-TrkB and truncated TrkB (NM_008745.3)

Tissue preparation for Immunohistochemistry

Following behavioral assessment, mice were deeply anesthetized with isoflurane and perfused via the heart with calcium-free Tyrode's solution (in mM: 116 NaCl, 5.4 KCl, 1.6 MgCl2·6H20, 0.4 MgSO4·7H2O, 1.4 NaH2PO4, 5.6 glucose, and 26 Na2HCO3) followed by fixative (4% paraformaldehyde and 0.2% picric acid in 0.1 M phosphate buffer, pH 6.9). The spinal cord was removed, cryoprotected in 10% sucrose overnight, covered with OCT and frozen using liquid CO_2, and cryostat-sectioned into 14 μm sections that were slide-mounted. Sections were preabsorbed in T/T/T buffer (TBS containing 0.2% Triton-X 100 and 0.2% Tween 20) for 30 min followed by incubation with a rabbit anti-pTrkB (Y816) 1:500 (Millipore Sigma-Aldrich ABN1381), along with Chicken anti-GFP (1:1000, Abcam ab13970) or Rat anti-tdTomato (1:1000) diluted in T/T/T overnight at 4^0C in a humidified chamber. Tissue sections were then washed 3X 10 mins each in TBS and incubated with secondary antibody for 1 hour at room temperature in a humidified chamber. Slides that were incubated with Chicken anti-GFP and Rabbit anti-pTrkB antibodies, were incubated with Cy3 donkey anti-rabbit (1:300 Jackson labs) and Alexa488 donkey anti-chicken (1:100 Jackson labs), while the slides previously treated with rabbit anti-pTrkB and Rat anti-tdTomato antibodies were incubated in Cy3 donkey anti-rat (1:300) and Alexa 488 donkey anti-rabbit (1:100) antibodies. Slides were then washed in TBS 3X10 mins each and cover slipped with FluorSave™ (Millipore 345789). Sections were allowed to dry and stored at room temperature until being imaged.

Image Acquisition and Analysis

Images were captured using a confocal Nikon A1R multiphoton confocal microscope or Olympus Fluoview upright confocal microscope at the University of Minnesota Imaging Center, with guidance from Dr. Guillermo Marquis. All images were collected on the same day or consecutive days with identical settings for all groups for direct comparison. Three equally spaced spinal cord sections were imaged for each animal and values were averaged to obtain one value per animal for between group comparisons. All data were tested for normality and the appropriate test was chosen.

Image Quantification

All image quantification was conducted by an experimenter blinded to the treatment conditions or animal groupings using FIJI. Images were auto-thresholded using max entropy setting and ROI size, and the Area of measured signal (um^2) as well as %Area of thresholded signal (measure of signal controlled for ROI size) were measured. Representative images were selected by finding the datapoint close to the mean to represent the average staining or fluorescence pattern. All representative images were manipulated to enhance brightness and contrast for visualization, however, all images across groups were adjusted similarly.

Data Analysis

Results from FIJI were stored as csv files and excel VBA macros were created to streamline the editing excel files to minimize human error. Prism 8 was used for all statistical analyses presented in this chapter and mean and SEM are graphed.

RESULTS

BDNF and TrkB mRNA in microglia

To determine if we could detect BDNF mRNA in microglial profiles after nerve injury, we combined *in situ* hybridization to detect BDNF mRNA and immunohistochemistry to visualize spinal microglia in ipsilateral dorsal horn 3 days after nerve injury in male mice. We did not detect any overlap between BDNF mRNA (Figure 3.1 a1) and Iba1-ir (figure 3.1 a2). Higher magnification images of ipsilateral DH of two other animals from this cohort 3 days after SNI are included as representative images from a set of images collected from about 10 nerve injured male and female mice (Fig. 3.1 b, c). Therefore, overall, we did not detect any instances of BDNF mRNA overlap with spinal microglia in ICR WT males 3 days post-SNI.

In contrast to BDNF mRNA, we observed that TrkB mRNA colocalized with Iba1-ir profiles at day 3 post-SNI in ICR WT mice. A representative image from a female ICR WT mouse 3 days post-SNI shows TrkB mRNA (figure 3.2 a1) and Iba1-ir (figure 3.2 a2) composite image (figure 3.2 a3). High-resolution magnified images were collected from several SNI and sham animals 3 days post-injury was collected to determine whether in the instances where TrkB mRNA appeared to overlap with Iba1-ir cell the TrkB mRNA was located inside the cell. One of these high-resolution magnified images are displayed in an orthogonal view (on the side panels) shows the intensity along the axis and confirmed that TrkB mRNA is located within the Iba1-ir positive nucleus (figure 3.2 b).

TrkB receptor expression and activity in microglia

Further confirmation of the expression of TrkB in microglia came from the observation of pTrkB-ir in microglia after SNI. Since the well validated and widely used antibody directed against Iba1 is grown in rabbit, we could not use the rabbit anti-pTrkB antibody that we validated (data presented in chapter 2). We attempted to visualize spinal microglia with other commercially available antibodies but recognized that immunohistochemistry would not allow visualization of microglial processes and often has a punctate or patchy staining pattern. Therefore, we utilized a transgenic mouse model in which GFP is driven by Iba1 promoter, and immunostained spinal cord sections from these mice at 3-, 7-, and 28-day post-SNI in male and female animals to determine the degree of pTrkB in microglia. Representative images of ipsilateral and contralateral dorsal horn at 7 days post-SNI show increased pTrkB-ir and Iba1-GFP staining in ipsilateral (figure 3.3 b1, b2) DH as compared to contralateral (figure 3.3 a1, a2), and a composite image shows the overlap (figure 3.3 a3 and b3). The total area of pTrkB-ir and Iba1-GFP in DH was measured as the percentage of the total area of DH ROI that is occupied by pTrkB-ir. DH contralateral to the nerve injury had little to no pTrkB signal which matched sham levels of pTrkB and was not quantified. Similarly, in the absence of nerve injury, contralateral DH in SNI animals or ipsilateral DH in sham operated animals had very little Iba1-GFP expression. The pTrkB-ir in DH of male and female mice was equally elevated at days 3-, 7-, and 28-days post SNI (figure 3.3 g). Concomitantly, the injured mice had increased area of Iba1-GFP profiles in the ipsilateral DH as compared to contralateral side and no sex differences at any time-points in the degree of microglial activation (as measured by the area of DH occupied by Iba1-GFP profiles) were detected (figure 3.3 d) or the pTrkB-ir in microglia (figure 3.3 e). Lastly, to determine whether the

data collected with this transgenic mouse line is generalizable to WT animals, we quantified pTrkB-ir in WT and Iba1-GFP mice and noticed that SNI induced increase in pTrkB-ir in ipsilateral DH of Iba1-GFP mice was much greater than that seen in WT SNI mice ($p<0.0001$, One way ANOVA with Sidak's post hoc, figure 3.3 f). Data from male and female mice were combined for comparisons between genotypes because no sex-differences were detected in any of the groups.

Since we noticed significant effect of genotype on pTrkB-ir with the Iba1-GFP mouse line, we used another transgenic line to visualize microglial profiles and immunostain spinal cord tissue. This mouse line is a cross between a microglial tamoxifen inducible cre line ($Cx3Cr1^{creERT2}$) and Ai14 (tdTomato reporter line). Naïve $Cx3Cr1^{creERT2}$; Ai14 mice were injected with 50mg/kg (i.p.) tamoxifen for 3 consecutive days after baseline threshold measurement. On Day 3 of tamoxifen injections, SNI or sham surgeries were performed. Spinal cord tissue was collected 7 days post-SNI since previous studies measuring pTrkB-ir indicated peak levels at this timepoint. Representative images show pTrkB-ir in ipsilateral DH of SNI and sham operated animals (figure 3.4 a1, b1), along with staining for tdTomato protein to visualize microglial profiles (figure 3.4 a2, b2). A merged or composite image confirms the overlap between pTrkB-ir and endogenous fluorescence driven by a microglial promoter (figure 3.4 a3, b3). A slightly higher magnification image from a different SNI operated male mouse allows for better visualization of the fine microglial processes (figure 3.4 c2) and the pTrkB-ir (figure 3.4 c1) present in these regions (figure 3.4 c3). Image quantification revealed that SNI increased pTrkB-ir in females at day 7 post-SNI but not in males ($p<0.05$, Two-way ANOVA, Tukey's HSD, figure 3.4 d). The overall area of

microglia in the DH was unchanged (figure 4.3 e), while the proportion of TrkB-ir in microglia was significantly higher in female SNI mice as compared to sham females ($p<0.05$, Two-Way ANOVA with Tukey's HSD, figure 3.4 f). These data suggest that female system is more responsive to SNI induced immune changes, but the low sample size of the male groups cannot be ignored and likely skewed the results. Lastly, we compared SNI induced pTrkB-ir increase between C57/Bl6 WT and $Cx3Cr1^{creERT2}$ X Ai14 mouse line on C57/Bl6 background which indicated that SNI increased pTrkB-ir to similar degrees in WT and transgenic mouse line used for better visualization of the entire microglial profile (figure 3.4 g). Unlike the Iba1-GFP line that expressed significantly higher pTrkBir, this transgenic mouse line does not differ from WT animals in its response to SNI induced TrkB activation. Furthermore, the proportion of overlap between pTrkB-ir and Iba1-GFP-ir was also higher in the Iba1-GFP line (Mean=56.3±6.8 (SD) on day 7 post-SNI) as compared to the mean overlap value seen in $Cx3Cr1^{creERT2}$ X Ai14 mouse line (Mean = 37±6.6 (SD)).

Functional role of microglial TrkB on SNI induced tactile hypersensitivity

Since we detected TrkB mRNA in microglia instead of BDNF mRNA and considerable portion of pTrkB-ir in microglial profiles after nerve injury, we next wanted to test whether the microglial TrkB is functionally required for maintaining nerve injury induced neuroplasticity. To determine functionality, a tamoxifen inducible microglial cre line was crossed with a homozygous TrkB floxed line to generate a mouse line in which microglia specific TrkB could be knocked down in a time-dependent manner without affecting normal neural development. $Cx3Cr1^{CreERT2/+;}$ $TrkB^{fl/fl}$ mice or $Cx3Cr1^{+/+}$;$TrkB^{fl/fl}$ (littermate controls) were tested to establish baseline tactile thresholds and injected with

50mg/kg (i.p) of 4-OHT (hydroxytamoxifen) once daily for 3 consecutive days. On third day of 4-OHT treatment, SNI surgeries were performed, and tactile thresholds were measured on days 3-, 7-, and 28- post-SNI. Behavioral testing did not show any sex- or treatment- differences between any of the groups on the side ipsilateral (figure 3.5 a) or contralateral to the injury (figure 3.5 b).

To verify the degree of microglial TrkB mRNA knockdown, spinal cord tissues were collected on day 29 post-SNI and RNAscope was performed for quantification. Representative images of ipsilateral DH from $Cx3Cr1^{creERT2/+;}$ $TrkB^{fl/fl}$ (henceforth referred to cre+ or microglial TrkB KO, figure 3.6 b1-4) or $Cx3Cr1^{+/+}$;$TrkB^{fl/fl}$ (henceforth referred to as cre- or littermake controls) SNI operated animals (figure 3.6 a1-4). Surprisingly, overall BDNF and TrkB mRNA was unchanged in the cre+ animals (microglial TrkB KO) as compared to their cre- littermate controls that were treated with 4-OHT and underwent SNI surgeries (figure 3.6 c, d). The microglial activation, defined by the area of DH occupied by Iba1-ir profiles, as well as proportion of TrkB mRNA in Iba1-ir profiles were significantly higher in male ($p<0.01$, Two-way ANOVA with Tukey's HSD) and female ($p<0.05$, Two-way ANOVA with Tukey's HSD) Cre+ animals as compared to their cre- counterparts (figure 3.6 e, f). These data indicate that microglia in DH of cre+ animals were more abundant and larger and occupied greater proportion of DH than microglia in cre- animals (figure 3.6 e). Similarly, the greater proportion of TrkB mRNA relative to DH ROI area, indicates higher proportion of TrkB mRNA in cre+ mice as compared to cre- mice (figure 3.6 f). The increased TrkB mRNA in cre+ DH might be due to a compensatory increase in TrkB mRNA in other cell types of the DH. To evaluate whether the TrkB mRNA density in microglia increases in cre+ animals,

the total area occupied by microglial portion of TrkB was normalized to the surface area of microglial profiles. When microglial TrkB mRNA was normalized to the size of microglia, the differences in animals of the two genotypes disappears (figures 3.6 g) which indicates that the increased TrkB mRNA was elevated proportionally with microglial profile expansion and proliferation.

These data collectively indicate that our microglial TrkB KD strategy was either unsuccessful, or it produced a greater immune response that resulted in elevated TrkB mRNA expression that outweighed the KD, or both situations contributed to the increased TrkB mRNA in microglia. Although our experimental strategy was ineffective, the verification efforts elucidated the potential compensatory mechanisms that may be triggered due to these genetic and pharmacological manipulations.

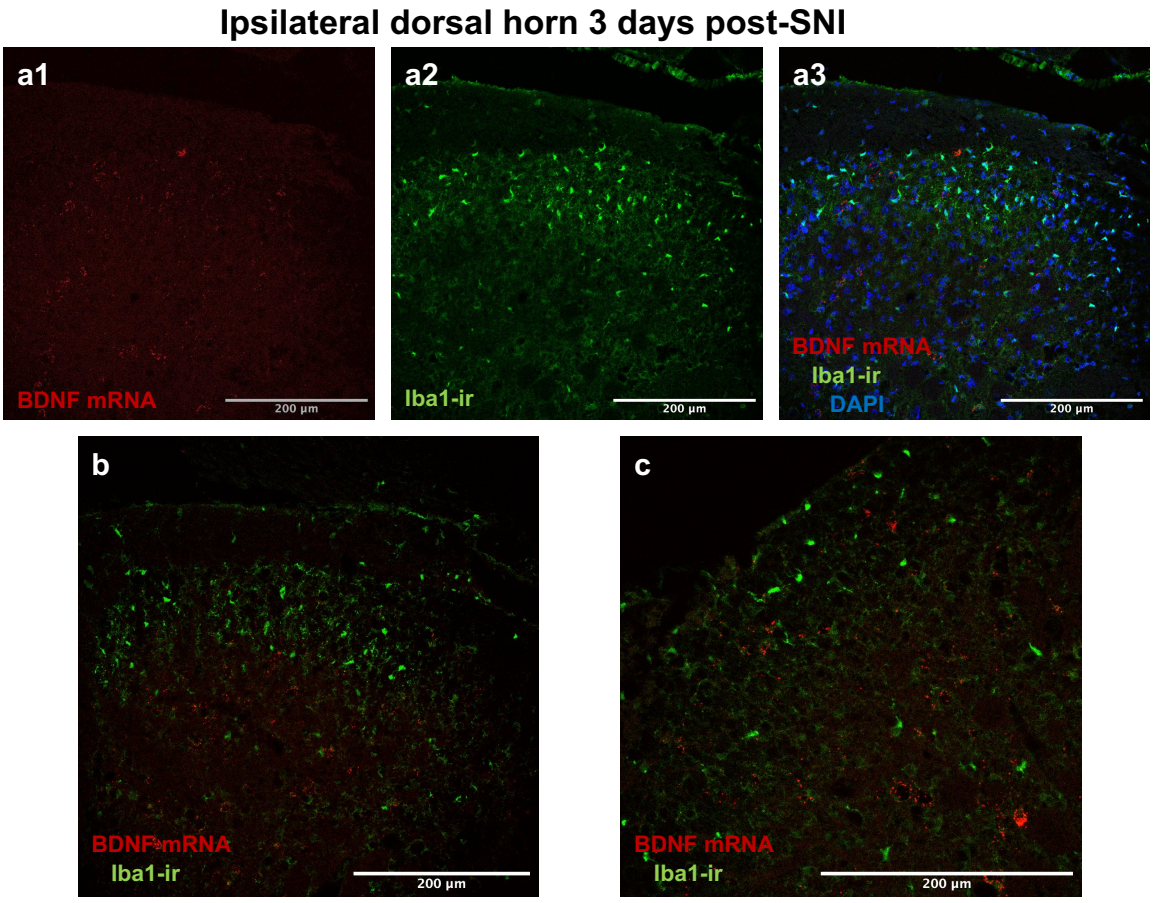

Figure 3.1: Visualization of BDNF mRNA in microglia. Representative images of DH sections collected from nerve injured ICR WT male mouse 3 days post-SNI (a1-3). BDNF mRNA (a1), Iba1-ir (a2) and DAPI stain were used to determine whether BDNF mRNA colocalizes with microglial profiles (a3). Scale bar = 200um. Additional images were collected from SNI operated ICR WT animals 3 days post-SNI, two of the representative images are included (b, c) and these images do not contain any overlap of BDNF mRNA signal with Iba1-ir.

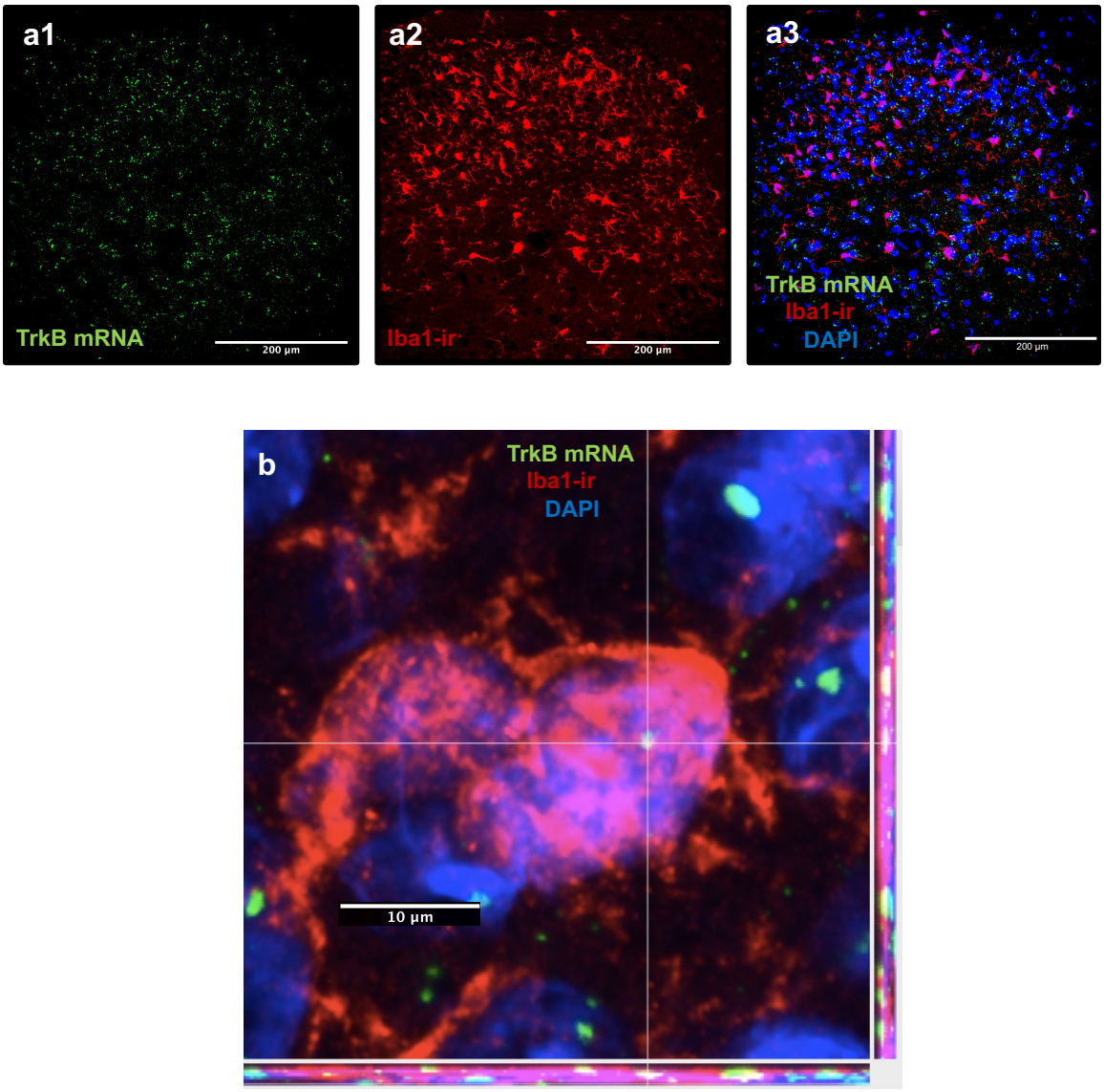

Figure 3.2: Visualizing and verifying TrkB mRNA expression in spinal microglia. Representative images of DH of a male mouse 3 days post-SNI show TrkB mRNA visualized using RNAscope® (a1), Iba1-ir visualized using anti-Iba1 antibody (a2), and nuclei visualized with DAPI staining (a3) Scale bars = 200um. A high-resolution image of an Iba1-ir and DAPI positive profile was collected to confirm that TrkB mRNA was located inside DAPI stained Iba1-ir wrapped structure (b); An orthogonal view (side panels) shows fluorescence intensity in that plane. Scale bar = 10um.

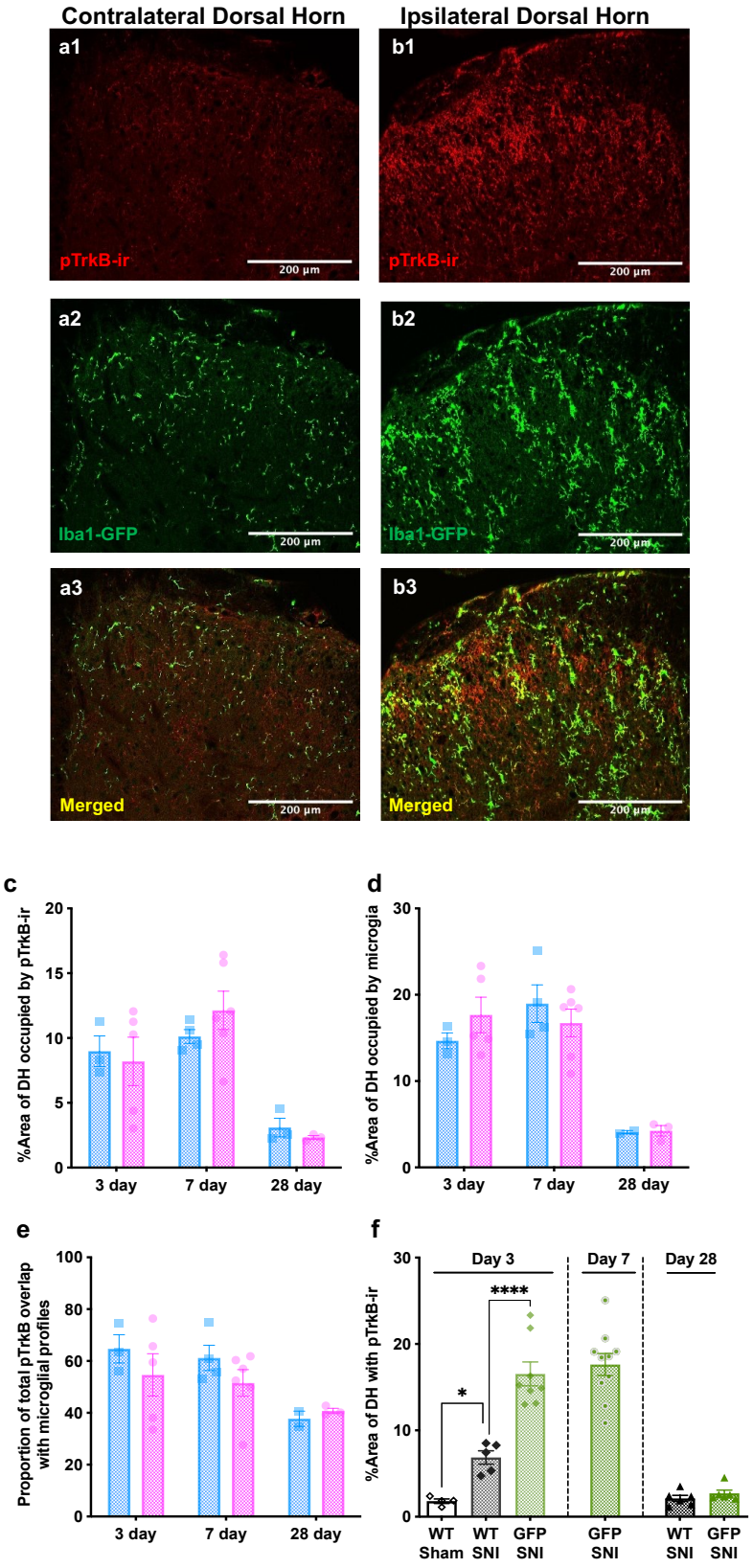
Contralateral Dorsal Horn
Ipsilateral Dorsal Horn
a1
pTrkB-ir
200 μm
b1
pTrkB-ir
200 μm
a2
Iba1-GFP
200 μm
b2
Iba1-GFP
200 μm
a3
Merged
200 μm
b3
Merged
200 μm
c
%Area of DH occupied by pTrkB-ir
0
5
10
15
20
3 day
7 day
28 day
d
%Area of DH occupied by microgia
0
10
20
30
3 day
7 day
28 day
e
Proportion of total pTrkB overlap with microglial profiles
0
20
40
60
80
100
3 day
7 day
28 day
f
%Area of DH with pTrkB-ir
Day 3
Day 7
Day 28
*
****
0
10
20
30
WT Sham
WT SNI
GFP SNI
GFP SNI
WT SNI
GFP SNI

Figure 3.3: Immunohistochemical analysis of pTrkB in spinal microglia using a Iba1-GFP transgenic mouse line. Representative image of pTrkB-ir and Iba1-GFP-ir in spinal DH contralateral (a1-3) and ipsilateral (b1-3) to nerve injury 7 days after SNI. pTrkB-ir (a1, b1) and Iba1-ir (a2, b2) in ipsilateral DH is higher as compared to the contralateral DH of the same animal. Scale bar = 200um, 20X magnification. Composite image shows considerable overlap between pTrkB-ir and Iba1-ir in ipsilateral DH as compared to the contralateral DH (a3, b3). Quantification of the pTrkB-ir in ipsilateral DH of male and female animals at day 3-, day 7- and day 28-post SNI as a percent of total DH area shows similar levels of pTrkB-ir in male and female mice (g). The percent area of DH occupied by Iba1-ir was used as a measure of microglial activation (h), and the proportion of total pTrkB-ir overlap with Iba1-ir profiles was used to determine localization of pTrkB in microglia(i). No sex-differences were observed in any of these measures at any timepoint. pTrkB-ir in Iba1-GFP mice and balb/c WT littermate controls indicate a greater increase in pTrkB-ir in Iba1-GFP mice (j). One way ANOVA (WT sham vs WT SNI vs GFP SNI) with Tukey's HSD. $p<0.05$*, $p<0.0001$****. Sample sizes (for g, h, i): 3day male (n=3), 3day female (n=5), day7 male (n=4), day7 female (n=6), 28day male (n=3), 28day female (n=3). Day 3: WT sham (n=4), WT SNI (n=5), GFP SNI (n=8). Day 7 GFP SNI (n=10). Day 28 WT SNI (n=6), GFP SNI (n=6).

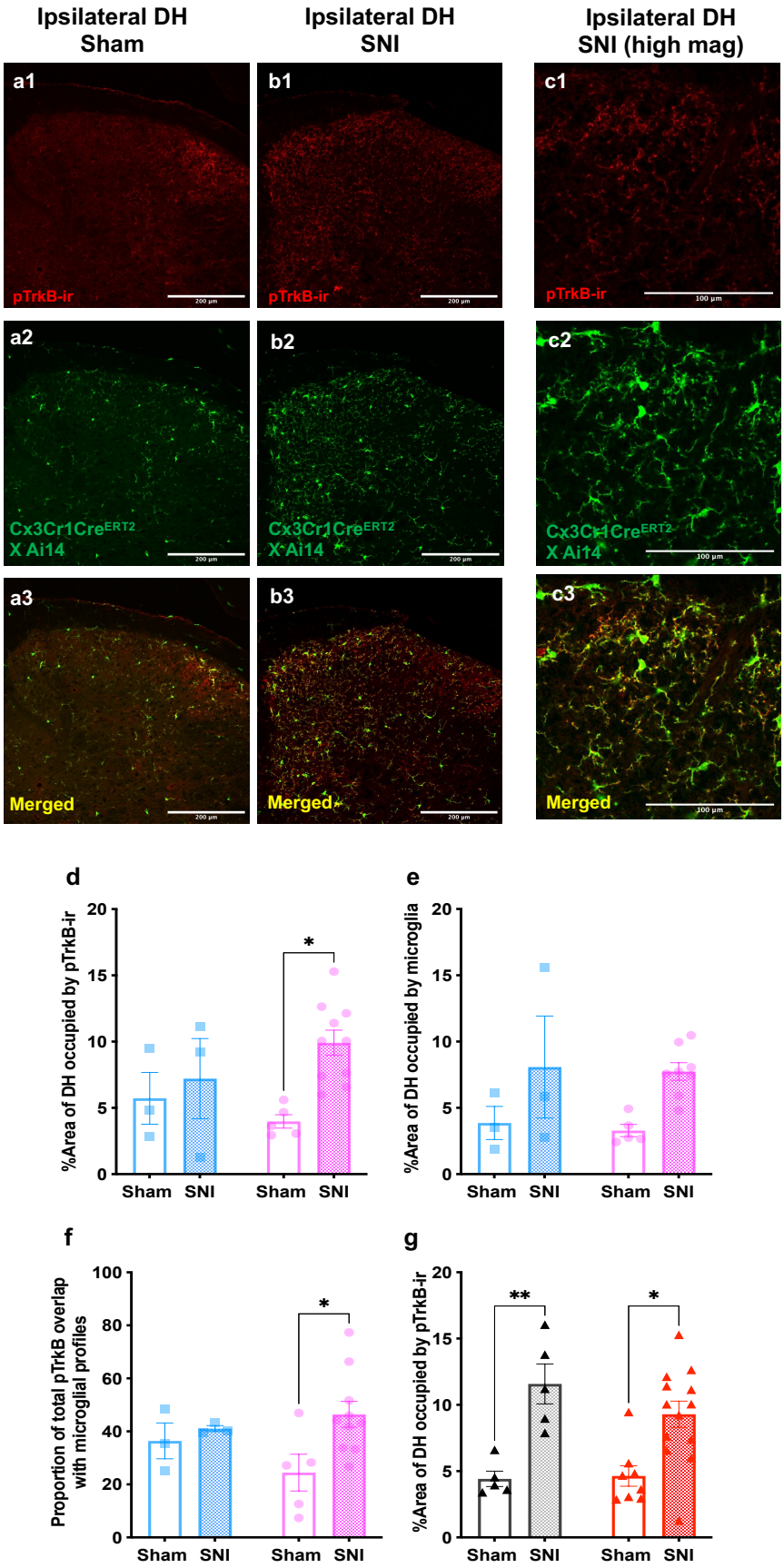
Ipsilateral DH
Sham
Ipsilateral DH
SNI
Ipsilateral DH
SNI (high mag)
a1
pTrkB-ir
b1
pTrkB-ir
c1
pTrkB-ir
a2
Cx3Cr1CreERT2
X Ai14
b2
Cx3Cr1CreERT2
X Ai14
c2
Cx3Cr1CreERT2
X Ai14
a3
Merged
b3
Merged
c3
Merged
d
%Area of DH occupied by pTrkB-ir
20
15
10
5
0
*
Sham
SNI
Sham
SNI
e
%Area of DH occupied by microglia
20
15
10
5
0
Sham
SNI
Sham
SNI
f
Proportion of total pTrkB overlap with microglial profiles
100
80
60
40
20
0
*
Sham
SNI
Sham
SNI
g
%Area of DH occupied by pTrkB-ir
20
15
10
5
0
**
*
Sham
SNI
Sham
SNI

Figure 3.4 Quantification of pTrkB-ir in spinal dorsal horn 7 days post-SNI in Cx3Cr1creERT2 X Ai14 mice and littermate controls. Representative images of ipsilateral DH from sham operated and SNI males 7 days post-SNI show higher pTrkB-ir (a1, b1) and microglial surface area visualized by microglial tdTomato expression (a2, b2) in injured animals. Higher magnification images collected from another animal at 7 days post-SNI shows the presence of pTrkB-ir (c1) in microglial profiles (c2) in a composite image (c3) Scale bar = 200um. Quantification of pTrkB-ir in injured mice shows increased pTrkB in injured females compared to sham females at day 7 post-SNI (d). Similarly, the surface area of DH occupied by microglia and the proportion of microglial pTrkB was also higher in SNI females as compared to sham females (e, f). A comparison of SNI induced increase in pTrkB-ir in C57/Bl6 WT (male and female) vs the transgenic (male and female) mice created on the C57/Bl6 background did not show significant effect of genotype on pTrkB-ir (g). The data from male and female mice of each genotype were combined for following comparison between genotypes since sex-differences were not observed within genotypes. Two-way ANOVA with Tukey's post-hoc test. $p<0.05$*, $p<0.01$**. Group sample sizes (d, e, f): Male sham (n=3), Male SNI (n=3), female sham (n=5), female SNI (n= 10). Sample size of WT sham (n=5), WT SNI (n=5), transgenic sham (n=8), transgenic SNI (n=13).

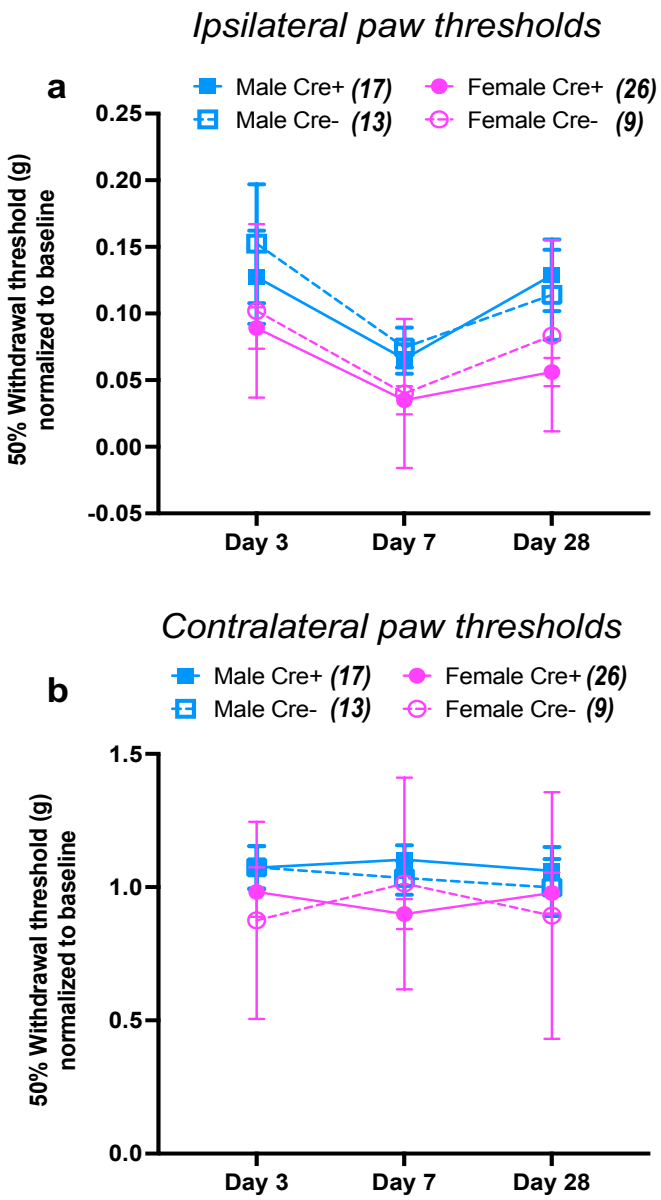

Figure 3.5: Measurement of tactile thresholds in hind paws ipsilateral (a) and contralateral (b) to nerve injury in tamoxifen inducible microglial TrkB KO male and female mice along with littermate controls. Cx3Cr1$^{creERT2/+}$ TrkB$^{fl/fl}$ (microglial TrkB KO) animals and littermate controls (Cx3Cr1$^{+/+}$;TrkB$^{fl/fl}$) were injected with 50mg/kg (i.p) 4-OHT from day -2, -1, and 0 relative to SNI and tested days 3-, 7- and 28-post-SNI did not show any reduction of behavioral hypersensitivity in microglial TrkB KO as compared to SNI operated control littermates (Two-way ANOVA). Number of animals: male Cre+ (n=17), male Cre- (n=13), female Cre+ (n=26), female Cre- (n=9).

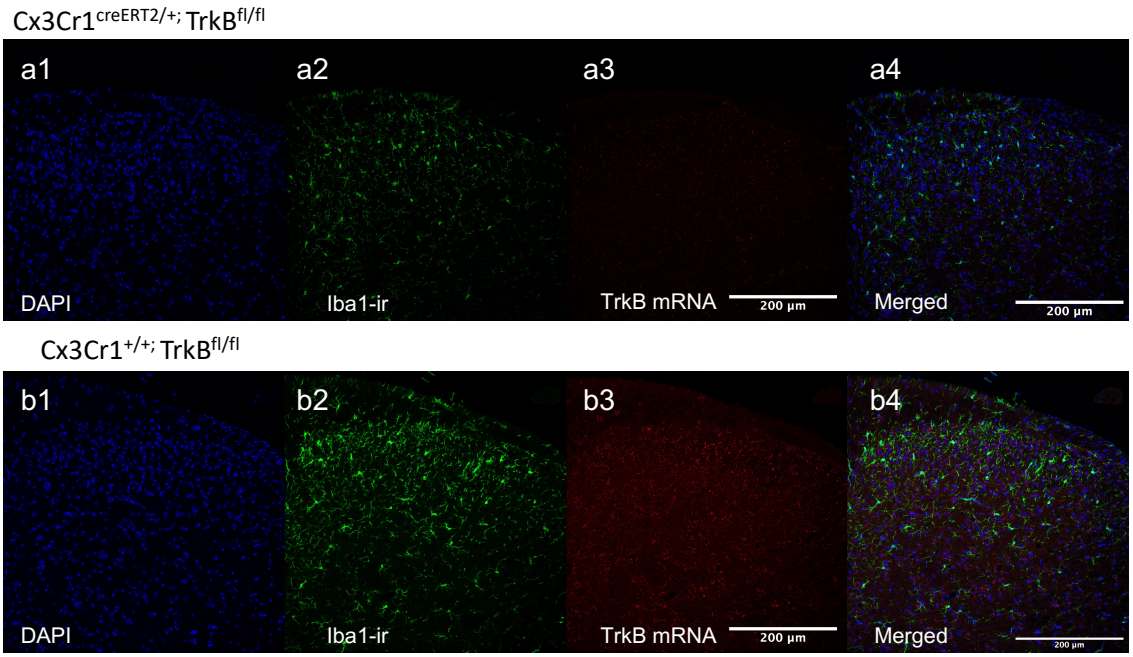
Cx3Cr1creERT2/+; TrkBfl/fl
a1
a2
a3
a4
DAPI
Iba1-ir
TrkB mRNA
200 μm
Merged
200 μm
Cx3Cr1+/+; TrkBfl/fl
b1
b2
b3
b4
DAPI
Iba1-ir
TrkB mRNA
200 μm
Merged
200 μm

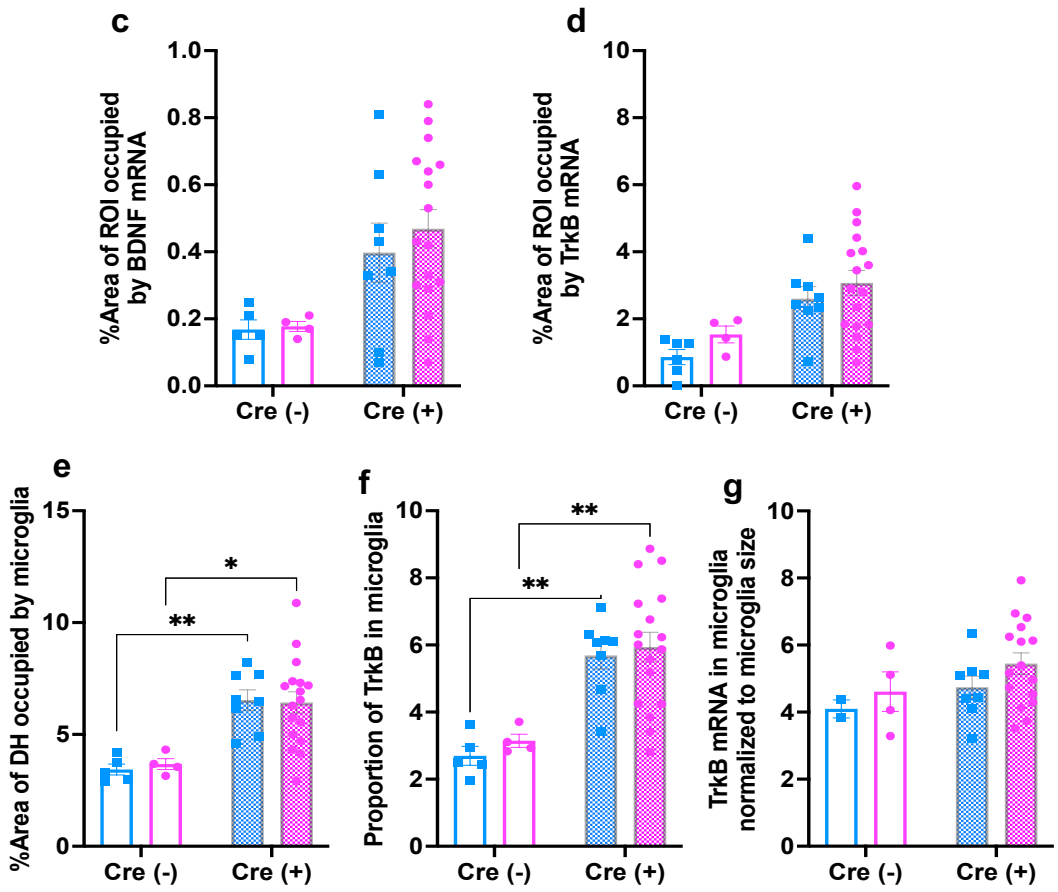
c
%Area of ROI occupied by BDNF mRNA
1.0
0.8
0.6
0.4
0.2
0.0
Cre (-)
Cre (+)
d
%Area of ROI occupied by TrkB mRNA
10
8
6
4
2
0
Cre (-)
Cre (+)
e
%Area of DH occupied by microglia
15
10
5
0
*
**
Cre (-)
Cre (+)
f
Proportion of TrkB in microglia
10
8
6
4
2
0
**
**
Cre (-)
Cre (+)
g
TrkB mRNA in microglia normalized to microglia size
10
8
6
4
2
0
Cre (-)
Cre (+)

Figure 3.6: Evaluating degree of microglial TrkB knockdown in DH of spinal cord. Representative images of DH of $Cx3Cr1^{+/+}$;$TrkB^{fl/fl}$ (control littermates a1-4) and $Cx3Cr1^{CreERT2/+}$:$TrkB^{fl/fl}$ (microglial TrkB KO, b1-4) shows increased Iba1-ir and elevated TrkB mRNA in microglial TrkB KO mice. 25X magnification, scale bars = 200um. DAPI staining (a1,b1), Iba1-ir (a2, b2), TrkB mRNA (a3, b3), and merged image (a4, b4). The proportion of ipsilateral dorsal horn occupied by BDNF and TrkB mRNA in $Cx3Cr1^{CreERT2/+}$:$TrkB^{fl/fl}$ tamoxifen treated SNI males and females as compared to SNI operated tamoxifen treated $Cx3Cr1^{+/+}$;$TrkB^{fl/fl}$ (c,d) was not different between any of the groups. The area of DH occupied by iba1-ir profiles (e) and proportion of *TrkB* mRNA overlap with Iba1-ir cells (f) is higher in the Cre+ group as compared to their cre negative counterpart in males ($p<0.01$) and females ($p<0.05$) (Two-way ANOVA with Tukey's HSD). However, when the area of microglial *TrkB* mRNA is normalized to the area of iba1+ profiles, there is no difference in the amount of microglial *TrkB* expression between groups (g). $p<0.05$*, $p<0.01$**. Sample sizes: Male Cre- (n= 5), male cre+ (n= 8), female cre- (n= 4), female cre+ (n= 17).

DISCUSSION

Microglia are considered an important cell type in nociceptive signaling due to their role in injury induced neuroplasticity. They are thought to contribute to the massive neural reorganization by releasing BDNF which on its own produces LTP, increases excitability of spinal neurons, and triggers a multitude of signaling cascades. However, there is no direct evidence indicating that microglia produce or express BDNF. One study measured miniscule amounts of BDNF release from neonatal cortical microglial cultures stimulated with ATP in vitro (Coull et al., 2005), and a follow up study performed immunohistochemical analysis on spinal cord dorsal horn to show BDNF-ir in microglia using an unvalidated anti-BDNF antibody (Ulmann et al., 2008). Most of the data that suggest the importance of microglia in BDNF-TrkB signaling include the study of functional changes in downstream effectors or behavior (Ulmann et al., 2008; Inoue, 2009; Zhou et al., 2011; Chen et al., 2014b). In these instances, the contribution of microglia to the BDNF-TrkB signaling specifically is difficult to assess since microglia serve many other neuroprotective and pro-inflammatory roles in the CNS (Ledeboer et al., 2005; Moalem and Tracey, 2006; Vallejo et al., 2010; Ji et al., 2013; Ramesh et al., 2013). Given the lack of clarity regarding the expression and release of BDNF, we aimed to use new and improved *in situ* hybridization method RNAscope® to visualize *BDNF* expression in microglia which would allow us to detect very small amounts of mRNA. We did not detect *BDNF* mRNA colocalization with microglial profiles, but instead we noted considerable microglial *TrkB* mRNA expression. The mRNA signal overlap with microglial profiles was not quantified because the tissue processing required for mRNA visualization destroys antigen epitopes, while tissue processing for IHC does not label

mRNA. Given this inverse relationship, to visualize both simultaneously, we underestimate both signals. This discrepancy is not problematic to demonstrate co-localization, but any quantification of the overlap would not be informative or accurate. that was verified with high resolution imaging to confirm the localization of *TrkB* mRNA in nuclei of microglia.

Limited information is available regarding the role of microglial BDNF-TrkB in injury induced maladaptive neuroplasticity. It is possible that microglia contribute to BDNF-TrkB signaling by engaging in an autocrine signaling loop that is triggered and maintained by continuous TrkB activation via fl-TrkB in microglia.

To determine the extent of injury induced changes in microglial TrkB activation, we utilized two transgenic mouse lines to genetically encode fluorescent molecules in microglia. Using these mouse lines, we discovered that about half of the activated TrkB signal can be localized to microglia. We confirmed the generalizability of these lines by comparing the injury induced changes in WT animals to estimate the degree of change in TrkB activation in genetically unaltered mice. Furthermore, we generated a tamoxifen inducible microglial TrkB knock-out line to selectively delete microglial TrkB around the time of injury and test its requirement on the development and maintenance of behavioral hypersensitivity as well as spinal microglial activation. We found that microglial cre expressing mice had tactile thresholds that were indistinguishable from the control animals, suggesting that microglial TrkB is dispensable in spinal neuroplasticity that results in behavioral hypersensitivity. However, further characterization of the tissues from these mice confirmed that the experimental manipulations were either unsuccessful or had compensatory changes that increased microglial activation and pTrkB-ir in

animals that were supposed to lack microglial *TrkB*. One possible explanation is that a subset of spinal microglia and macrophages that do not express Cx3Cr1 transcription factor increase their own expression of *TrkB* which compensated for the lack of *TrkB* mRNA in cre+ mouse DHs.

Taken together, these data present a complicated view of TrkB function in microglia but also the challenges of selectively manipulating receptor expression in specific cell types. Finally, the studies presented here also emphasize the need for data collection to verify success rate and efficacy of any manipulation or treatment employed in experimental manipulation. Collectively, the data presented here will significantly contribute to our collective understanding of the function of microglia in nociceptive circuitry and its involvement in BDNF-TrkB signaling.

OVERALL SUMMARY

BDNF-TrkB signaling is widely studied for its role in neuroplasticity in general, and in maladaptive plasticity in nociceptive systems following nerve injury. The wide range of studies investigating functional consequences of exogenous BDNF application or sequestration of endogenous BDNF on the system of interest (Miki et al., 2000; Eaton et al., 2002; Coull et al., 2005; Constandil et al., 2011; Chen et al., 2014b; Ding et al., 2015; Li et al., 2017; Wu et al., 2021), provide evidence for the myriad of short- and long-term changes in neural signaling that can be attributed to BDNF. Despite the ubiquity of research on effects of BDNF, very little direct evidence of its expression (Geng et al., 2010), localization, and regulation after nerve injury exists. Similarly, the evidence for the BDNF receptor, TrkB, is also lacking. Given the importance of this signaling system in producing a chronic neuropathic pain state, we aimed to understand the expression patterns of the two molecules, as well as any injury induced changes in its expression and functional roles of this signaling.

Information presented in this thesis fills gaps in the existing literature regarding BDNF-TrkB signaling and provides a comprehensive characterization of expression patterns of these molecules and their activity. First, mRNA expression of BDNF and TrkB in DRG neurons, satellite cells, and spinal cord dorsal horn after nerve injury was examined in detail, along with TrkB protein expression in spinal cords of male and female mice (Chapter 1). The extent of TrkB activity following nerve injury in male and female animals was quantified and no sex-differences were detected in the degree of TrkB activation, which disputes the notion that female mice lack BDNF-TrkB signaling in spinal cord (Sorge et al., 2015) (Chapter 2). The functional role of TrkB activity was

also investigated by using a TrkB inhibitor, ANA-12, and surprising results indicated an inverse relationship between TrkB activation and behavioral hypersensitivity in both sexes (Chapter 2). Lastly, high resolution images indicated an absence of BDNF mRNA in microglia, which contradicts the assumptions in the field regarding the source of BDNF (Tsuda et al., 2005; Moalem and Tracey, 2006; Ji and Suter, 2007; Scholz and Woolf, 2007; Vallejo et al., 2010; Sorge et al., 2015) in chronic neuropathic pain (Chapter 3). Interestingly, we detected TrkB mRNA in microglia, and conducted additional investigation to quantify the extent of TrkB activity in microglia after nerve injury and generated conditional knockout mice to determine the functional role of microglial TrkB in the injury-induced pain behaviors (Chapter 3). Collectively, these data provide a thorough characterization of the expression and activity patterns of BDNF and its receptor in a time- and sex-dependent manner in a model of chronic neuropathic pain.

FUTURE DIRECTIONS

BDNF and TrkB protein expression patterns

Although we quantified TrkB protein levels (fl-TrkB and truncated TrkB) after nerve injury using Western blot assay, we could not detect TrkB levels via IHC due to the lack of validated antibodies. Future studies should utilize specific antibodies directed against the TrkB isoforms to understand its spatial expression patterns in the DH after injury. A similar study of the BDNF protein is crucial to our understanding of the role and mechanism by which BDNF participates in injury related changes. As mentioned previously, only few studies have attempted to measure BDNF levels in spinal cord, and even fewer have been able to successfully detect it. A careful and thorough characterization of BDNF protein expression and localization in different cell types of spinal cord is necessary for the fundamental understanding of the role of BDNF in neuroplasticity in a nociceptive system. A greater emphasis needs to be placed on development and testing of antibodies specific to BDNF and its receptors, and widely and uniformly used by different research groups to generate a cohesive narrative of the role of BDNF-TrkB signaling in chronic pain.

TrkB function in injury induced hypersensitivity in male and female animals

Disruption of BDNF activity rather than altering TrkB function is commonly used in studies of BDNF/TrkB signaling, mostly due to lack of proper TrkB tools. The only study in which TrkB activity was blocked included a transgenic line in which TrkB containing sensory neurons were photoablated (Dhandapani et al., 2018), while another generated a knock-in line in which the endogenous TrkB receptor was replaced with a genetically modified TrkB receptor that can be blocked with a synthetic ligand (Wang et

al., 2009). Both studies included female mice, but either they did not detect and therefore did not report sex-differences, or any sex-differences were not highlighted or mentioned. This is an important point because other studies that manipulate microglial function (Sorge et al., 2015; Taves et al., 2016) have shown sex-differences, and this has led to the overinterpretation of the data considering the lack of information regarding BDNF-TrkB signaling in females. However, a recent study reported that changes downstream of BDNF-TrkB signaling, KCC2 channel downregulation, occurs in both sexes suggesting that pathways in male and female mice converge downstream of BDNF-TrkB (Mapplebeck et al., 2019). This could be due to an alternate pathway in females (separate from BDNF-TrkB) leads to the same downstream outcomes as BDNF-TrkB signaling accomplishes in males. Regardless of the pathways involved, the sites at which the male and female systems converge is crucial in developing therapeutic strategies for chronic pain that are effective in male and female systems.

New pharmacological tools to inhibit TrkB function need to be characterized and efficacy confirmed each time the drugs are used. Existing literature regarding contribution of TrkB signaling to neuronal excitability or downstream signaling pathways utilize a drug, K25a, assumed to be TrkB specific inhibitor, however it is now known to be a pan-Trk and PKC inhibitor. A novel small-molecule TrkB specific inhibitor (Cazorla et al., 2011) is now available but has not been widely used and therefore the stability, efficacy, and specificity of the drug has not been well characterized. In our experiments, ANA-12 had modest effects, but the vehicle required to dissolve the drug had unexpected side-effects that should be explored further. In addition, other studies that have reported using ANA-12 (Chen et al., 2014b; Moy et al., 2019) need to be transparent with their

methods sections and include control groups to determine existence of side-effects from the vehicle. Finally, additional experiments need to be done to determine the effect of the manipulations used to alter TrkB functions on the underlying neurophysiological systems to verify the treatment, tools, and reagents have similar effects in male and female animals.

The role of Microglia in BDNF-TrkB signaling

More research needs to be done to determine if spinal microglia produce BDNF and the exact role of microglia in BDNF-TrkB signaling. Although we did not detect BDNF mRNA using a highly sensitive and specific *in situ* hybridization method, we cannot rule out the possibility that *BDNF* mRNA is present in spinal microglia at levels that are below the detection limit of this method. Different assays may be required to visualize, quantify, and detect *BDNF* mRNA in microglia. Furthermore, additional studies are required to understand the role and function of microglial TrkB, and whether it is functionally relevant for nerve injury induced neuroplasticity. Given the variety of tools used to investigate function of BDNF-TrkB signaling, the efficacy and specificity of the manipulations should be verified.

FINAL CONCLUSIONS

Chronic pain affects millions of people in the US and costs billions in health care and lost productivity (CDC, 2018; CE et al., 2020). Neuropathic pain is notoriously difficult to treat, and current pain treatments are only about 60% effective (Stemkowski et al., 2013; Abdulrahman and Alsafi, 2020). Basic science research has provided and continues to generate new knowledge regarding the mechanisms underlying neuroplasticity in chronic pain (Khan and Smith, 2015; Abdulrahman and Alsafi, 2020). Many novel therapies have been developed based on the mechanistic information provided through pre-clinical research (Abdulrahman and Alsafi, 2020). BDNF continues to garner great interest as a potential target for pain therapies due to its involvement in many aspects and types of processes involved in maladaptive neuroplasticity underlying neuropathic pain. Data presented in this thesis contributes to the enormous literature on the role of BDNF-TrkB signaling in neuroplasticity that underlies chronic neuropathic pain. Specifically, this thesis provides a broad framework by evaluating BDNF and TrkB expression and function at multiple timepoints after nerve injury and in both sexes. Majority of the data in this field was collected only in male subjects, and often at a single timepoint or a single region of the CNS. Although the data presented here are by no means comprehensive, they do serve an important function in contextualizing existing literature on BDNF-TrkB activity, the role of microglia in this signaling, and a basic framework in which to interpret sex-differences in this signaling. A holistic and nuanced understanding of these neurobiological process is crucial for the development of therapies that are safe, effective, and equitable.

BIBLIOGRAPHY

Abdulrahman NSH, Alsafi MYB (2020) Discovery of Novel Analgesic Agents Targeting Neuropathic Pain: Computer-Aided Drug Design. Chem Pharm Res 2.

Barbacid M (1994) The Trk family of neurotrophin receptors. J Neurobiol 25:1386–1403.

Bardoni R, Merighi A (2009) Synaptic Plasticity in Pain. :89–108.

Berkley KJ (1997) Sex differences in pain. Behav Brain Sci 20:371–380.

Biggs JE, Lu VB, Stebbing MJ, Balasubramanyan S, Smith PA (2010) Is BDNF sufficient for information transfer between microglia and dorsal horn neurons during the onset of central sensitization? Mol Pain 6:44.

Borodinova AA, Salozhin SV (2017) Differences in the Biological Functions of BDNF and proBDNF in the Central Nervous System. Neurosci Behav Physiology 47:251–265.

Bramham CR, Messaoudi E (2005) BDNF function in adult synaptic plasticity: The synaptic consolidation hypothesis. Prog Neurobiol 76:99–125.

Buchholz RA, Dundore RL, Cumiskey WR, Harris AL, Silver PJ (2018) Protein kinase inhibitors and blood pressure control in spontaneously hypertensive rats. Hypertension 17:91–100.

Cao T, Matyas JJ, Renn CL, Faden AI, Dorsey SG, Wu J (2020) Function and Mechanisms of Truncated BDNF Receptor TrkB.T1 in Neuropathic Pain. Cells 9:1194.

Cazorla M, Prémont J, Mann A, Girard N, Kellendonk C, Rognan D (2011) Identification of a low–molecular weight TrkB antagonist with anxiolytic and antidepressant activity in mice. J Clin Invest 121:1846–1857.

CDC (2018) P revalence of chronic pain and high-impact chronic pain among adults—United States, 2016. MMWR Morb Mortal Wkly Rep 67:1001–1006.

CE Z, JM D, JW L, EM C (2020) Chronic pain and high-impact chronic pain among U.S. adults, 2019. Hyattsville, MD: National Center for Health Statistics.

Chaplan SR, Bach FW, Pogrel JW, Chung JM, Yaksh TL (1994) Quantitative assessment of tactile allodynia in the rat paw. J Neurosci Meth 53:55–63.

Chen JT, Guo D, Campanelli D, Frattini F, Mayer F, Zhou L, Kuner R, Heppenstall PA, Knipper M, Hu J (2014a) Presynaptic GABAergic inhibition regulated by BDNF contributes to neuropathic pain induction. Nat Commun 5:5331.

Chen W, Walwyn W, Ennes HS, Kim H, McRoberts JA, Marvizón JCG (2014b) BDNF released during neuropathic pain potentiates NMDA receptors in primary afferent terminals. European J Neurosci 39:1439–1454.

Clark AK, Yip PK, Grist J, Gentry C, Staniland AA, Marchand F, Dehvari M, Wotherspoon G, Winter J, Ullah J, Bevan S, Malcangio M (2007) Inhibition of spinal microglial cathepsin S for the reversal of neuropathic pain. Proc National Acad Sci 104:10655–10660.

Constandil L, Aguilera R, Goich M, Hernández A, Alvarez P, Infante C, Pelissier T (2011) Involvement of spinal cord BDNF in the generation and maintenance of chronic neuropathic pain in rats. Brain Res Bull 86:454–459.

Coull JAM, Beggs S, Boudreau D, Boivin D, Tsuda M, Inoue K, Gravel C, Salter MW, Koninck YD (2005) BDNF from microglia causes the shift in neuronal anion gradient underlying neuropathic pain. Nature 438:1017–1021.

Decosterd I, Woolf CJ (2000) Spared nerve injury: an animal model of persistent peripheral neuropathic pain. Pain 87:149–158.

Dembo T, Braz JM, Hamel KA, Kuhn JA, Basbaum AI (2018) Primary afferent-derived BDNF contributes minimally to the processing of pain and itch. Eneuro 5:ENEURO.0402-18.2018.

Dhandapani R, Arokiaraj CM, Taberner FJ, Pacifico P, Raja S, Nocchi L, Portulano C, Franciosa F, Maffei M, Hussain AF, Reis F de C, Reymond L, Perlas E, Garcovich S, Barth S, Johnsson K, Lechner SG, Heppenstall PA (2018) Control of mechanical pain hypersensitivity in mice through ligand-targeted photoablation of TrkB-positive sensory neurons. Nat Commun 9:1640.

Ding X, Cai J, Li S, Liu X-D, Wan Y, Xing G-G (2015) BDNF contributes to the development of neuropathic pain by induction of spinal long-term potentiation via SHP2 associated GluN2B-containing NMDA receptors activation in rats with spinal nerve ligation. Neurobiol Dis 73:428–451.

Dixon WJ (2012) The Up-and-Down Method for Small Samples. J Am Stat Assoc 60:967–978.

Doyle HH, Eidson LN, Sinkiewicz DM, Murphy AZ (2017) Sex Differences in Microglia Activity within the Periaqueductal Gray of the Rat: A Potential Mechanism Driving the Dimorphic Effects of Morphine. J Neurosci 37:3202–3214.

Eaton MJ, Blits B, Ruitenberg MJ, Verhaagen J, Oudega M (2002) Amelioration of chronic neuropathic pain after partial nerve injury by adeno-associated viral (AAV) vector-mediated over-expression of BDNF in the rat spinal cord. Gene Ther 9:1387–1395.

Fillingim RB, King CD, Ribeiro-Dasilva MC, Rahim-Williams B, Riley JL (2009) Sex, Gender, and Pain: A Review of Recent Clinical and Experimental Findings. J Pain 10:447–485.

Foster E, Robertson B, Fried K (1994) trkB-like immunoreactivity in rat dorsal root ganglia following sciatic nerve injury. Brain Res 659:267–271.

Fukuoka T, Kondo E, Dai Y, Hashimoto N, Noguchi K (2001) Brain-Derived Neurotrophic Factor Increases in the Uninjured Dorsal Root Ganglion Neurons in Selective Spinal Nerve Ligation Model. J Neurosci 21:4891–4900.

Garraway SM, Huie JR (2016) Spinal Plasticity and Behavior: BDNF-Induced Neuromodulation in Uninjured and Injured Spinal Cord. Neural Plast 2016:1–19.

Geng S-J, Liao F-F, Dang W-H, Ding X, Liu X-D, Cai J, Han J-S, Wan Y, Xing G-G (2010) Contribution of the spinal cord BDNF to the development of neuropathic pain by activation of the NR2B-containing NMDA receptors in rats with spinal nerve ligation. Exp Neurol 222:256–266.

Greenspan JD, Craft RM, LeResche L, Arendt-Nielsen L, Berkley KJ, Fillingim RB, Gold MS, Holdcroft A, Lautenbacher S, Mayer EA, Mogil JS, Murphy AZ, Traub RJ, IASP the CWG of the S Gender, and Pain SIG of the (2007) Studying sex and gender differences in pain and analgesia: A consensus report. Pain 132:S26–S45.

Groth R, Aanonsen L (2002) Spinal brain-derived neurotrophic factor (BDNF) produces hyperalgesia in normal mice while antisense directed against either BDNF or trkB, prevent inflammation-induced hyperalgesia. Pain 100:171–181.

Guan Z, Kuhn JA, Wang X, Colquitt B, Solorzano C, Vaman S, Guan AK, Evans-Reinsch Z, Braz J, Devor M, Abboud-Werner SL, Lanier LL, Lomvardas S, Basbaum AI (2015) Injured sensory neuron–derived CSF1 induces microglial proliferation and DAP12-dependent pain. Nat Neurosci 19:94–101.

Ha SO, Kim JK, Hong HS, Kim DS, Cho HJ (2001) Expression of brain-derived neurotrophic factor in rat dorsal root ganglia, spinal cord and gracile nuclei in experimental models of neuropathic pain. Neuroscience 107:301–309.

Hildebrand ME, Xu J, Dedek A, Li Y, Sengar AS, Beggs S, Lombroso PJ, Salter MW (2016) Potentiation of Synaptic GluN2B NMDAR Currents by Fyn Kinase Is Gated through BDNF-Mediated Disinhibition in Spinal Pain Processing. Cell Reports 17:2753–2765.

Ikeda K, Hazama K, Itano Y, Ouchida M, Nakatsuka H (2020) Development of a novel analgesic for neuropathic pain targeting brain-derived neurotrophic factor. Biochem Bioph Res Co.

Imai Y, Kohsaka S (2002) Intracellular signaling in M-CSF-induced microglia activation: Role of Iba1. Glia 40:164–174.

Inoue K (2009) The mechanism and control of neuropathic pain. Rinsho Shinkeigaku 49:779–782.

Ito D, Imai Y, Ohsawa K, Nakajima K, Fukuuchi Y, Kohsaka S (1998) Microglia-specific localisation of a novel calcium binding protein, Iba1. Mol Brain Res 57:1–9.

Ji R-R, Berta T, Nedergaard M (2013) Glia and pain: Is chronic pain a gliopathy? Pain 154:S10–S28.

Ji R-R, Suter MR (2007) p38 MAPK, Microglial Signaling, and Neuropathic Pain. Mol Pain 3:1744-8069-3–33.

Jin S-X, Zhuang Z-Y, Woolf CJ, Ji R-R (2003) p38 Mitogen-Activated Protein Kinase Is Activated after a Spinal Nerve Ligation in Spinal Cord Microglia and Dorsal Root Ganglion Neurons and Contributes to the Generation of Neuropathic Pain. J Neurosci 23:4017–4022.

Kanazawa H, Ohsawa K, Sasaki Y, Kohsaka S, Imai Y (2002) Macrophage/Microglia-specific Protein Iba1 Enhances Membrane Ruffling and Rac Activation via Phospholipase C-γ-dependent Pathway*. J Biol Chem 277:20026–20032.

Khan N, Smith MT (2015) Neurotrophins and Neuropathic Pain: Role in Pathobiology. Molecules 20:10657–10688.

Kitayama T, Morita K, Motoyama N, Dohi T (2016) Down-regulation of zinc transporter-1 in astrocytes induces neuropathic pain via the brain-derived neurotrophic factor - K+-Cl− co-transporter-2 signaling pathway in the mouse spinal cord. Neurochem Int 101:120–131.

Klein R, Nanduri V, Jing S, Lamballe F, Tapley P, Bryant S, Cordon-Cardo C, Jones KR, Reichardt LF, Barbacid M (1991) The trkB tyrosine protein kinase is a receptor for brain-derived neurotrophic factor and neurotrophin-3. Cell 66:395–403.

Ledeboer A, Sloane EM, Milligan ED, Frank MG, Mahony JH, Maier SF, Watkins LR (2005) Minocycline attenuates mechanical allodynia and proinflammatory cytokine expression in rat models of pain facilitation. Pain 115:71–83.

León A de, Gibon J, Barker PA (2020) NGF- and BDNF-dependent DRG sensory neurons deploy distinct degenerative signaling mechanisms. Eneuro 8:ENEURO.0277-20.2020.

Li S, Cai J, Feng Z-B, Jin Z-R, Liu B-H, Zhao H-Y, Jing H-B, Wei T-J, Yang G-N, Liu L-Y, Cui Y-J, Xing G-G (2017) BDNF Contributes to Spinal Long-Term Potentiation and Mechanical Hypersensitivity Via Fyn-Mediated Phosphorylation of NMDA Receptor GluN2B Subunit at Tyrosine 1472 in Rats Following Spinal Nerve Ligation. Neurochem Res 42:2712–2729.

Lu B, Pang PT, Woo NH (2005) The yin and yang of neurotrophin action. Nat Rev Neurosci 6:603–614.

Mannion RJ, Costigan M, Decosterd I, Amaya F, Ma Q-P, Holstege JC, Ji R-R, Acheson A, Lindsay RM, Wilkinson GA, Woolf CJ (1999) Neurotrophins: Peripherally and centrally acting modulators of tactile stimulus-induced inflammatory pain hypersensitivity. Proc National Acad Sci 96:9385–9390.

Manson JE (2010) Pain: sex differences and implications for treatment. Metabolis 59:S16–S20.

Mapplebeck JCS, Beggs S, Salter MW (2017) Molecules in pain and sex: a developing story. Mol Brain 10:9.

Mapplebeck JCS, Dalgarno R, Tu Y, Moriarty O, Beggs S, Kwok CHT, Halievski K, Assi S, Mogil JS, Trang T, Salter MW (2018) Microglial P2X4R-evoked pain hypersensitivity is sexually dimorphic in rats. Pain 159:1752–1763.

Mapplebeck JCS, Lorenzo L-E, Lee KY, Gauthier C, Muley MM, Koninck YD, Prescott SA, Salter MW (2019) Chloride Dysregulation through Downregulation of KCC2 Mediates Neuropathic Pain in Both Sexes. Cell Reports 28:590-596.e4.

Marchand F, Perretti M, McMahon SB (2005) Role of the Immune system in chronic pain. Nat Rev Neurosci 6:521–532.

Marcol W, Kotulska K, Larysz-Brysz M, Kowalik JL (2007) BDNF contributes to animal model neuropathic pain after peripheral nerve transection. Neurosurg Rev 30:235–243.

Merighi A, Salio C, Ghirri A, Lossi L, Ferrini F, Betelli C, Bardoni R (2008) BDNF as a pain modulator. Prog Neurobiol 85:297–317.

Mestre C, Pélissier T, Fialip J, Wilcox G, Eschalier A (1994) A method to perform direct transcutaneous intrathecal injection in rats. J Pharmacol Toxicol 32:197–200.

Michael GJ, Averill S, Shortland PJ, Yan Q, Priestley JV (1999) Axotomy results in major changes in BDNF expression by dorsal root ganglion cells: BDNF expression in large trkB and trkC cells, in pericellular baskets, and in projections to deep dorsal horn and dorsal column nuclei. Eur J Neurosci 11:3539–3551.

Middlemas DS, Lindberg RA, Hunter T (1991) trkB, a neural receptor protein-tyrosine kinase: evidence for a full-length and two truncated receptors. Mol Cell Biol 11:143–153.

Miki K, Fukuoka T, Tokunaga A, Kondo E, Dai Y, Noguchi K (2000) Differential effect of brain-derived neurotrophic factor on high-threshold mechanosensitivity in a rat neuropathic pain model. Neurosci Lett 278:85–88.

Milligan ED, Watkins LR (2009) Pathological and protective roles of glia in chronic pain. Nat Rev Neurosci 10:23–36.

Milosavljević A, Jančić J, Mirčić A, Dožić A, Boljanović J, Milisavljević M, Ćetković M (2020) Morphological and functional characteristics of satellite glial cells in the peripheral nervous system. Folia Morphol.

Minichiello L (2009) TrkB signalling pathways in LTP and learning. Nat Rev Neurosci 10:850–860.

Mitre M, Mariga A, Chao MV (2016) Neurotrophin signalling: novel insights into mechanisms and pathophysiology. Clin Sci 131:13–23.

Moalem G, Tracey DJ (2006) Immune and inflammatory mechanisms in neuropathic pain. Brain Res Rev 51:240–264.

Mogil JS (2012) Sex differences in pain and pain inhibition: multiple explanations of a controversial phenomenon. Nat Rev Neurosci 13:859–866.

Mogil JS (2020) Qualitative sex differences in pain processing: emerging evidence of a biased literature. Nat Rev Neurosci 21:353–365.

Moy JK, Szabo-Pardi T, Tillu DV, Megat S, Pradhan G, Kume M, Asiedu MN, Burton MD, Dussor G, Price TJ (2019) Temporal and sex differences in the role of BDNF/TrkB signaling in hyperalgesic priming in mice and rats. Neurobiology Pain 5:100024.

Obata K, Noguchi K (2006) BDNF in sensory neurons and chronic pain. Neurosci Res 55:1–10.

Obata K, Yamanaka H, Fukuoka T, Yi D, Tokunaga A, Hashimoto N, Yoshikawa H, Noguchi K (2003) Contribution of injured and uninjured dorsal root ganglion neurons

to pain behavior and the changes in gene expression following chronic constriction injury of the sciatic nerve in rats. Pain 101:65–77.

Obata N, Mizobuchi S, Itano Y, Matsuoka Y, Kaku R, Tomotsuka N, Morita K, Kanzaki H, Ouchida M, Yokoyama M (2011) Decoy strategy targeting the brain-derived neurotrophic factor exon I to attenuate tactile allodynia in the neuropathic pain model of rats. Biochem Bioph Res Co 408:139–144.

Ohira K, Hayashi M (2009) A New Aspect of the TrkB Signaling Pathway in Neural Plasticity. Curr Neuropharmacol 7:276–285.

Ohsawa K, Imai Y, Kanazawa H, Sasaki Y, Kohsaka S (2000) Involvement of Iba1 in membrane ruffling and phagocytosis of macrophages/microglia. J Cell Sci 113:3073–3084.

Pezet S, Malcangio M, McMahon SB (2002) BDNF: a neuromodulator in nociceptive pathways? Brain Res Rev 40:240–249.

Raghavendra V, Tanga F, DeLeo JA (2003) Inhibition of Microglial Activation Attenuates the Development but Not Existing Hypersensitivity in a Rat Model of Neuropathy. J Pharmacol Exp Ther 306:624–630.

Ramesh G, MacLean AG, Philipp MT (2013) Cytokines and Chemokines at the Crossroads of Neuroinflammation, Neurodegeneration, and Neuropathic Pain. Mediat Inflamm 2013:1–20.

Reichardt LF (2006) Neurotrophin-regulated signalling pathways. Philosophical Transactions Royal Soc B Biological Sci 361:1545–1564.

Richner M, Bjerrum OJ, Koninck YD, Nykjaer A, Vaegter CB (2017) Sortilins in neuropathic pain. Scand J Pain 3:183–184.

Richner M, Pallesen LT, Ulrichsen M, Poulsen ET, Holm TH, Login H, Castonguay A, Lorenzo L-E, Gonçalves NP, Andersen OM, Lykke-Hartmann K, Enghild JJ, Rønn LCB, Malik IJ, Koninck YD, Bjerrum OJ, Vægter CB, Nykjær A (2019) Sortilin gates neurotensin and BDNF signaling to control peripheral neuropathic pain. Sci Adv 5:eaav9946.

Scholz J, Woolf CJ (2007) The neuropathic pain triad: neurons, immune cells and glia. Nat Neurosci 10:1361–1368.

Shaw S, Uniyal A, Gadepalli A, Tiwari V, Belinskaia DA, Shestakova NN, Venugopala KN, Deb PK, Tiwari V (2020) Adenosine receptor signalling: Probing the potential pathways for the ministration of neuropathic pain. Eur J Pharmacol 889:173619.

Sikandar S, Minett MS, Millet Q, Santana-Varela S, Lau J, Wood JN, Zhao J (2018) Brain-derived neurotrophic factor derived from sensory neurons plays a critical role in chronic pain. Brain 141:1028–1039.

Smith PA (2014) BDNF: No gain without pain? Neuroscience 283:107–123.

Sorge RE et al. (2015) Different immune cells mediate mechanical pain hypersensitivity in male and female mice. Nat Neurosci 18:1081–1083.

Sorge RE, Totsch SK (2016) Sex Differences in Pain. J Neurosci Res 95:1271–1281.

Squinto SP, Stitt TN, Aldrich TH, Davis S, Blanco SM, RadzieJewski C, Glass DJ, Masiakowski P, Furth ME, Valenzuela DM, Distefano PS, Yancopoulos GD (1991) trkB encodes a functional receptor for brain-derived neurotrophic factor and neurotrophin-3 but not nerve growth factor. Cell 65:885–893.

Stemkowski PL, Biggs JE, Chen Y, Bukhanova N, Kumar N, Smith PA (2013) Understanding and Treating Neuropathic Pain. Neurophysiology+ 45:67–78.

Taves S, Berta T, Liu D-L, Gan S, Chen G, Kim YH, Ven TV de, Laufer S, Ji R-R (2016) Spinal inhibition of p38 MAP kinase reduces inflammatory and neuropathic pain in male but not female mice: Sex-dependent microglial signaling in the spinal cord. Brain Behav Immun 55:70–81.

Terada Y, Morita-Takemura S, Isonishi A, Tanaka T, Okuda H, Tatsumi K, Shinjo T, Kawaguchi M, Wanaka A (2018) NGF and BDNF expression in mouse DRG after spared nerve injury. Neurosci Lett 686:67–73.

Tsuda M, Inoue K, Salter MW (2005) Neuropathic pain and spinal microglia: a big problem from molecules in 'small' glia. Trends Neurosci 28:101–107.

Tsuda M, Mizokoshi A, Shigemoto-Mogami Y, Koizumi S, Inoue K (2004) Activation of p38 mitogen-activated protein kinase in spinal hyperactive microglia contributes to pain hypersensitivity following peripheral nerve injury. Glia 45:89–95.

Ulmann L, Hatcher JP, Hughes JP, Chaumont S, Green PJ, Conquet F, Buell GN, Reeve AJ, Chessell IP, Rassendren F (2008) Up-Regulation of P2X4 Receptors in Spinal Microglia after Peripheral Nerve Injury Mediates BDNF Release and Neuropathic Pain. J Neurosci 28:11263–11268.

Vaegter CB, Jansen P, Fjorback AW, Glerup S, Skeldal S, Kjolby M, Richner M, Erdmann B, Nyengaard JR, Tessarollo L, Lewin GR, Willnow TE, Chao MV, Nykjaer A (2011) Sortilin associates with Trk receptors to enhance anterograde transport and neurotrophin signaling. Nat Neurosci 14:54–61.

Vallejo R, Tilley DM, Vogel L, Benyamin R (2010) The role of glia and the immune system in the development and maintenance of neuropathic pain. Pain Pract Official J World Inst Pain 10:167–184.

Verge GM, Milligan ED, Maier SF, Watkins LR, Naeve GS, Foster AC (2004) Fractalkine (CX3CL1) and fractalkine receptor (CX3CR1) distribution in spinal cord and dorsal root ganglia under basal and neuropathic pain conditions. Eur J Neurosci 20:1150–1160.

Wang X, Ma W, Wang T, Yang J, Wu Z, Liu K, Dai Y, Zang C, Liu W, Liu J, Liang Y, Guo J, Li L (2019) BDNF-TrkB and proBDNF-p75NTR/Sortilin Signaling Pathways are Involved in Mitochondria-Mediated Neuronal Apoptosis in Dorsal Root Ganglia after Sciatic Nerve Transection. Cns Neurological Disord - Drug Targets 19:66–82.

Wang X, Ratnam J, Zou B, England PM, Basbaum AI (2009) TrkB Signaling Is Required for Both the Induction and Maintenance of Tissue and Nerve Injury-Induced Persistent Pain. J Neurosci 29:5508–5515.

Wu Y, Shen Z, Xu H, Zhang K, Guo M, Wang F, Li J (2021) BDNF Participates in Chronic Constriction Injury-Induced Neuropathic Pain via Transcriptionally Activating P2X7 in Primary Sensory Neurons. Mol Neurobiol:1–11.

Xiaodi Y, Shuangqiong Z, Qianbo C, Chengwen C, Hongbin Y (2010) P2X4 receptor and brain-derived neurotrophic factor in neuropathic pain. J Medical Coll Pla 25:275–284.

Yajima Y, Narita M, Narita M, Matsumoto N, Suzuki T (2002) Involvement of a spinal brain-derived neurotrophic factor/full-length TrkB pathway in the development of nerve injury-induced thermal hyperalgesia in mice. Brain Res 958:338–346.

Yan Q, Radeke MJ, Matheson CR, Talvenheimo J, Welcher AA, Felnstein SC (1997) Immunocytochemical localization of TrkB in the central nervous system of the adult rat. J Comp Neurol 378:135–157.

Zhang X, Wang J, Zhou Q, Xu Y, Pu S, Wu J, Xue Y, Tian Y, Lu J, Jiang W, Du D (2011a) Brain-derived neurotrophic factor–activated astrocytes produce mechanical allodynia in neuropathic pain. Neuroscience 199:452–460.

Zhang X, Xu Y, Wang J, Zhou Q, Pu S, Jiang W, Du D (2011b) The effect of intrathecal administration of glial activation inhibitors on dorsal horn BDNF overexpression and hind paw mechanical allodynia in spinal nerve ligated rats. J Neural Transm Vienna Austria 1996 119:329–336.

Zhou L-J, Yang T, Wei X, Liu Y, Xin W-J, Chen Y, Pang R-P, Zang Y, Li Y-Y, Liu X-G (2011) Brain-derived neurotrophic factor contributes to spinal long-term potentiation

and mechanical hypersensitivity by activation of spinal microglia in rat. Brain Behav Immun 25:322–334.

Zhuang Z-Y, Gerner P, Woolf CJ, Ji R-R (2005) ERK is sequentially activated in neurons, microglia, and astrocytes by spinal nerve ligation and contributes to mechanical allodynia in this neuropathic pain model. Pain 114:149–159.